CREEP MEASUREMENTS IN IGNEOUS ROCKS WITH SOME APPLICATIONS TO AFTERSHOCK THEORY

Thesis by

Cinna Lomnitz

In Partial Fulfillment of the Requirements

for the Degree of

Doctor of Philosophy

California Institute of Technology

Pasadena, California

1955

ACKNOWLEDGMENTS

Deepest appreciation is expressed to all those who made this work possible, and particularly to the following:

Professor Hugo Benioff, who suggested its subject and who designed the apparatus, giving of his advice and experience at all stages in the development of the experiments; Professor C. Hewitt Dix, who gave freely of his time in informal discussions and stimulating criticism; Professor Beno Gutenberg, who in his capacity as Director of the Seismological Laboratory helped generously in providing the specimens, photographic materials and accessories, and the use of Laboratory facilities.

Special thanks are due to Professor C. F. Richter for his encouragement and support, and to the entire staff of the Seismological Laboratory.

Mr. F. Lehner gave technical advice in the assembly of the apparatus, helped in procuring the specimens and was frequently consulted in technical matters. Mr. R. von Huene prepared the thin sections and the photomicrographs. Professor A. Erdelyi suggested the solution of an integral equation in Chapter VIII. Dr. S. R. Valluri made available an invaluable bibliographic file on creep. Dr. C. W. Burnham checked and completed the petrographic descriptions of the rocks. The late Professor J. P. Buwalda gave much encouragement and practical advice during the early part of the experiments. Professors F. J. Converse, G. W. Housner, Ian Campbell, C. R. De Prima and J. A. Noble contributed valuable advice on several occasions.

This work was initiated under a UNESCO Fellowship grant and completed under a California Institute of Technology Scholarship. Deep gratitude is hereby expressed to all persons who, in official capacities or as private citizens made our stay in this country a pleasant and fruitful one.

As in all our undertakings, an equal share of credit is due to my wife, Larissa. Without her inspiration, hard work and unfailing collaboration the present effort would be unthinkable. Our baby George woke me up every morning at daybreak, thereby earning a considerable portion of whatever credit may be left.

Above all, my deep gratitude goes to my parents in Santiago, Chile, to whom this volume is humbly and lovingly dedicated.

ABSTRACT

First Part

Cylindrical specimens of Southern California granodiorite and gabbro were creep-tested at constant torques in a high-magnification torsion apparatus. Complete creep and creep recovery curves at room temperature were recorded for periods of about 10,000 minutes.

The results are represented by an empirical equation of the form:

$$s = p\,(a+b \log t)$$

where s is the strain, p the stress and t the time. No evidence was found of creep behavior suggestive of the Michelson equation.

For some granodiorite samples the viscosity was of the order of 3×10^{15} poises. The behavior of the rocks under prevailing test conditions was not appreciably different from that of other polycrystalline materials.

Second Part

A quantitative treatment of the Benioff aftershock sequences on the basis of the theory of viscoelasticity is given. The minimum coefficient of viscosity found by this method is of the order of 10^{19} poises, in good agreement with accepted viscosity values for the earth's crust.

TABLE OF CONTENTS

NOTATION

Some of the more frequently used symbols are given below. A dot above a symbol denotes derivation with respect to time.

p	stress in gr/cm^2
s	strain in radians
t	time in minutes (First Part)
	id. in days (Second Part)
M	torque in gr-cm
E, a	moduli of elasticity (unspecified)
G	modulus of rigidity in gr/cm^2
θ	twist per unit length, in radians/cm
η	viscosity in poises
r	radial distance in cm.
R	radius of specimen in cm.
K	magnification constant
U	crustal strain rate in radians/day
V	volume in cm^3
T	time (of main earthquake) in days
F, ϕ, ψ, Ψ, N	various functions as defined

INTRODUCTION

When, in 1951, Professor Hugo Benioff published his first paper on Earthquakes and Rock Creep, the question of the origin and mechanism of earthquakes was in the stage of scientific conjecture. Intents of proving the connection between earthquakes and astronomical, meteorological or chronological events had been shown statistically unsound.

The relation of tectonic earthquakes to geologic faulting had been known for a long time. The seismicity of the globe had been exhaustively studied by Gutenberg and Richter, and the approximate recurrence of shocks of a given magnitude was known for well-covered regions such as Southern California and New Zealand. The elastic constants of different layers of the earth's crust had been obtained from seismic wave velocities. However, earthquakes still remained essentially unpredictable events and there was no known relation between one shock and the next, either in magnitude or in time.

The Benioff aftershock theory reported its first success in predicting the occurrence of an earthquake of magnitude 7.5 in a region of relatively low seismicity in the Indian Ocean, where no shock of that magnitude had been recorded previously. This earthquake (and a smaller one preceding it by two years) occurred after a period of quiet of 16 years (fig. 1). In some of the earthquake sequences studied by Benioff (1951) the aftershock strains followed very closely a curve of the form

$$S = A + B\left(1 - e^{-a\sqrt{t}}\right).$$

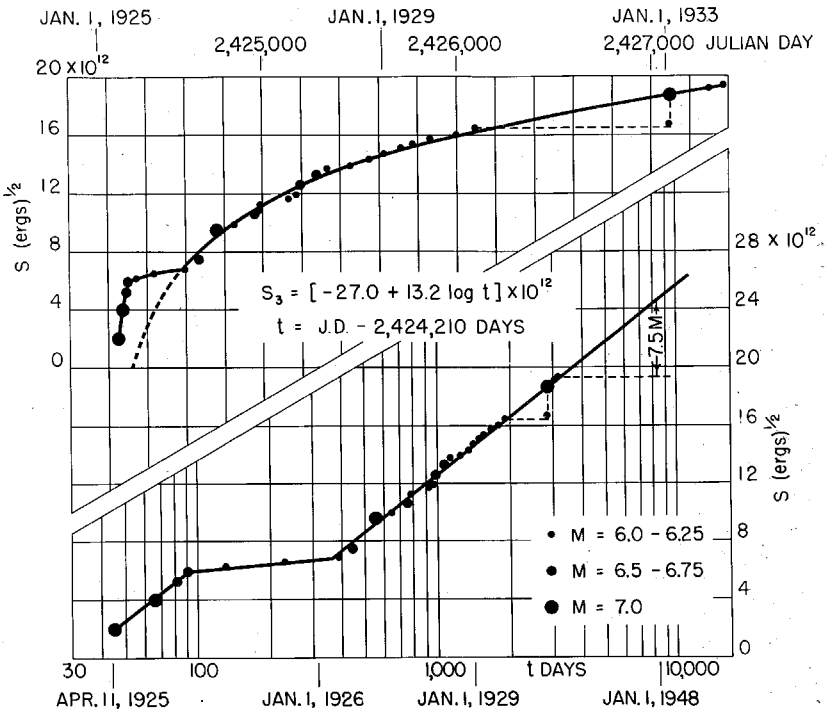

INDIAN OCEAN. SHALLOW FOCUS SWARM. ϕ = 34° S., λ = 58° E.

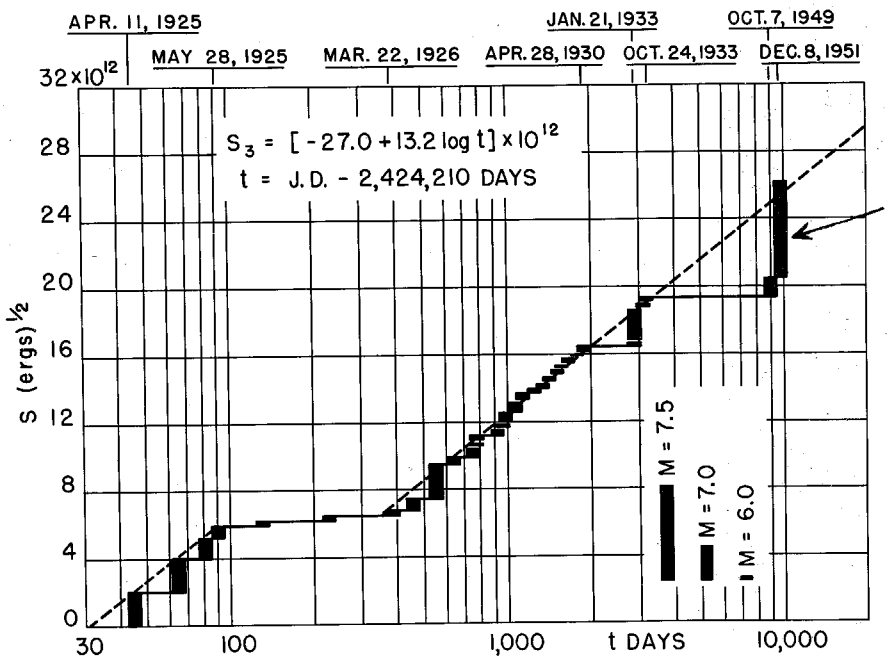

INDIAN OCEAN SEQUENCE. ϕ = 34° ± S., λ = 58° ± E.

H. BENIOFF, JAN. 1952 FIG. 1

* ARROW INDICATES EARTHQUAKE PREDICTED IN EARLIER GRAPH (ABOVE)

An expression of this form had been proposed by A. A. Michelson (1917; 1920) for the creep recovery of many materials in torsion testing.

The lack of creep test data on igneous rocks, and the unusual form of the Michelson equation which had not received confirmation from subsequently published work on creep, induced Professor Benioff to plan an experiment for testing the creep of igneous rocks in torsion.

On the basis of the scant observations available it was expected to find very low rates of creep in these rocks, a fact which made large instrumental magnifications essential. At the same time, the nature of the investigation precluded the use of expensive equipment, and made the qualities of ruggedness and some measure of self-operation desirable.

A torsion apparatus fulfilling these requisites was designed by Professor Benioff and built under his supervision at the workshops of the Seismological Laboratory. The use of this apparatus for the purpose of determining the validity of the Michelson equation for igneous rocks, was proposed to the author as a doctorate research project, late in 1952.

The bulk of the experiments to be described in the following, were carried out in the Arms Laboratory of the Geological Sciences at California Institute of Technology, during the period between November 1954 to April 1955. Rock specimens, photographic materials and various accessories were supplied by the Seismological Laboratory of the Institute.

In the course of the experimental work a more challenging

objective was always kept in mind, namely, to find a quantitative correlation between the aftershock sequences and the creep properties of the earth's crust. Some tentative results of this quest are given in the last two chapters, together with the rudiments of a mathematical treatment of aftershock curves. This treatment is far from exhaustive but may be of some interest in view of the rather good agreement obtained with independent estimates of the viscosity of the earth's crust.

CHAPTER I

FUNDAMENTALS OF CREEP TESTING

1. Definitions. When a substance is subjected to an external force it is bodily accelerated in the direction of the force. If one applies also an external restraint opposing the force, the body undergoes a change in shape, in volume or in both. This change is known as deformation, and its magnitude is dependent at least upon the material, the external force, temperature, pressure and time.

A part of the deformation in a solid is known to occur practically instantaneously. This we shall call the elastic deformation in an unrestricted sense (i.e. without implying anything about linearity of the stress-strain relation). All time-dependent deformation occurring after the elastic deformation will be termed creep.

Creep may be more in the nature of a transient or of a steady-state deformation. This depends a great deal upon temperature and pressure, the scales of time and strain used in the test, and the point of view of the observer. In engineering design at ordinary temperature creep is usually neglected altogether, or it may be embodied in a general "factor of safety". In metallurgy and high-temperature design it is customary to distinguish a steady and a transient component of creep; the latter is often neglected. This procedure is increasingly being recognized as artificial in view of the evidence of long-duration creep tests, that the creep rate may continue to change slowly over periods of years (Robinson 1933).

When the force acting upon the sample is released a reversed deformation occurs, the instantaneous part of which is termed

elastic rebound, and the time-dependent part creep recovery. The elastic rebound tends to be equal to the initial elastic deformation, while creep recovery mostly proceeds at a slower rate than the corresponding direct creep. Experience also shows that a certain amount of creep deformation is often practically unrecoverable.

If instead of an external force of known magnitude one imposes upon the sample a given deformation, the material is stressed instantly an amount equal to the force needed to produce the same deformation. With increasing time the stress in the sample is observed to decrease to a constant value which may or may not be zero. This variation of stress with time is known as relaxation. The phenomena of creep, creep recovery and relaxation are significantly interrelated and the exact form of their relationship has recently been derived for one important case (Sips, 1950).

2. Background of creep testing. Actual deformation tests are extremely complex. The need of using different specimens of a substance raises the questions of uniformity and homogeneity. Lack of isotropy may introduce additional uncertainties in test results. All materials do also exhibit an appreciable dependence upon previous strain history. Since all specimens subjected to testing must have been strained previously in a way that is largely unknown, even the best-conducted creep test cannot hope to give more than one point in a statistical array representing the strain properties of the material.

Nevertheless, great progress has been made since the formulation by Hooke (1618) of his law of elasticity:

$$p = Es \tag{1}$$

which is among the most durable linear relations in physics. Since the development by Cauchy (1822) of the concepts of strain and stress it has formed the basis of the important mathematical-physical structure of the Theory of Elasticity.

A group of materials such as concrete, cast iron, rocks and others, deviate from Hooke's Law to a certain degree, which often is of no great consequence in technology.

The study of creep has gained great importance during the last 50 years, paralleling the development of metallurgy. Among the earlier tests, many were confined to the study of stress-strain-time relations. Temperature was introduced early as an important variable, and pressure much later. Relaxation tests are of recent date.

Empirical creep formulas may be classified as follows:

a. "constant strain rate" formulas:

$$\dot{s} = f(p) \tag{2}$$

b. "aging" formulas:

$$s = f(p, t) \tag{3}$$

c. "strain hardening" formulas:

$$s = f(p, \dot{s}) \tag{4}$$

The functions proposed are too varied to be discussed in detail. A useful review will be found in Schwope and Jackson (1951). Formulas corresponding to the "aging" hypothesis are very common. It had been observed at an early date (Trouton and Rankine, 1904) that many materials at ordinary temperature often give a logarithmic

relation:

$$s = a + b \log t \tag{5}$$

where b is approximately a linear function of stress.

At higher temperatures the constant strain rate hypothesis is more convenient to use, and one finds expressions such as the "logarithmic strain rate law":

$$\log \dot{s} = a + b\, p \tag{6}$$

or the hyperbolic sine law (Nadai and McVetty, 1943):

$$\dot{s} = a \sinh (bp + c) . \tag{7}$$

Both relations receive some measure of theoretical justification through Eyring's theory of rate processes as applied by Kauzmann (1941) and Nowick and Machlin (1946). A theoretical derivation of the semi-logarithmic law (5) was given by Goranson (1940).

3. Rheological approach. Closely paralleling this empirical development is the progress of the Theory of Plasticity, based upon fundamental work by Saint Venant (1871) and others. A plastic body deforms indefinitely at a certain magnitude of stress k. Below this so-called "yield stress" the body is assumed to obey Hooke's Law.

There is occasionally some confusion between the concepts of plasticity and viscosity, and it may be convenient to define these terms as they will be used here. The law of viscous flow, given by Newton (1685):

$$p = \eta \dot{s} \tag{8}$$

may be used to define ideal viscosity. It is seen that Hooke's and Newton's laws are similar in structure; thus many solutions obtained in the Theory of Elasticity (see, for instance, Love, 1934) may be written directly for a viscous medium by replacing the stress by its time derivative.

The ideal plastic body is defined by Saint Venant's relation:

$$p = k \, . \tag{9}$$

When $k = 0$ we have the perfect fluid, which has no viscosity and no strength.

It is observed that one cannot impose on a plastic body any stress larger than k. It is somewhat hard to see what this implies physically; in effect it means that one may only specify an arbitrary velocity at the point of application of the stress. If one tries to increase the stress the sample deforms in such a way as to defeat the attempt.

The Theory of Plasticity (see, for example, Prager and Hodge, 1951) is valuable chiefly in the technology of such materials as steel and bronze in the vicinity of the yield point. However, as one increases the temperature and pressure it becomes applicable to a great many other materials as well (Bridgman, 1952).

In 1868 Maxwell proposed a new law for a combined Hooke-Newton substance which he used to describe the behavior of fluids showing stress relaxation:

$$\dot{s} = \frac{1}{E} \dot{p} + \frac{1}{\eta} p \tag{10}$$

which defines the state of elastico-viscosity or visco-elasticity. Maxwell's visco-elastic substance was the first of a series of rheological models that have been proposed, combining the properties of elasticity, plasticity and viscosity (see Reiner, 1949).

A convenient way to objectivize these models is to represent them as a combination of springs, dashpots and weights sliding on friction surfaces. In these "models" the stress is represented by the applied force, and the strain by the displacement. Thus the Maxwell model may be represented by a spring and a dashpot in series (fig. 2).

The same elements combined in parallel constitute the "firmo-viscous" model, proposed independently by Voigt and Lord Kelvin:

$$p = Es + \eta\dot{s} \quad . \tag{11}$$

The term "firmo-viscosity" is due to Jeffreys. This model exhibits transient creep and creep recovery; the Maxwell model gives constant-rate creep (non-recoverable) as well as stress relaxation. It seemed natural to combine both models into one, called "standard linear solid" (Zener, 1946) and studied by Jeffreys (1917) and Burgers (1935).

Finally, Alfrey (1944) and other workers in the field of organic polymers analyzed the general case of a model having an arbitrary number of Maxwell elements in parallel, or Voigt elements in series. This generalized viscoelastic model is

RHEOLOGICAL ELEMENTS

SPRING

$p = Es$

DASHPOT

$p = \eta \dot{s}$

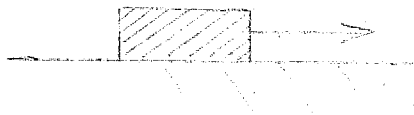

SLIDING WEIGHT

$p = k$

RHEOLOGICAL MODELS

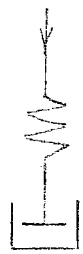

MAXWELL

$\dot{s} = \frac{1}{E}\dot{p} + \frac{1}{\eta} p$

$\phi(t) = \frac{E}{\eta} t$

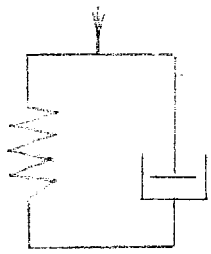

VOIGT

$p = Es + \eta \dot{s}$

$\phi(t) = -e^{-\frac{E}{\eta}t}$

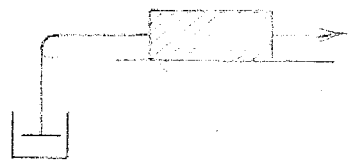

BINGHAM

$p = k + \eta \dot{s}$

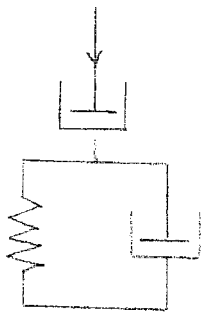

STANDARD LINEAR SOLID

$Es + \eta \dot{s} = p + \frac{1}{\tau}\int p\,dt$

$\phi(t) = \left(1 - \frac{\eta}{E\tau}\right)\left(1 - e^{-\frac{E}{\eta}t}\right) + \frac{t}{E\tau} - 1$

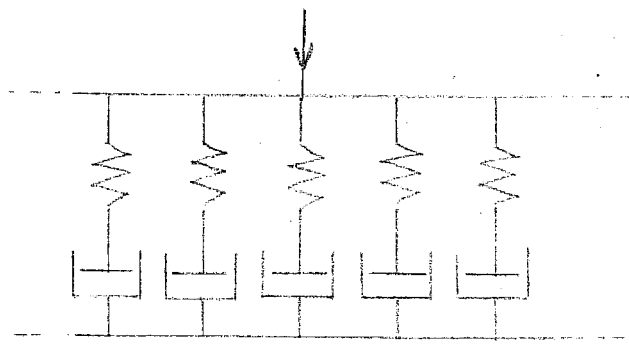

GENERAL VISCOELASTIC SOLID

$s = \frac{p}{E}\left[1 + \phi(t)\right]$

$\phi(t)$ any increasing function

$\phi(0) \geq -1$

susceptible of mathematical treatment (e.g. Biot, 1954) and is receiving increasing practical application.

4. Creep tests. The most widely used among methods of creep testing remains the tension test. It has been standardized by the American Society for Testing Materials (Specification E22-41), as well as abroad. Its great advantage is that it reproduces critical conditions of loading to which a majority of structural parts will be subjected.

Routine tests are often required to give only relative information, leading to the acceptance or rejection of a certain material. For more exact work the tensile test has an important drawback in the phenomenon known as necking. When a specimen is tested in tension, each increase in strain is accompanied by a progressive narrowing-down in localized regions of the sample. This results in greater stress concentrations and proportionally higher creep rates in the "necks".

An exact solution of the problem would require at least current measurements of the radius of curvature at the neck for the duration of the test. Lacking these, assumptions are made which may lead to important errors at high stresses.

The situation is similar for compression tests, with the added complication of buckling. However, compression tests may be the only practical ones for sedimentary rocks or specimens in which bedding or cleavage planes may be present (D. T. Griggs, oral communication).

Torsion tests are common to a certain extent, although far less so than tension tests. They have the obvious advantage that in cylindrical specimens the shape is not altered even at quite large strains.

Moreover, the internal path of deformation is simpler than in tension. In the latter

"...the planes of shear envelop a cone and hence interfere with each other. In simple shear, on the other hand, any plane of shear retains its direction and all the atoms in the plane retain their separation....It is natural to think that in any actual case of shear the total disorganization must be less than in tension." (Bridgman, Large Plastic Flow, p. 273).

Creep tests in tension and in torsion have been compared experimentally (Ludwig and Scheu, 1925; Shepherd, 1948; Bridgman, 1952), but no differences in the behavior of the material were found except for large strains. In these cases strain hardening was somewhat less pronounced in torsion, as would be expected from the passage quoted.

The advantage of having plane strains in torsion is offset by the fact that stresses are inhomogeneous in the section, i.e. varying from a maximum at the surface to zero at the core. The stress distribution in the section depends upon the kind of stress-strain relation which can be assumed valid for the material. The conditions for which this problem can be solved will be examined in the following chapter.

CHAPTER II

TORSION OF CYLINDRICAL BAR

1. The superposition range. Let a constant moment of torsion M be applied at the free end of a rod of circular cross-section (fig. 3), and let the strain S(t) at the periphery be an experimental datum. It may be shown (Appendix I, p. 86) that the stress distribution in the section must be constant with time. Although this conclusion is valid for any kind of material, we shall begin by confining the analysis to a certain range of stresses and temperatures, such that Boltzmann's principle of superposition is valid. It was pointed out (C. H. Dix, oral communication) that Boltzmann's principle is exactly equivalent to assuming a linear relation between stress and strain.

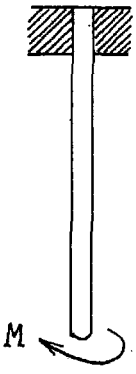

Fig. 3

Such a condition may be written in the form

$$s(t) = \frac{p}{E}\left[1 + \phi(t)\right] \tag{12}$$

which is reduced to Hooke's Law for $t = 0$. The function $\phi(t)$, called the "creep function", is characteristic of the material, temperature and pressure. We also have $\phi(0) = 0$.

The moment M can be expressed (Appendix I, Eq. 85):

$$M = 2\pi \int_0^R p r^2 dr \tag{13}$$

R being the radius of specimen. Substituting from (12):

$$M = \frac{2\pi E}{1+\phi(t)} \int_0^R s(t)\, r^2\, dr \tag{14}$$

which is exactly similar to the expression for M in the elastic case, except for the function of time in the denominator.

The elastic torsion problem was first solved by Coulomb, who assumed the strain to be proportional to the axial distance. It has been shown (Saint Venant) that this assumption is equivalent to requiring plane cross-sections to remain plane during torsion. It is found that these conditions are verified only for the circular cross-section.

Accordingly, we may write:

$$s(t) = S(t) \frac{r}{R} \quad . \tag{15}$$

S(t) is the maximum strain at the periphery, which is found from experiment. Equation (14) then becomes:

$$M = \frac{2\pi E\, S(t)}{R\left[1+\phi(t)\right]} \int_0^R r^3\, dr \quad . \tag{16}$$

Integrating:

$$M = \frac{\pi}{2} E\, R^3 \frac{S(t)}{1 + \phi(t)} \quad . \tag{17}$$

In actual testing it is customary to use the angle of twist per unit length of sample as a more convenient parameter:

$$\theta(t) = \frac{S(t)}{R} \tag{18}$$

$$M = \frac{\pi}{2} E\, R^4 \frac{\theta(t)}{1 + \phi(t)} \tag{19}$$

$$\phi(t) = \frac{\pi}{2M} ER^4\, \theta(t) - 1 \quad . \tag{20}$$

Equation (20) permits us to obtain the creep function from direct experimental data. It also represents the time-creep relation of a material for a constant stress.

In fig. 2 this relation is shown for the Maxwell, Voigt and standard linear models of solid. The derivation is found in Appendix II. With the use of Alfrey's generalized viscoelastic model $\phi(t)$ may be any continuously increasing function.

2. The plastic range. Let us imagine a cylindrical rod made of ideally plastic material. If such a specimen is subjected to an increasing torque it will deform elastically until the yield stress k is reached along the periphery. If the torque is increased further a plastic zone will spread concentrically inwards, reaching the center of the rod at infinite strains.

Thus the problem of plastic torsion is one of two domains governed by different laws of deformation, the position of the boundary being unknown. In the case of a circular cross-section the problem may be solved analytically if one assumes two conditions of continuity at the boundary. For most other sections the geometrical form of the boundary is unknown, but a graphical or experimental solution can be found by Nadai's sand-hill method (1931).

Let us write the solution for the circular case (Prager and Hodge, 1951):

$$M = \frac{2}{3}\pi R^3 k \left[1 - \frac{1}{4R^3}\left(\frac{k}{E\theta}\right)^3\right]. \qquad (21)$$

The presence of θ indicates that (21) is an equilibrium condition. No flow occurs in plastic torsion until the entire section has reached the plastic state. The torque necessary to produce this state is only 1/3 higher than the torque upon reaching the yield point (fig. 4). No greater torque can be imposed upon the sample in theory. If one does nevertheless it may be presumed that the specimen is accelerated to the point of failure.

In order to introduce creep one may postulate a Maxwell, Voigt or Zener material having a plastic yield point; or one may imagine a model combining plasticity and viscosity. Such a model has been proposed by Bingham (1922) to describe the "visco-plasticity" of paints:

$$p = k + \eta \dot{s} \quad . \tag{22}$$

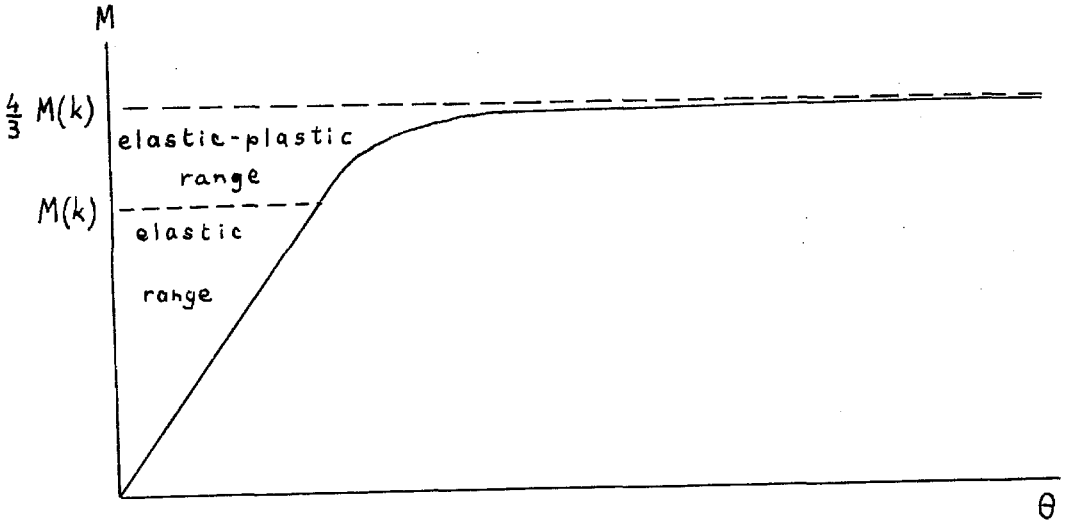

FIG. 4

The derivation of the plastic torsion formula for this material may be readily carried out (Appendix III, p. 90). The solution is:

$$M = \frac{2}{3}\pi R^3 k\left[1 - \frac{1}{4R^3}\left(\frac{k}{E\theta_o}\right)^3\right] + \frac{\pi}{6}\eta R\dot{\theta}\left(3R^3 - \frac{R^2 k}{E\theta_o} - \frac{Rk^2}{E^2\theta_o^2} - \frac{k^3}{E^3\theta_o^3}\right) . \tag{23}$$

The first term is identical to (21), θ_o being the elastic part of the angle of twist. The total angle is given by:

$$\theta = \theta_o + \int_o^t \dot{\theta}\, dt \tag{24}$$

or, if η is a constant:

$$\theta = \theta_o + \dot{\theta}t \quad . \tag{25}$$

The rate of angular strain is constant and proportional to the applied torque M.

While this model appears to be more realistic than the purely plastic one, it has no real advantage over a viscoelastic model, which has no two-domain problem.

3. Non-linearity . Whenever Boltzmann's principle of superposition ceases to apply, a problem of non-linearity is created. Deviations from linearity have been known for a long time, both in fluids and in solids. Some of the most useful empirical creep equations (such as Eq's. (6) and (7)) are non-linear.

These equations belong to the constant-rate group which is applied at high temperatures for which Boltzmann's principle is not expected to apply. However, Orowan (1946) has given a treatment of primary creep that is non-linear, being based upon

rate theory and upon Becker's theory of crystal slip (1925). Orowan's equation does not fit the experimental data and has been modified by several authors with contradictory results.

It is felt that a linear approach to the creep problem may still be preferable, particularly in low-temperature creep and, more generally, for all those cases in which the constant strain rate simplification is not admissible. Great progress has been made in the field of molecular physics, particularly in dislocation theory and thermodynamics of irreversible processes. However, no unified theory of creep has been forthcoming, the work by Goranson (1940) constituting an isolated attempt to the exception.

4. The Michelson equation. In 1919 A. A. Michelson published the results of a series of torsion creep tests covering a wide range of substances (including lead, tin, copper, aluminum, zinc, iron, steel, quartz, glass, pitch, calcite, limestone, slate, marble, gelatin, rubber, ebonite, bakelite and sealing wax). His results were described by the formula:

$$S = F_1 + F_2 (1-e^{-a\sqrt{t}}) + F_3 t^{\frac{1}{3}} \tag{26}$$

in which

$$F_i = C_i P e^{h_i P} \tag{27}$$

where S is the twist and P is the weight applied to produce the torque. The formula may be represented by a mechanical model

(fig. 5) which is similar to the standard linear solid except that it has both linear and non-linear elements. The constants C, h and a for the various materials tested were published in a second paper (Michelson, 1920). The experimental data have remained unpublished, with the exception of a table of creep recovery data for vulcanite. The dimensions of the apparatus are relevant to the interpretation of formula (26) because it does not contain either stress or strain explicitly.

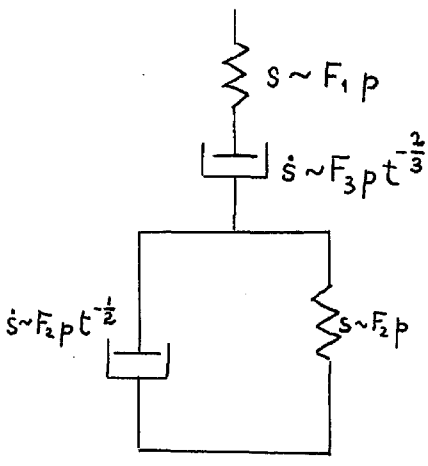

FIG. 5

The apparatus is described as a horizontal frame which accommodated cylindrical samples 12 mm in diameter at the ends. One end of the specimen was clamped to the frame and the other to a pulley resting on a knife edge. The diameter of the central part of the sample was 4 mm and its length was 7.5 cm.

Due to an unfortunate misprint the diameter of the pulley is given once as 8 cm (first paper) and once as 5 cm (second paper). The uncertainty cannot be removed by referring to the published constants, because of insufficient description of the materials tested.

Test readings were made by "measuring the angular position of the pulley by a micrometer at intervals of one minute while it is under a constant torque" (first paper). This seems to indicate that the duration of tests was not very long. The published table of data for vulcanite goes as far as 100 minutes, and it may be

assumed that this was the order of duration for the other experiments as well. If the arm of the micrometer was of the order of diameter of the pulley, the accuracy of reading may be estimated at $\pm 10^{-3}$ radians (as compared to 10^{-7} in our experiments). The unit of P is given as 100 grams. The unit of S is not given.

The aim of Michelson's experiments was chiefly a qualitative one in connection with his work on the rigidity of the earth (Michelson, 1914, 1919). His published data do not appear to be sufficiently detailed to afford an exact check. However, it may be of interest to study the behavior of Eq. (26). In fig. 6 some of these curves have been plotted from constants published in Table IV (second paper). They can be approximated by semi-logarithmic expressions without great strain.

This agreement is lost if we plot the corresponding recovery curves, for which the "viscous" term $F_3 t^{\frac{1}{3}}$ should of course be zero. In this connection we may refer to a footnote in the second paper:

"It was found by experiment that for stresses not too great the 'direct' curve (on applying the stress) and the 'return' curve (on releasing) were the same; or rather, if the former is S and the latter R then S + R = constant."

This statement, apparently contradicting Michelson's own conclusions as well as ordinary creep test experience, may be taken as an indication of the sensitivity of the apparatus used. It should be borne in mind that for most of the substances tested

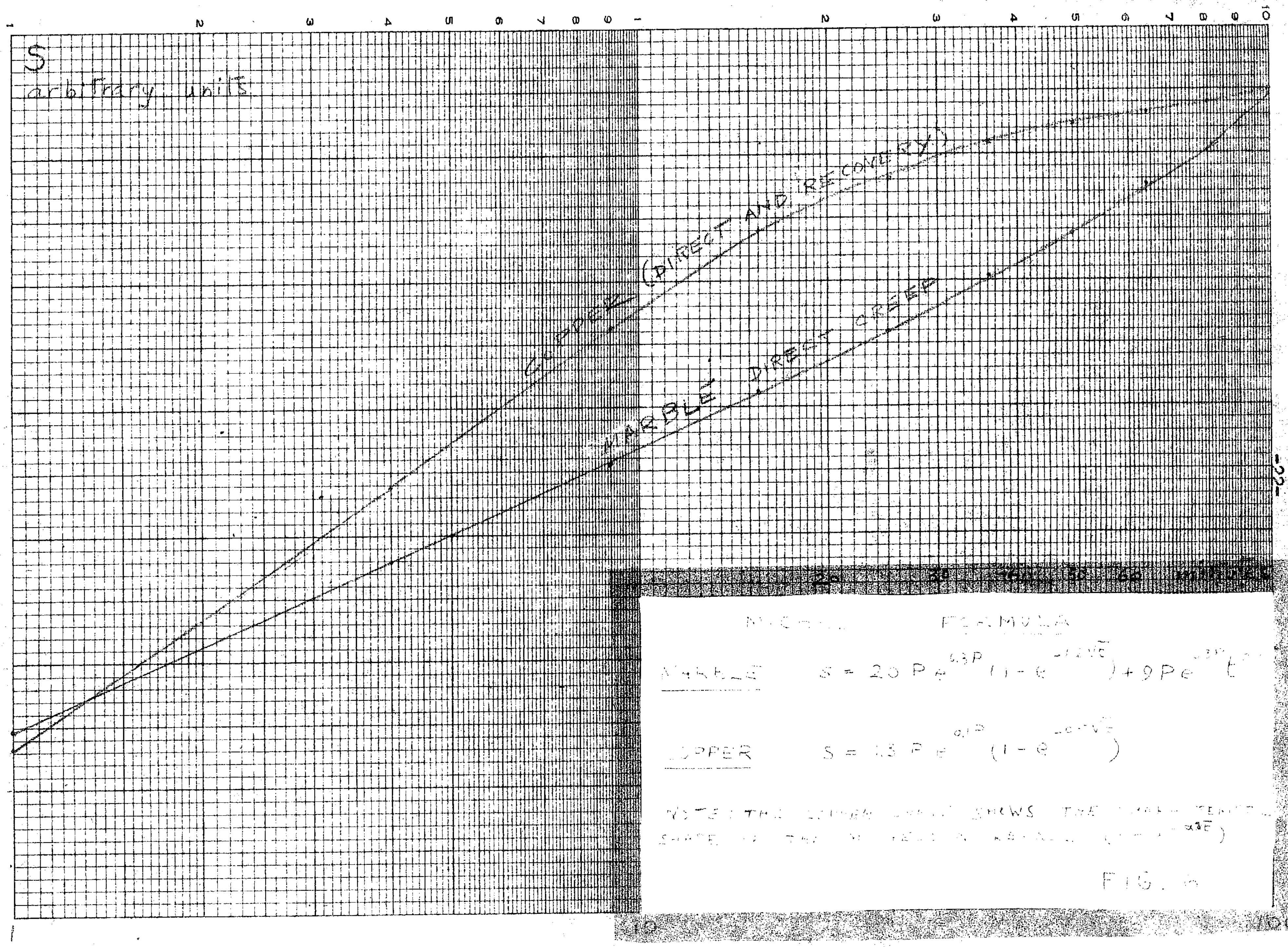
S
arbitrary units
COPPER (DIRECT AND RECOVERY)
MARBLE DIRECT CREEP
20
30
FORMULA
MARBLE
COPPER

by Michelson the rates of creep and of recovery were rather small at room temperature.

It is perhaps striking that Michelson should not have used the interferometer in these measurements. The fact could be taken to mean that the priority attached to this particular investigation was not very great at the time. In effect, as is apparent from their publication in the Journal of Geology, the results were intended as a basis for a discussion of the interferometric measurements of the earth tides, published by Michelson in the same Journal (1914, 1919). In view of the difficult form of Eq. (26) it is not surprising that such a discussion should not have taken place. In any case its importance within the general framework of research of the great physicist may well have been a subordinate one.

In conclusion, the Michelson tests do not appear to give any clear evidence of a new fundamental result having been reached. An attempt to fit the behavior of such different materials as lead, gelatin, steel and pitch would have strained any empirical formula we know. As a consequence, the Michelson formula needs no less than seven different constants to describe the behavior of a material. It remains for experiment to decide whether this generality is meaningful in the light of our present knowledge of creep.

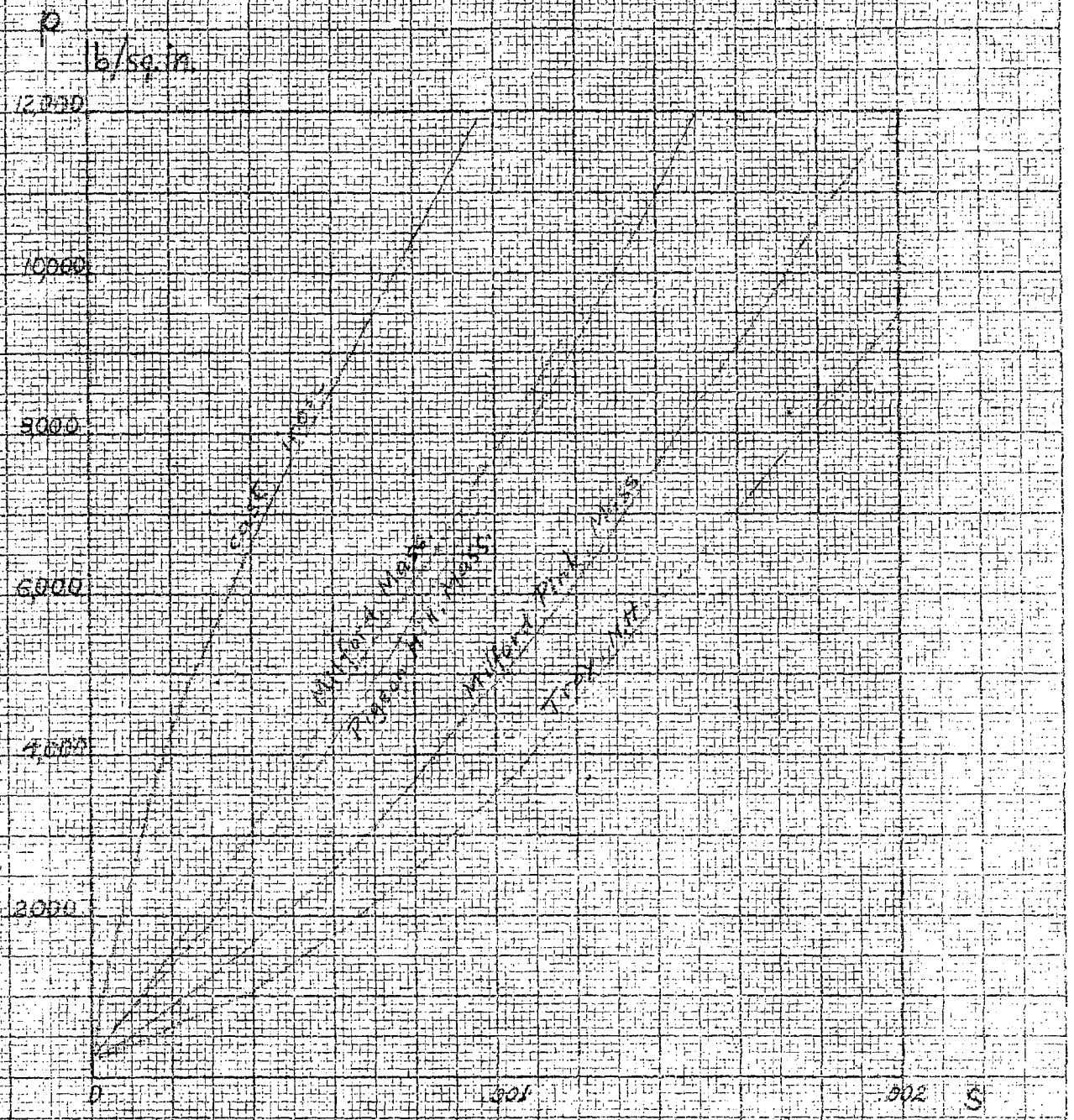

Typical Stress - Strain Curves

+ Eastern Granites (compression)
after Watertown Arsenal Report, 1887

Cast Iron (tension)
after Clapp & Clark, Engineering Materials

FIG. 7

CHAPTER III

TORSION TESTS IN IGNEOUS ROCKS

1. Background. The elastic properties of igneous rocks have been investigated in connection with their use as building materials. A fairly typical stress-strain curve is reproduced on fig. 7. It may be observed that rocks do not generally have a clear yield point or a well-defined proportionality limit.

Creep tests on igneous rocks are rare. Torsion tests were performed by Sokoloff and Skriabin (1936) with test durations of a few minutes only. Compression creep tests on diabase were conducted by Bridgman (1949). Dynamic determinations of viscosity and relaxation functions of igneous rocks were made by Birch and Bancroft (1938).

Work on sedimentary and metamorphic rocks is more abundant (D. T. Griggs, 1936; 1939).

2. Description of Apparatus. The apparatus shown in fig. 8 was originally developed by H. Benioff and was used in the present investigation with very few additions or modifications. It consists of a sturdy vertical steel frame accommodating a specimen 18" long. The upper end of the specimen is tightly clamped into a $\frac{1}{2}$" opening in the upper plate, while the lower end remains free and self-aligning. This lower end is clamped into a steel fitting which supports a dural pulley of 15 cm diameter.

Screwed to the base plate of the frame are two small pulleys on ball bearings. A steel or dural tape can slide over these pulleys and through openings in the base plate to the yoke

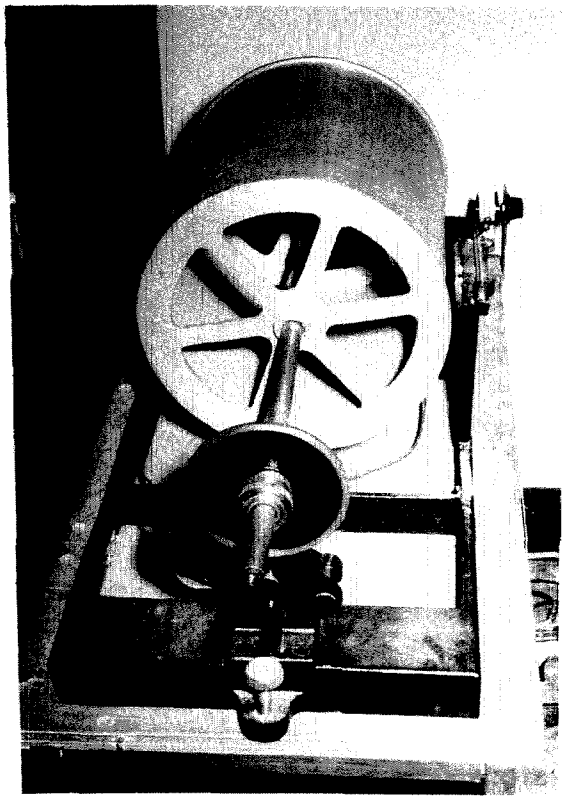

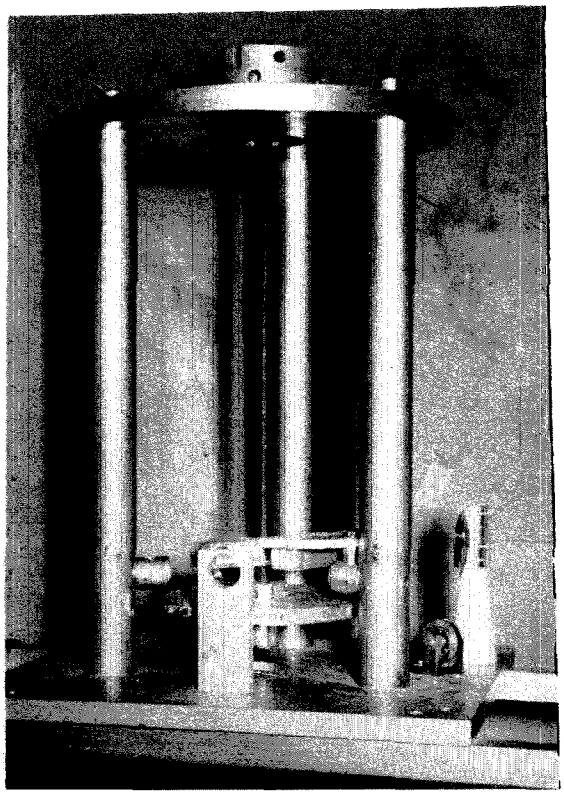

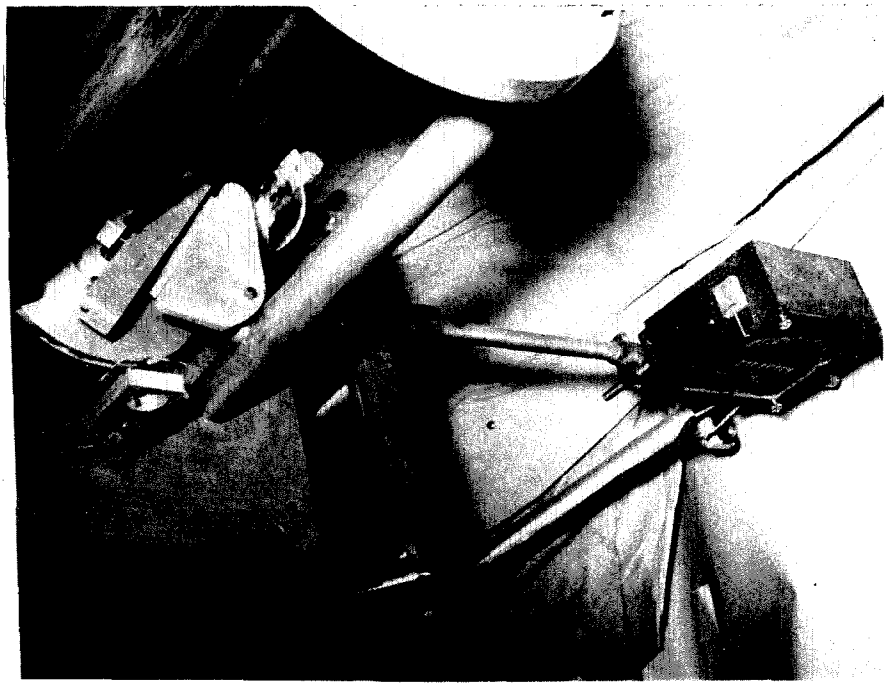

FIG. 8

FIG. 9

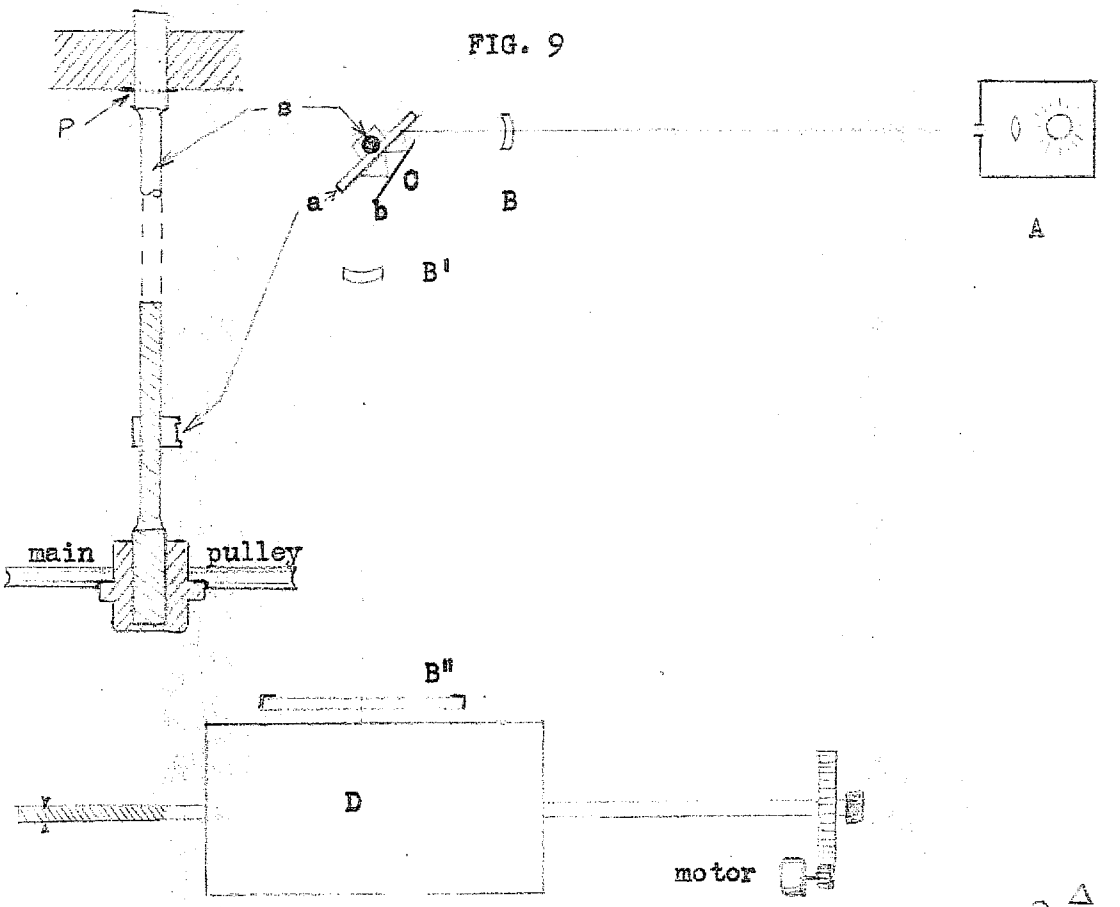
P
s
a
b
C
B
A
B'
main
pulley
B''
D
motor

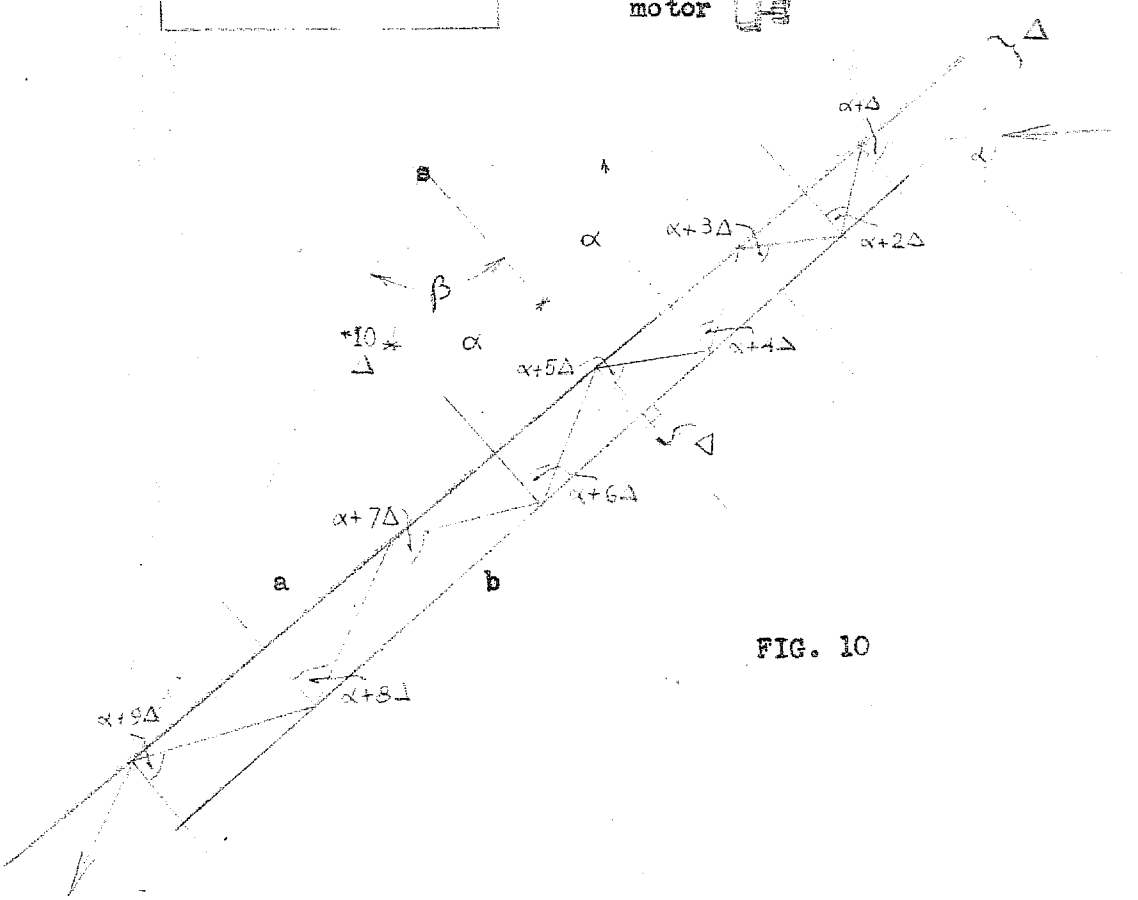
s
α
β
α
α+Δ
α+2Δ
α+3Δ
α+4Δ
α+5Δ
α+6Δ
α+7Δ
α+8Δ
α+9Δ
a
b

FIG. 10

or loading beam underneath. The other ends of the tape are connected to the main pulley which transmits the torque to the specimen.

The recording system is entirely optical. It consists of a light source A (fig. 9) having a vertical slit of adjustable width, a set of lenses B, B', B'', a multiplying mirror system C and a photographic recorder D.

Fig. 10 represents a diagram of the mirror system. Mirror a is mounted directly onto the specimen s (shown in cross-section), while mirror b remains fixed during the test. Let α be the angle of the incident ray with the normal to mirror b; then the corresponding angle of the outgoing ray with the same normal will be:

$$\beta = \alpha + (n + 1)\,\Delta \tag{28}$$

where Δ is the angle between the two mirrors and n is the total number of reflections. In the position illustrated, $n = 9$ and therefore $\beta = \alpha + 10\Delta$, meaning that the angular deflection of the specimen will be multiplied by 10. The system has proved to be very reliable, rugged and easily adjustable by hand. It introduces no frictional error and is independent of the exact position of the specimen and of possible temperature changes.

The linear magnification is proportional to the optical lever d (fig. 9), so that the total magnification is written:

$$K = d\,(n + 1)\ . \tag{29}$$

The number of reflections n may be varied by adjusting the angle of incidence and the angle between mirrors. An optical magnification $(n + 1) = 10$ was found to be practical for most tests. At $(n + 1) = 12$ the adjustment necessary to accommodate all reflections on the limited length of the mirrors became very delicate. For some larger creep deformations, however, the angular magnification was reduced to 8.

The system of lenses is shown diagrammatically on fig. 9. Lenses B and B' are toric with the axis in the vertical direction and selected in such a way that their foci coincide with the slit of the light source, and with the face of the light-sensitive paper, respectively. Thus the rays that travel between the mirrors are parallel. The sharp vertical image of the light source on the photographic paper is reduced to a luminous point by means of a cylindrical lens B'', whose axis is perpendicular to the direction of the image. The position of lens B'' is adjustable for precise focusing.

The recording drum is of the same kind used in seismic recording and accommodates a standard 30 cm wide photographic paper. A small synchronous motor is mounted on a movable arm which can be easily disengaged from the drum gear. The drum speed is one revolution per hour, corresponding to a recording speed of 1.5 cm per minute. A worm gear on the axis of the drum provides a lateral translation of 0.1 inch per revolution. It was found that one record could normally register four days consecutively without changing.

3. Sensitivity. In the preceding paragraphs K represented the magnification corresponding to a given angle of twist of the specimen at the level of the mirrors. In order to convert this to actual strains, let us introduce the effective length L of the sample, measured from the level of the mirror to the upper clamped section, and the radius R of the specimen. Then we have

$$K = d\,(n + 1)\,\frac{L}{R} \tag{30}$$

in cm. per radian of actual strain at the periphery of the sample.

Actually the clamped section is of larger diameter and may be disregarded, so that the effective length L is only measured up to the change in section. The following values of the constants were currently used in testing:

$$n = 9$$

$$L = 34 \text{ cm}$$

$$R = \tfrac{1}{2} \times \frac{7}{16} = 0.555 \text{ cm}$$

$$d = 117.6 \text{ cm}$$

which gives a magnification ratio

$$K = 72,000 \text{ cm per radian of strain}.$$

The photographic records were read to the nearest $\pm$ 0.01 cm (as in seismic work). This corresponds to a strain of $\pm$ 0.01/K, or $\pm$ 1.4×10^{-7} radian--a sensitivity which is quite satisfactory, considering the economy of means with which it is achieved.

The unusual stability and trouble-free performance of this high-sensitivity creep unit is well worth being emphasized.

4. Limitations and sources of error. The experimental method described, while adequate for the purpose of this investigation, may present certain inconveniences for more general applications.

An obvious disadvantage is the fact that the elastic deformation could not be recorded in many cases, its size being too large as compared to the creep deflections to be measured. A system of double recording with different magnifications might obviate this drawback. In our case it seemed sufficient to record the elastic deformation whenever possible, i.e. for small torques. The elastic modulus obtained in this fashion was consistent.

Possible errors may be analyzed as to their origin and importance, as follows:

a) Errors due to quality of sample: In spite of the care taken in selecting the chunks of rock from which the samples were cut, it was found that the specimens were not homogeneous. The inhomogeneity was apparently of minor importance in the granodiorite; however, gabbro specimens showed variations in the amount of dark minerals, and slightly greater scattering of points in the stress-strain graph. Possibly the grain size of the gabbro was near the limit of coarseness which can safely be used in this type of experiment. At any rate the results were fairly consistent even for the dark rock. The clean helical fractures indicated at least that there were no major discontinuities of any kind within one sample.

All specimens were hand-polished with grade "00" emery cloth in order to reduce surface irregularities. In the process of grinding the specimens, some residual stresses are likely to be introduced. This effect is difficult to estimate; it may be assumed that it is relatively constant for all specimens.

b) Errors attributable to environment: Humidity variations affect the dimensions of the photographic paper. The resulting error, for the type of paper used, was found to be of the order of 0.3% or less; it may become important, however, for measurements at large times ($t > 1000$ minutes), where it can easily be mistaken for constant-rate creep. All instances where it was necessary to correct for this error have been clearly indicated on the graphs.

No appreciable effect of humidity variations was expected on the creep behavior of igneous rocks of low porosity.

The room selected for the experiment--a tiny, completely closed and dark first basement room--proved to be practically temperature-invariant on the evidence of recording thermometer tests. The optical magnification system used is also quite independent of temperature changes.

The location of the tests (Arms Hall) is rather quiet. There is some low-level vibration from electric motors (thin-sections laboratory, fan room in the sub-basement) but the frequency is high. It is estimated that the site would not be ruled out as a seismograph location. Human traffic is low at all hours.

c) Errors due to friction. The only place where friction might have occurred was in the ball bearings of the two small pulleys over which the torque transmission tape ran.

The possibility of friction was minimized by keeping the ball bearings clean and well oiled.

d) Errors due to end effects. The importance of preventing slippage due to insufficient tightening of the upper or lower clamps, has been recognized at an early stage. Actual slip has been observed in one case, with a copper specimen subjected to an unusually high torque (over 200 lb-cm).

Special care was applied during the operation of clamping the specimens, and no instance of slip has been detected. At the low torque used in rock testing the clamping pressures were apparently adequate to prevent any slippage.

The possibility of localized plastic flow at the clamped section merits some attention. From inspection of fig. 9 it is apparent that a zone of stress concentration may be present at P.

The particular stress situation has not been solved to our knowledge. Thin sections (fig. 13) failed to show any evidence of unusual strains. Moreover, no specimen showed any tendency to fracture in the vicinity of the section of clamping.

Bridgman (1952) found that, for extreme torsion strains combined with axial compression, the flow occurring in the larger diameter parts of the specimen could still be disregarded. This is all the more notable as about 97% of the total length of the sample was of larger diameter, and the ratio of the diameters

was only 8:10.

In our specimens the free length of larger diameter section was about 3% of the total length, the ratio of diameters was 8.75:10 and the strains were about 10,000 times less than those attained by Bridgman. It seems safe to conclude that no appreciable end effects could have been present.

e) Errors of parallax. In the derivation of the magnification formula, Eq. (29), it is implied that the arc subtended by the angle of twist is identical with the chord described by the light point on the photographic paper.

The maximum error resulting from this assumption is easily calculated. The length of the cylindrical lens B'' limits the deflection of the light point to 5 cm on either side of the midpoint of the lens. The distance to the mirror on the specimen being 117.6 cm from the midpoint, we find that the angle corresponding to a maximum deflection is:

$$\tan \Delta = \frac{5}{117.6} = 0.04252$$

$$\Delta = 2^{\circ}26'05'' = 0.04249 \text{ radian}.$$

Therefore $\tan\Delta - \Delta = 0.00003$

corresponding to a linear error of

$$\Delta\epsilon = 0.00003 \cdot 117.6 = 0.0035 \text{ cm}$$

which is well within the limits of reading accuracy.

f) Human error. The most important item in this category is the error involved in reading the records. The last decimal figure (tenths of millimeter) is estimated, and it is occasionally

of the order of the thickness of the line on the record. In the experiments at low torques this error is large enough to be quite noticeable on the graphs. In these cases the points corresponding to the readings give an erroneous impression of accuracy and the amount of scattering appears to be greater than it is in reality. If all graphs are plotted to the same scale of strains it is seen that the amount of deviation from the best fit is equally small for all torques.

The adjustment of the apparatus is largely independent of the personal equation of the observer, and no error is expected from this source.

CHAPTER IV

TESTING PROCEDURE AND RESULTS

1. Description of specimens. Igneous rocks are brittle materials of very low ductility. In order to obtain measurable twist deformations it was necessary to use rather long, slender specimens (fig. 11), requiring considerable skill and care in their manufacture. Mr. Sandberg, formerly of the Seismological Laboratory of the California Institute of Technology, first succeeded in producing such specimens; all those used in the present research were machined by the Wm. I. Mann Company of Monrovia, California.

The choice of the rocks to be used was determined by qualities of homogeneity, fine grain and accessibility of the type locality. Two quarried rocks, one acid and one basic, belonging to the Southern California batholith complex, were selected. The specimens of each rock were taken from a single block which was cut into parallel prisms having the same orientation. The rocks were furnished by the firm of Thos. Holmes and Son, Pasadena.

2. Foster granodiorite. This fine-grained, light gray rock is probably identical with the Descanso granodiorite, named by W. J. Miller (1935). It has been quarried at least since 1889 and is commercially known as "Silver Gray Granite". The specimens used came from the quarry of the McGilvray, Raymond Corporation, about $1\frac{1}{2}$ miles NNW of Foster, San Diego Co., California. It occurs in massive ledges showing mainly horizontal

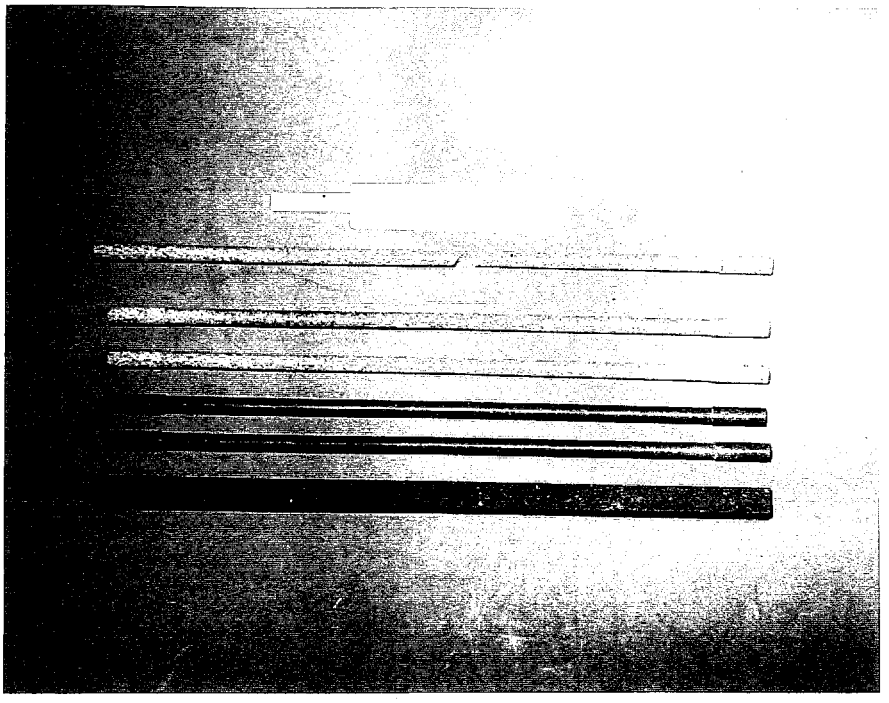

FIG. 11

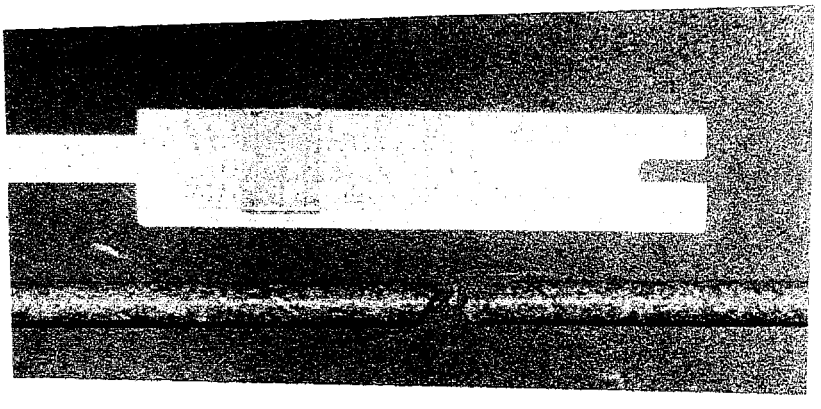

FIG. 12

UNSTRAINED

FIG. 13
FOSTER GRANODIORITE

STRAINED

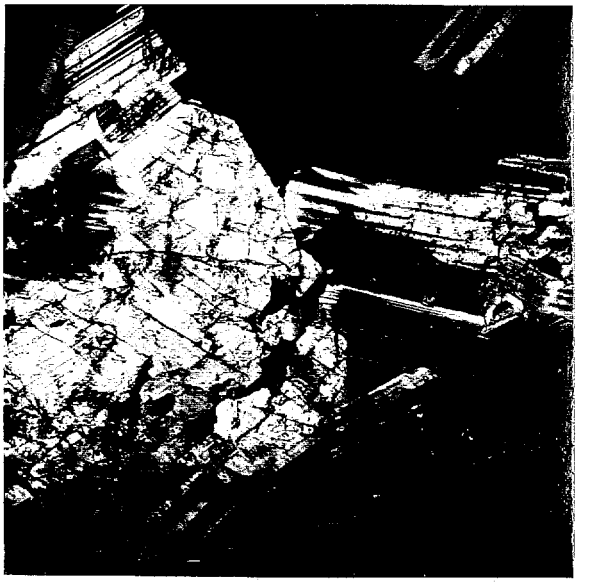

UNSTRAINED

FIG. 14
SAN MARCOS GABBRO

STRAINED

jointing. The rock may be termed leucogranodiorite because of the small amount of dark minerals present. The average diameter of grains is 0.5 mm for quartz and 0.3 mm for biotite.

A study of the thin section (fig. 13) yields the following composition:

Quartz (about 40%) showing wavy extinction.

Plagioclase Ab_{80} An_{20}, fairly altered to sericite, calcite and epidote.

Microcline.

Green and brown biotite, showing some chloritization.

Iron ore, very little apatite, very little sphene.

Formation of myrmekite is fairly abundant.

The structure is granular hypeutomorphic.

3. San Marcos Gabbro. This is a black medium-grained rock known commercially as "Black Diamond Granite". The type has been named and described by F. S. Miller (1937) and studied by Larsen (1948) and Hoppin and Norman (1950). The latter authors have also described briefly the Foster granodiorite.

The rock is a quartz-biotite-hornblende norite originally from the Ebony Black Diamond Granite Company quarry, located north of Escondido Creek, about 3 miles WSW of Escondido, San Diego County, California. It occurs in large residual boulders which are difficult to quarry because of absence of rift or grain.

The mineral composition is as follows (fig. 14):

Plagioclase (core Ab_{35} An_{65}, outer shell about $Ab_{40}An_{60}$) well developed tabular crystals, about 65% of rock.

Hornblende, formed at expense of augite and hypersthene.

Hypersthene and Augite.

Iron ore

Little quartz, associated with hornblende (less than 1%).

Little biotite, interstitial (less than 1%).

Small amounts of zircon and sphene.

The hornblende shows considerable chloritization.

The structure is granular hypeutomorphic. The grain size is 1-2 mm on the average.

A specimen of San Marcos quartz-biotite-norite collected less than a mile from the quarry was studied by F. S. Miller (1937) who obtained the following chemical analysis:

SiO_2	47.22
TiO_2	1.60
Al_2O_3	18.18
Fe_2O_3	6.14
FeO	7.80
MuO	.18
MgO	4.93
CaO	10.46
Na_2O	2.74
K_2O	.13
H_2O	.46
P_2O_5	--
S	.16
	100.00

Both the Foster granodiorite and the San Marcos gabbro

take a beautiful polish and are used mainly for monuments and ornamental facing.

4. Testing procedure. A total of 8 specimens of Foster granodiorite and 4 of San Marcos gabbro were tested in the torsion creep apparatus. For each specimen the direct creep deformation under torques from about 6000 gr-cm to failure, and the corresponding recovery creep for zero torque were recorded. The total duration of a combined creep and recovery test was one week or more.

The elastic modulus was calculated from the low torque tests whenever the elastic deflection was small enough to be recorded. For the larger torques there is always some uncertainty as to the exact beginning of the creep component. This is due to the fact that the creep rate in the vicinity of $t = 0$ becomes practically infinite, there being no clear break between the elastic and creep components of deformation. Thus the procedure of finding the boundary of zero creep often relies upon graphical interpolation.

The use of the logarithmic time scale makes it possible to obtain the true shape of the creep curve independently of the amount of deformation near the origin. The semi-logarithmic graph may later be used as an auxiliary in interpolation. Recovery tests mostly show rather clean breaks which allow exact reading of the initial recovery deformation.

The loads must be carefully lowered by hand in order to minimize dynamic effects. As a result, recording tends to be

erratic during the first 10 seconds of the test.

Experience with these departures from ideal testing evolved into the following test routine:

A. Specimen clamped in position.

B. Mirror clamped on specimen.

C. Light spot adjusted.

D. Red lights turned on; fresh record marked and slipped over drum.

E. Drum put in gear; light spot starts recording.

F. Loading yoke with attached weights carefully lowered into position.

G. Light spot (which may have wandered off the record) is adjusted back into recording position.

F. Red lights out.

This procedure has the advantage of recording the exact time of beginning of the test. The first few seconds of the test are lost, but experience shows that there is nothing to be gained by recording them. In any case the initial point must be gotten by interpolation. The determination by this method is always close and the error is not critical, since we are mainly interested in the creep rate and its variation with time and stress.

5. General results. The experimental data are given graphically on figs. 15 to 19 and at the end of this volume. A summary is given in Table I.

Semi-logarithmic plotting is found to be very convenient because of the tendency of the data to give straight alignments over practically the entire range of times. This is characteristic

of the behavior of many materials at low temperatures and low stresses.

The creep curves may deviate from the straight logarithmic line at small times and large times. A "sigmoidal" equation

$$s = a + b \log \frac{\alpha + t}{\beta + t} \tag{31}$$

could be used as a very close fit. However, it is seen that for practically all of the data it is quite sufficient to use the straight logarithmic form:

$$s = a + b \log t \ . \tag{32}$$

The tendency of some curves to become concave upwards at large times corresponds to a straightening out in the arithmetic plot, i.e. an approximation to constant creep rate. This is characteristic of the behavior at higher stresses and may indicate that the principle of superposition ceases to be valid.

In order to check this assumption, experiments were made on two copper rods of different diameter. The principle of superposition proved to be closely valid as long as the creep curve did not deviate substantially from Eq. (32). In the range of "constant creep rate" the creep rate increased faster than the stress (fig. 20).

Deviations from Eq. (32) at low times are to be expected. This is seen clearly if one puts $t = 0$. Then, from Eq. (32), $s = -\infty$ whereas one should have

TABLE I

SAMPLE #	APPLIED WEIGHT lbs	TORQUE kg-cm	SHEAR STRESS, kg/cm^2 surface	SHEAR STRESS, kg/cm^2 average	ELASTIC STRAIN AT SURFACE radians	CREEP RATE AT t = 1 in radians/minute DIRECT	CREEP RATE AT t = 1 in radians/minute RECOVERY
A. GRANODIORITE							
1	2	6.8	25.5	7.1	140	.1	.2
2	2½	8.5	31.8	8.8	170	(.7)	(.6)
3	3	10.2	38.2	10.6	-	4.0	-
4	3 3/4	12.8	47.8	13.2	-	5.2	2.9
5	5	17.0	63.7	17.6	-	5.8	-
6	6	20.4	71.4	19.8	-	8.1	4.2
7	11	37.5	140	38.8	-	20.0	failed
B. GABBRO							
1	3	10.2	38.2	10.6	85	.55	-
2	4	13.6	50.9	14.1	120	.8	.25
3	6	20.2	71.4	19.8	-	1.7	
4	11	37.5	140	38.8	-	1.5	

FIG 15 page 45

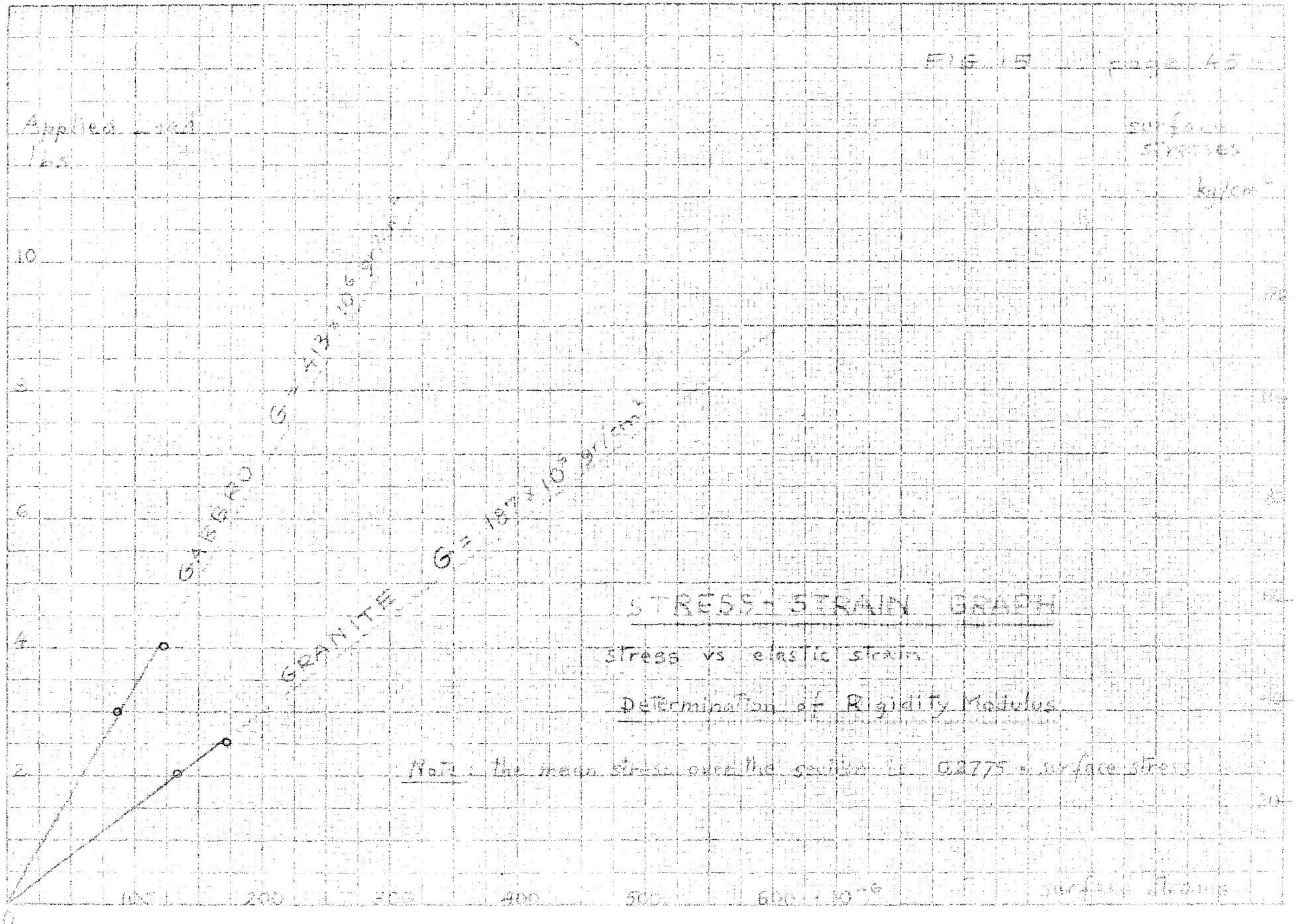

STRESS - STRAIN GRAPH

Stress vs elastic strain

Determination of Rigidity Modulus

Note : the mean stress over the section = 0.275 × surface stress

STRESS vs STRAIN RATE

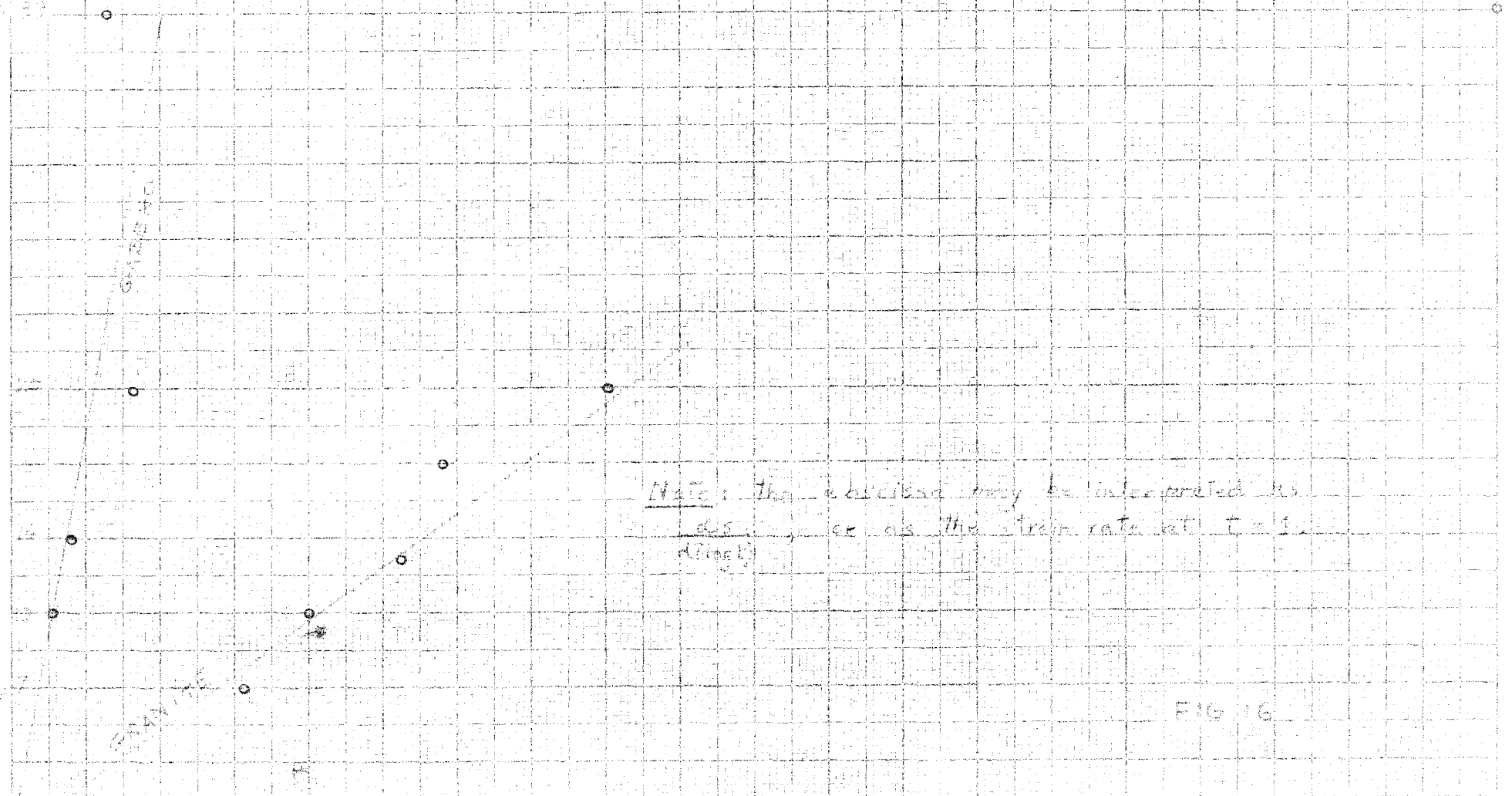

Note: the gradient may be interpreted as $\frac{d\sigma}{d(\log \dot{\varepsilon})}$, or as the stress rate at $t = 1$.

Fig. 6

FIG. 17

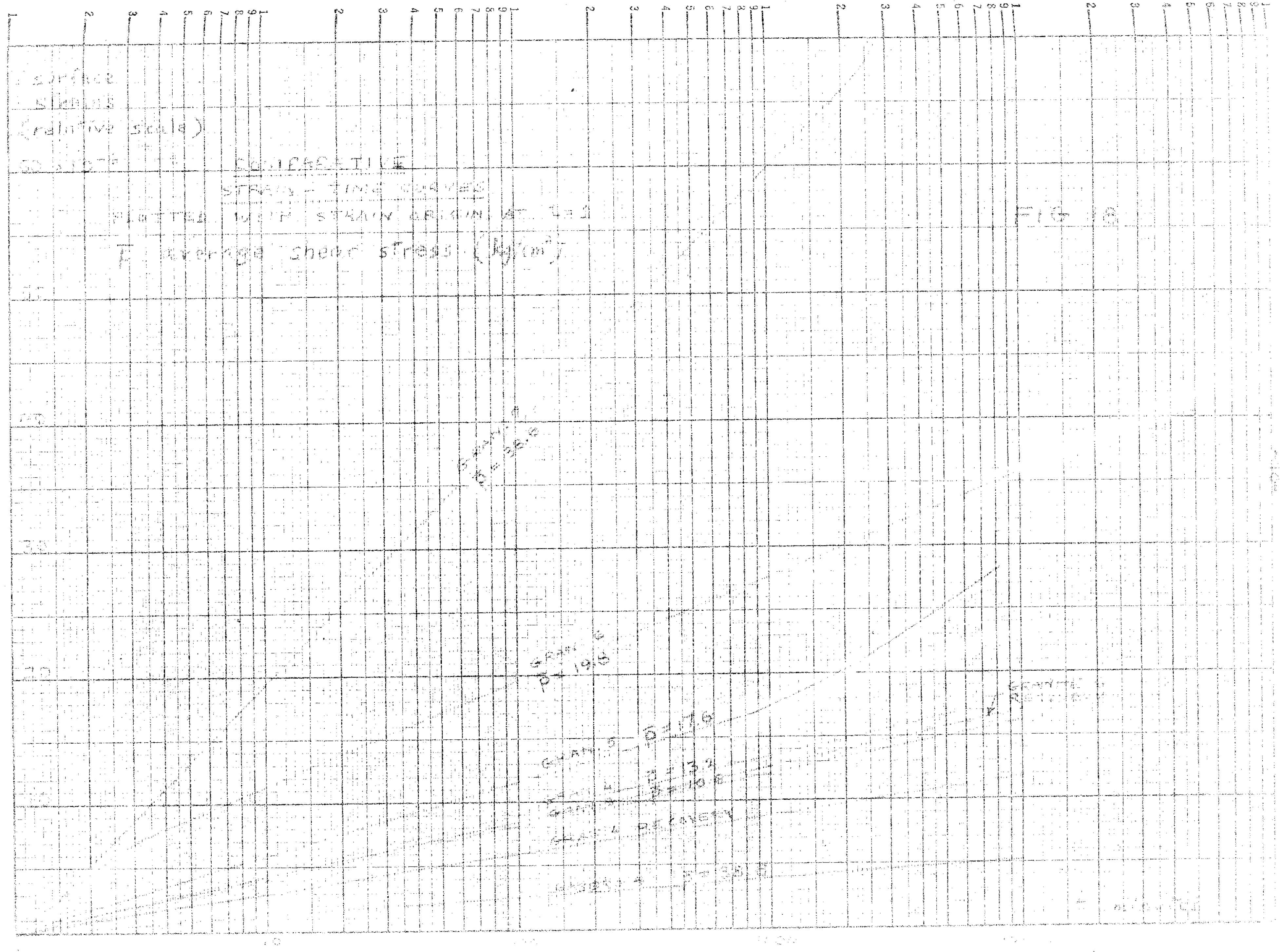
surface
strains
(relative scale)
COMPARATIVE
STRAIN - TIME CURVES
PLOTTED WITH STRAIN ORIGIN AT t=1
τ average shear stress (kg/cm²)
FIG 18
τ = 36.8
τ = 19.5
GRAN. 5
τ = 17.6
τ = 13.2
GRAN. 4 RECOVERY
GRANITE RECOVERY

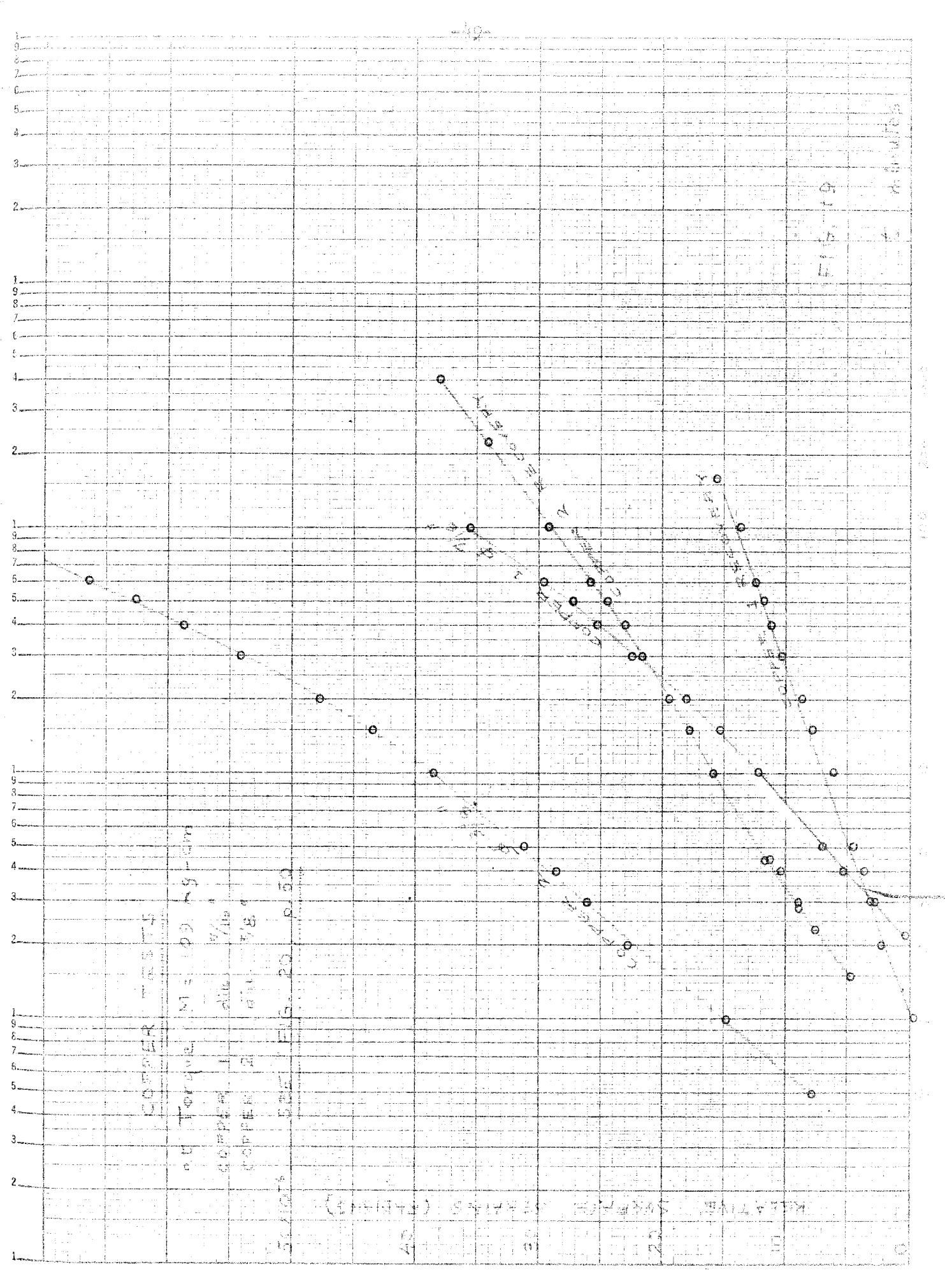

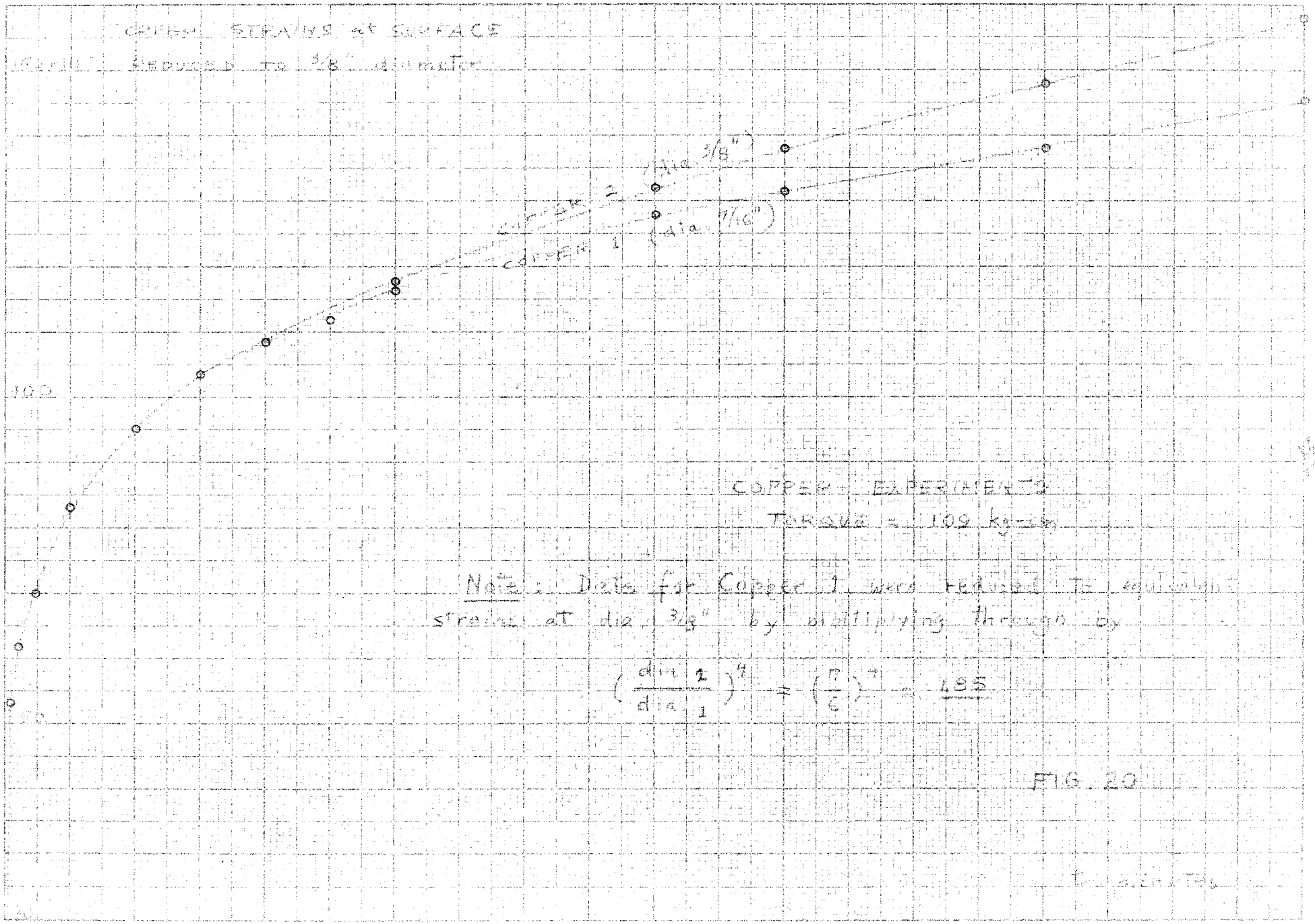

Note: Data for Copper 1 were reduced to equivalent stresses at dia 3/8" by multiplying through by

$$\left(\frac{\text{dia } 1}{\text{dia}_1}\right)^4 = \left(\frac{7}{6}\right)^4 = 1.85$$

FIG. 20

$$s = \frac{p}{E}$$

which is the elastic deformation. Thus Eq. (32) cannot be used for very small times. The discrepancy tends to increase with stress.

A plot of strain rate against stress (fig. 16) shows that the principle of superposition is valid over most of the range:

$$p \propto \dot{s} \quad . \tag{33}$$

The scattering seems to be due to lack of uniformity of samples; there is no systematic deviation from linearity.

At larger stresses one expects an increase of strains that is faster than linear. This effect is observed but it is not very large. Even near failure the strain rate is much nearer to linearity than to the logarithmic law:

$$p \propto \log \dot{s} \tag{34}$$

which is found in high-temperature creep of metals.

There were a few irregularities in the creep curves. The behavior of specimen Gran. 5 is not understood. Beginning at a rather low logarithmic rate it attains a constant rate near $t = 1000$ minutes. The creep recovery rates for the two first gabbro specimens were too low for accurate reading. Creep recovery curves for specimens Gran. 3 and 5 were lost due to failure of the light source.

The creep curve of Gran. 7 gives a remarkable example of brittle failure. The creep rate becomes slightly accelerated about two hours before rupture. The actual failure is quite sudden. The ruptured specimen is shown on fig. 12.

CHAPTER V

CONCLUSIONS

1. Creep Properties of Rocks. Under the conditions of the experiments the creep of the Foster granodiorite and San Marcos gabbro may be represented closely by an equation of the form:

$$s = p\,(a + b \log t) \qquad (35)$$

where the constants are given as follows:

	a	b
Foster granodiorite	59.4×10^{-10}	1.05×10^{-10}
San Marcos gabbro	24.7×10^{-10}	0.167×10^{-10}

In formula (35) s is in radians, p in gr/cm^2 and t in minutes.

The San Marcos gabbro is found to have considerably greater rigidity, creep resistance and brittleness than the Foster granodiorite. The ratio of the coefficients a is about the same as the inverse ratio of the rigidities:

$$\frac{G_{\text{gabbro}}}{G_{\text{granod}}} = 2.2\ ; \qquad \frac{a_{\text{granod}}}{a_{\text{gabbro}}} = 2.7\ .$$

Equation (35) is similar to the one found by Griggs (1939) for sedimentary and metamorphic rocks in compression. The linear relation between stress and strain is an expression of the finding that the rocks followed Boltzmann's principle of superposition (on the average). If rocks behave like other crystalline materials this condition should not be fulfilled at higher temperatures, due mainly to the appearance of phase changes and recrystallization processes.

2. Viscosity of Rocks. By differentiation of formula (35) one obtains:

$$\dot{s} = p \frac{b}{t} \tag{36}$$

indicating that the strain rate decreases linearly with time. Eventually the strain rate may reach a constant value $\dot{s}_c$; in this case we may write the viscosity of the rock:

$$\eta = \frac{\dot{s}_c}{p} \quad . \tag{37}$$

If the strain rate does not approach a constant value but decreases indefinitely according to (36), the viscosity η is infinite.

In practice η is not entirely independent of the stress. In the Foster granodiorite the viscosity was practically infinite at low stresses, but at least in two specimens subjected to higher stress a constant rate was approximated. In these cases the viscosity was of the order of $\eta = 3 \times 10^{15}$ poises. For the San Marcos gabbro the viscosity appears to be considerably higher.

There is a possibility of obtaining the value of η without the use of constant-rate approximations. The method was given by Sips (1950). If we have the creep equation of any linear solid (Eq. (12)):

$$s = \frac{p}{G} \left[1 + \phi(t) \right] \tag{38}$$

we can obtain the relaxation function $\psi(t)$ which is analogous to $\phi(t)$ for the constant-strain case. The analytical relation may be shown to be:

$$L(\dot{\psi}) = \frac{L(\dot{\phi})}{1+L(\dot{\phi})} \tag{39}$$

where L represents the Laplace transform operator.

Since our logarithmic formula cannot be used in the form (38) on account of its behavior near $t = 0$, we may approximate it by a curve of the type:

$$s = \frac{p}{G}(1 + At^n) \tag{40}$$

whence

$$\phi(t) = At^n \quad . \tag{41}$$

According to Sips, the application of (39) yields:

$$\psi(t) = En(x) - 1 \tag{42}$$

where

$$x = -A\ \Gamma(n+1)\ t^n \tag{43}$$

and

$$En(x) = 1 + \frac{x}{\Gamma(n+1)} + \frac{x^2}{\Gamma(2n+1)} + \ldots . \tag{44}$$

is the Mittag-Leffler function.

Once the value of $\psi(t)$ is known, one may calculate the viscosity by means of the formula given in Chapter VII (Eq. 75):

$$\eta = G \int_0^\infty \left[1 - \psi(t)\right]\ dt\ . \tag{45}$$

The Mittag-Leffler function has not been tabulated. The relaxation function may be calculated by points, using Eq. (42) through (44), although one may be doubtful about the accuracy of the result in view of the approximate nature of our assumption, Eq. (40).

3. Comparison with Michelson equation. The complete form of the Michelson equation, Eq. (26), may be fitted to most of the creep or recovery curves without too much strain.

In general, however, the result of the comparison with the Michelson formula is negative. The characteristic kernel of the equation $(1 - e^{-\alpha \sqrt{t}})$ has not been found experimentally. In particular the recovery tests were conclusive in this respect.

Additional tests on copper (fig. 20) and nylon (fig. 21) equally failed to show any similarity of behavior with the Michelson kernel. It is definitely inadequate to describe the experimental data herein.

4. Geological inferences. Igneous rocks have been made to creep experimentally at low stresses and ordinary surface temperatures. This fact may not be surprising in itself, but if one considers igneous rocks as the constituents of the earth's crust, it may be of importance to analyze the possible implications in terms of geological processes.

The earth's crust is capable of supporting the weight of mountain massifs up to 10 km high without any observable yielding.

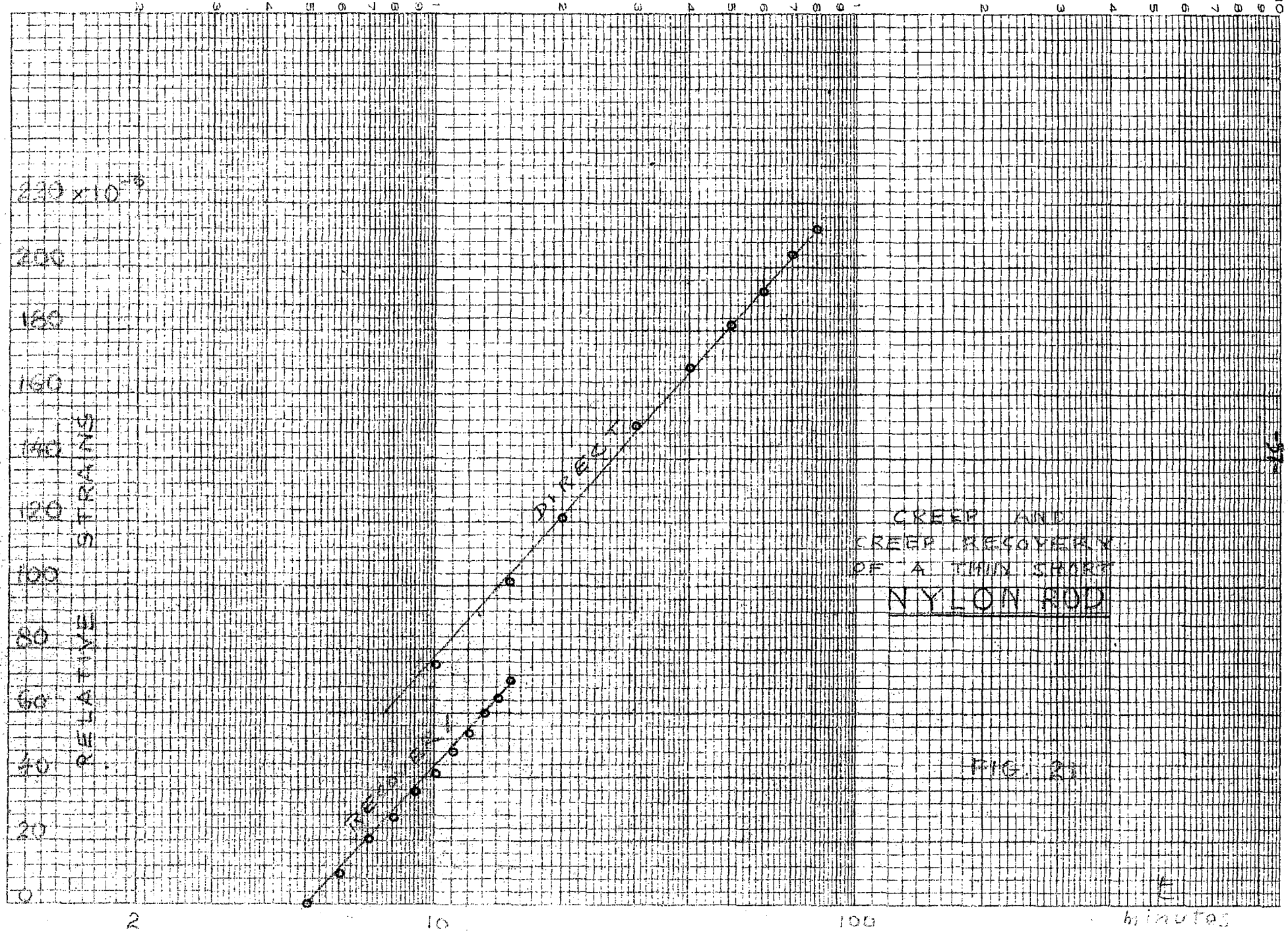
220 x 10⁻⁶
200
180
160
140
120
100
80
60
40
20
0
2
10
100
minutes
CREEP AND
CREEP RECOVERY
OF A THIN SHEET
NYLON ROD
FIG. 22

It must therefore possess an appreciable strength. The question arises as to whether this geologic fact can be reconciled with the experimental evidence of rock creep at ordinary temperature and stresses.

It should be noted firstly that the presence of low-temperature creep in rocks does not imply lack of strength, any more than it does in steel or other metals. In fact, below a certain stress threshold the creep is logarithmic in form and soon reaches a rate so slow that it is negligible. If this were otherwise no structures of any kind could ever be built, since creep in a universal feature in all construction materials.

Thus the concept of a stress threshold ("strength", "yield point", etc.) is indispensable, although it is important to remember its relativity with respect to the span of time one wishes to consider. Creep deformation, even if at a diminishing rate, may become important if the time is long enough.

Whatever the strength of the crust at depth may be, it appears that the continued activity of orogenic forces is necessary to explain why the continents have not been completely levelled off by the combined agents of creep and erosion. An attempt to reach an indirect conclusion as to the rate of creep deformation in the crust, will be made in the Second Part of this thesis.

The semi-logarithmic creep law which has emerged from the present series of tests has also been found by Benioff (1951) in aftershock strain sequences. However, this kind of deformation is so common in creep that a correlation is not necessarily

established.

The fact that rocks at room temperature exhibit certain similarities to polycrystalline metals should not lead to an extrapolation following the pattern known from metallurgy. Rocks are not homogeneous materials but an agglomeration of grains of different minerals, each of which has its own melting point, elasticity and creep properties.

It is possible, however, that in large-scale deformations the crust behaves more or less like a linear solid. The similarity between aftershock sequences and laboratory creep curves makes it seem plausible, at least, to try out such an assumption as a first approximation.

An attempt to apply this line of reasoning to the problem of aftershock generation, will be made in the following chapters.

PART TWO

CHAPTER VI

THE MECHANISM OF EARTHQUAKE GENERATION

1. Fundamentals of Benioff Theory. The discovery by Benioff (1951) of a general strain-time law which applies to aftershocks, has opened the possibility of a quantitative approach to the problem of earthquake generation.

The essence of the discovery is the following: whenever crustal strains corresponding to an aftershock sequence are plotted against time in a cumulative diagram, the result bears a striking resemblance to a creep recovery curve. On the basis of this analogy, Benioff formulates the hypothesis that aftershocks are generated by creep recovery (or elastic afterworking) of the strained rock in the vicinity of the earthquake fault. A series of papers developing this idea (Benioff, 1951+) constitute the basis for a physical theory of earthquake generation.

The strains freed by each earthquake are related to the seismic wave energy released, by means of the equation:

$$E = \tfrac{1}{2} q\, G\, V\, s^2 \qquad (46)$$

V is the column of rock assumed under uniform strain s at the instant preceding the earthquake. The elastic constant G is unspecified and its nature depends upon the prevailing type of deformation. An "efficiency factor" q measures the relative amount of elastic strain energy converted into seismic waves.

The assumptions and simplifications implied in Eq. (46) will not be discussed in detail. It should be mentioned that in any case, the quantities involved are known to the nearest order of

magnitude only. For the same reason the factor q may be taken as unity, an assumption which is probably not too far from the truth (H. Benioff, oral communication).

The energy E is computed from the new (1955) Gutenberg-Richter energy relation:

$$\log E = 9.1 + 1.75\, M + \log (9-M) \qquad (47)$$

in which M is the earthquake magnitude as defined by Richter (1935).

It is found that the aftershock graphs can be divided into two kinds:

a) Logarithmically increasing after the equation

$$s = a + b \log t \qquad (48)$$

b) Rapidly increasing and levelling off abruptly, according to the Michelson equation (see Chapter II, p. 19):

$$s = C_1 + C_2 (1 - e^{-a\sqrt{t}}) . \qquad (49)$$

Some aftershock sequences are discontinuous or composite, mainly with abrupt transitions from Eq. (48) into (49). The presence of the Michelson equation is interpreted as a possible predominance of shear over compression.

In the Kern County sequence (Benioff, 1955) it was discovered that the aftershocks with epicenters in the region SE to the main fault plotted according to Eq. (48) while those to the NW began more than a day late and followed the Michelson form

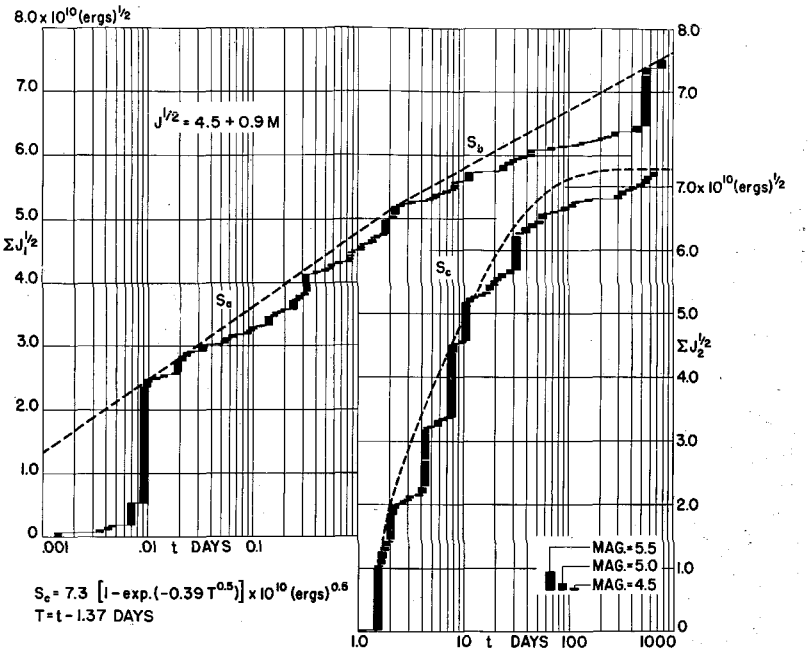

KERN COUNTY SEQUENCE
ELASTIC STRAIN REBOUND CHARACTERISTICS

SEPT., 1954 H. BENIOFF CURVES 177 & 178

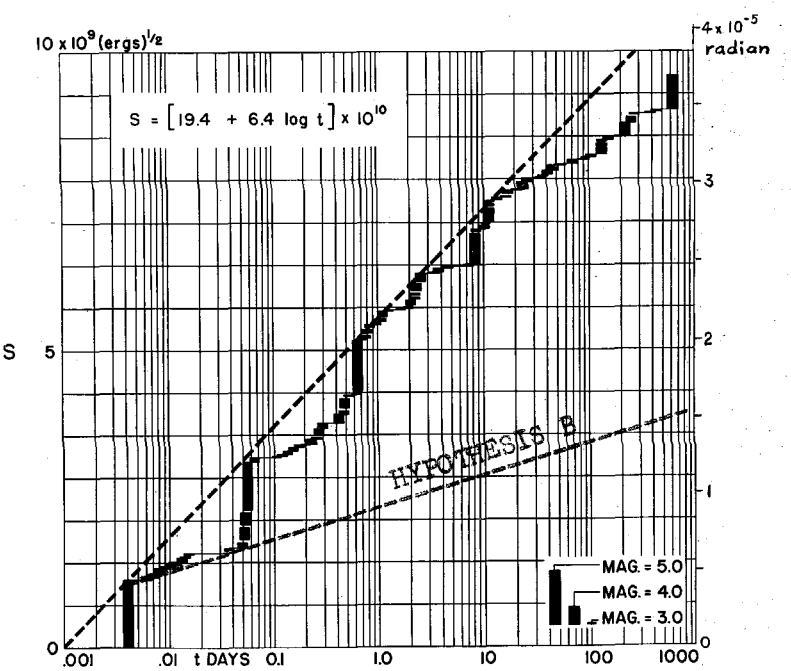

MANIX EARTHQUAKE AFTERSHOCK SEQUENCE

AUG. 1954 H. BENIOFF

FIG. 22

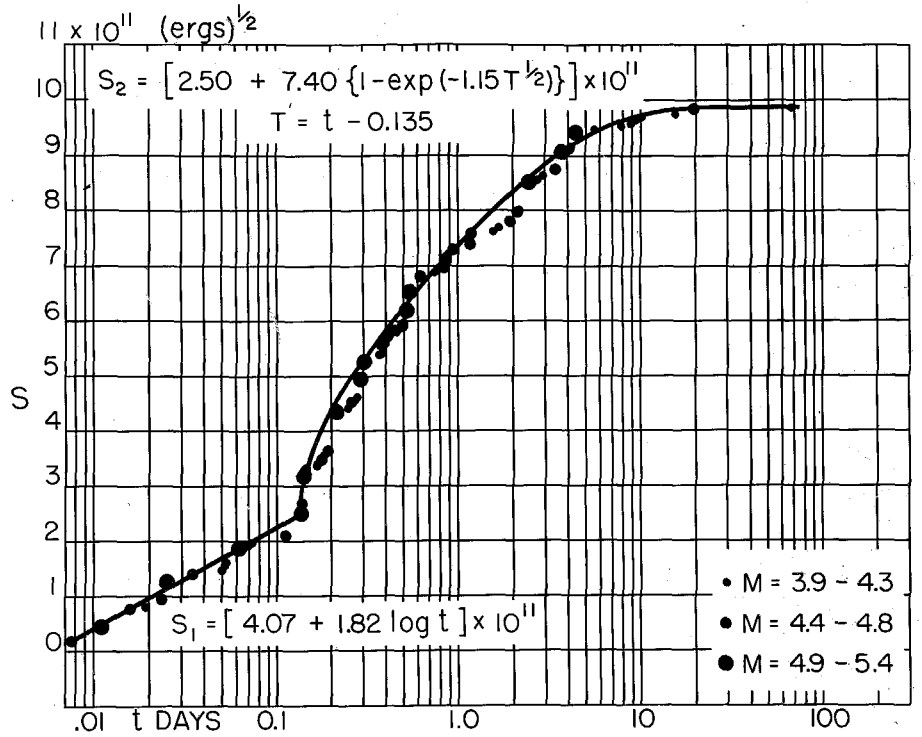

LONG BEACH EARTHQUAKE AFTERSHOCK SEQENCE

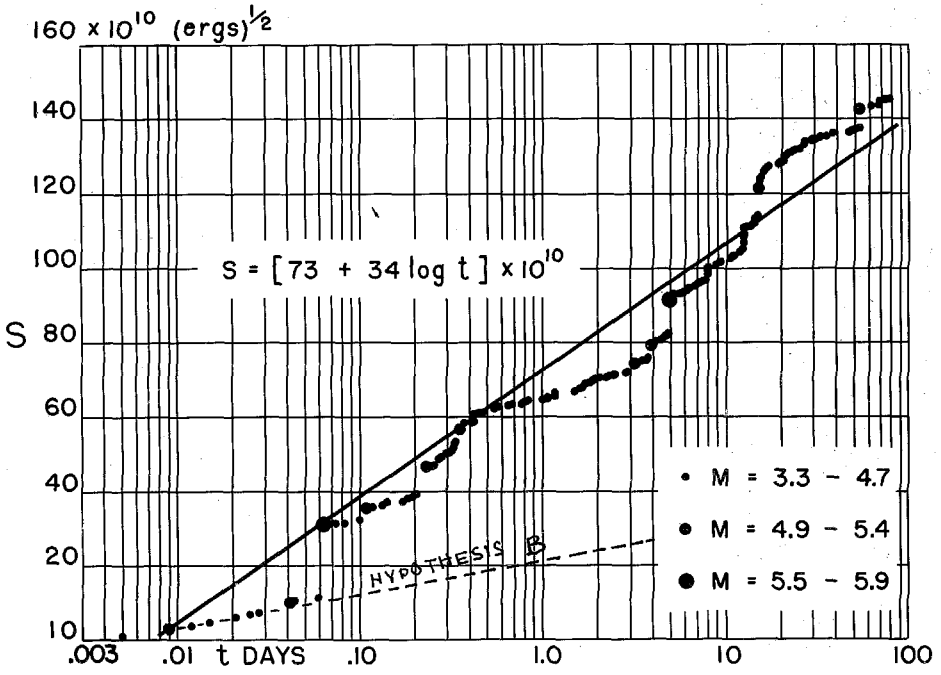

1932 DEC. 20 NEVADA EARTHQUAKE AFTERSHOCK SEQUENCE

FIG. 23

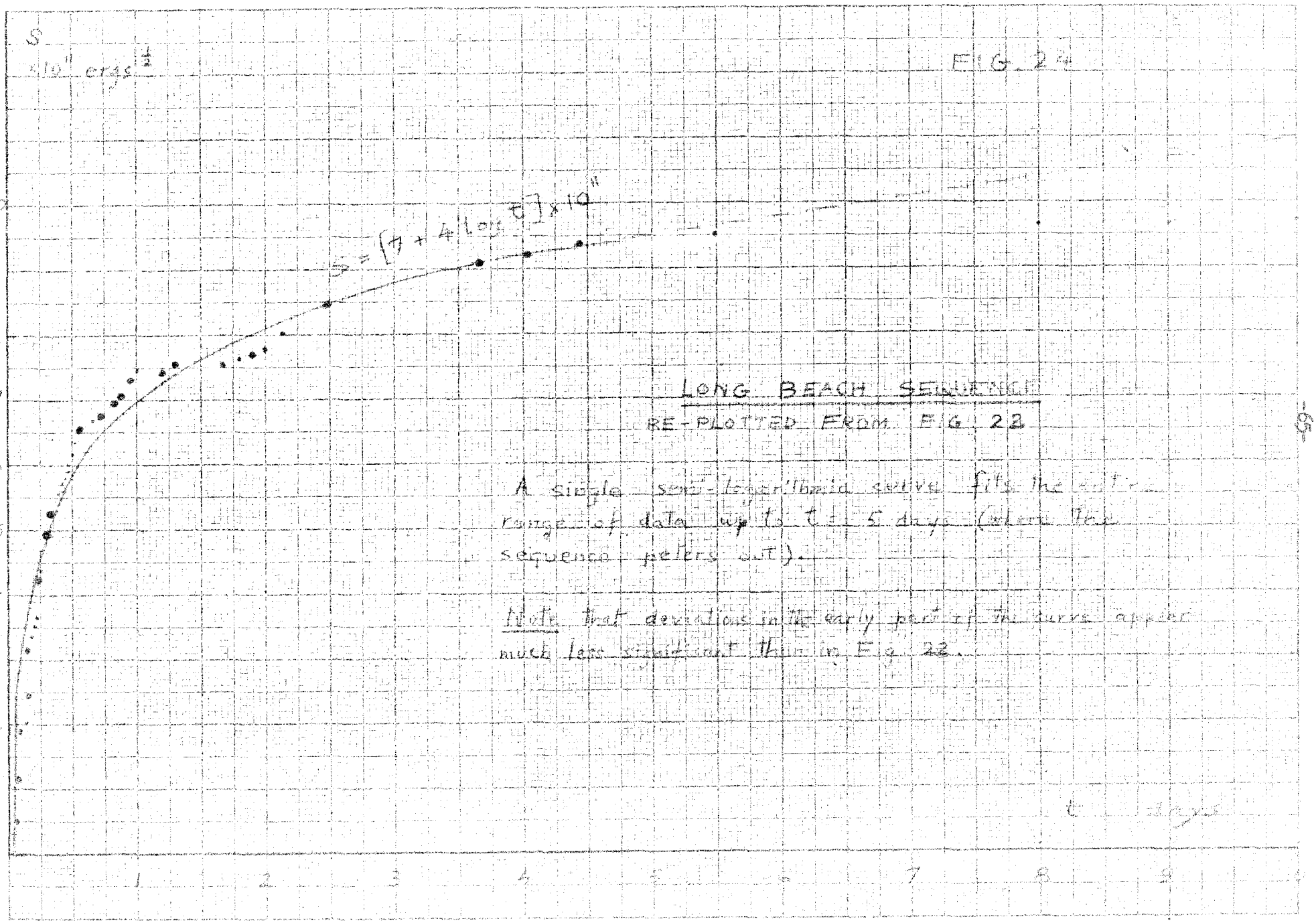

FIG. 24

LONG BEACH SEQUENCE
RE-PLOTTED FROM FIG. 22

A single semi-logarithmic curve fits the entire range of data up to $t = 5$ days (where the sequence peters out).

Note that deviations in the early part of the curve appear much less significant than in Fig. 22.

(Eq. (49)). Had the sequence been plotted as a whole, without discrimination of epicenters, it would have given a discontinuous, composite graph similar to the Long Beach sequence (fig. 22). In general it is found that the Michelson type of sequence is composed of a small number of larger shocks, while the logarithmic type features a larger amount of smaller shocks (Benioff, ibid.).

2. Properties of aftershock sequences. The occurrence of composite aftershock sequences and the peculiar aftershock distribution found in the Kern County sequence, pose a problem of some conceptual difficulty. Explanations in terms of random or secondary effects appear out of the question. On the contrary, it is likely that some basic mechanism is involved.

Figures 22, 23 reproduce several aftershock sequences by permission of Professor Benioff. In order to evaluate these sequences we shall begin by dealing with some objections that might possibly be raised.

In all these graphs the strains are cumulative; therefore no negative slopes can occur. It may be argued that such a plot can always be fitted to an arbitrarily small number of straight or curved segments.

Moreover, it is observed that the fits are not always very close. This is to be expected in view of the uncertainties of magnitude and energy involved in the processing of the data.

Finally, the curves of best fit are not representative of the average trend but rather of the trend of maxima of the data.

It is clear that one has to take the maxima because they represent the actual creep rebound which is interrupted by periods of relative quiet and strain accumulation. However, this could introduce a small factor of arbitrariness in the process of selecting the maxima to be used for fitting.

All this being said, let us consider the curves in more detail. Let us also imagine the data transferred onto a simple arithmetic graph (fig. 24), which has the property of smoothing out discontinuities that occur in the early part of the sequence. Then even such composite Michelson-type sequences as the Long Beach may be fitted rather smoothly by a logarithmic curve. In fact, a general semi-logarithmic trend seems to be the most conspicuous common feature in all the graphs.

No random distribution of aftershocks will give a semi-logarithmic sequence. If we imagine all earthquakes in a given sequence mixed together and "drawn" at random, the resulting distribution will be nearly linear. The only way of obtaining a semi-logarithmic distribution is by drawing the items at a logarithmic rate. In the physical picture this "rate" corresponds to the mechanism which governs the generation of aftershocks. Thus one may see in a simplified way how the Benioff aftershock sequences must be related to the seismic mechanism.

The Kern County sequence shows that this mechanism may be different on either side of the fault. It seems plausible to

assume that the difference is due to distinct subsidiary faulting patterns. For example, one of the blocks may be closely fractured and its creep energy be released in a swarm of small shocks; whereas the opposite block may contain relatively few faults which release the energy in greater "lumps" and possibly with some delay within the sequence. In the latter case, the strain release pattern becomes more complex because of secondary systems of stress concentration, the dimensions of which are not negligible in relation to the total earthquake zone. One may expect the resulting sequence to deviate from any simple strain curve, so that the Michelson equation would not be needed as an explanation (except perhaps in a descriptive way). It may be noted from the Kern County sequence that the amount of strain released is the same on either side of the fault; this shows that the difference lies only in the form and not the amount of strain release.

3. Two hypotheses. A direct quantitative interpretation of the aftershock theory is difficult because of our imperfect knowledge of the properties of the earth's crust. In the following discussion this objection is always kept in mind. Our purpose is to derive a value for the viscosity of the crust from the data given in the aftershock sequences. This problem would become solvable on the basis of some quantitative theory relating aftershock sequences to the creep properties of the material. In the absence of such a detailed theory we may resort to working hypotheses, two of which shall be considered here.

Hypothesis A. The aftershock sequence represents the pure creep recovery of the rock. This is the concept originally developed by Benioff. It implies that the entire elastic energy of the rock is released in the main earthquake, and that the entire aftershock energy is due to creep strain.

Hypothesis B. The aftershock sequence represents a succession of creep recovery patterns alternating with jumps of residual elastic recovery in the form of larger aftershocks. If the residual elastic energy is taken as zero one obtains the case of Hypothesis A, which thus may be considered a special case of B. No fundamental opposition exists between the two hypotheses.

A reason for advancing Hypothesis B may be found in the fact that some sequences have such a high ratio of aftershock strain to main earthquake strain that creep recovery alone can hardly account for it. Thus one may be led to conceive the possibility of some amount of elastic energy remaining stored in the rock after the earthquake, and being released gradually as aftershocks.

The question is raised as to what part of such a sequence can be attributed to creep recovery. There is no evident answer to this problem from first principles. However, many logarithmic aftershock graphs show a peculiar step-like structure not unlike that of a laboratory creep recovery curve obtained by successive decrements of load (Fig. 22). We shall assume tentatively that the slope of these steps (which appears to be fairly constant) gives a measure of the true creep rate in Hypothesis B.

Such a delay in elastic strain release is not the only

mechanism which might reduce the creep rate from the value originally expected by Hypothesis A. Especially in a large earthquake, the shock may be the prelude to a regional redistribution of stresses involving some transfer of elastic energy in the direction of the seismic zone. It will be shown, however, that Hypothesis A gives a sufficiently good approximation for the kind of computation attempted here.

4. Volumes and Strains in the Seismic Zone. The volume V of strained rock is an essential quantity in our computations. Its magnitude has been discussed and some agreement reached in spite of widely different initial assumptions.

Bullen (1955) finds a minimum $V = 6 \times 10^{19}$ cm^3 for an earthquake of magnitude 8.6. Benioff (1955) calculates that the volume involved in the Kern County aftershock sequence was about 7.6×10^{19} cm^3.

Geodetical measurements across the San Andreas fault show that the two fault blocks are moving at the rate of 2 inches per year relatively to each other. The region of measurable strains is confined to a 5 mile wide belt on each side of the fault. The same order of magnitude was found in the measurements of the extent of displacements after the San Francisco earthquake of 1906. Benioff (1955) has calculated that the rigidity G in the strained belt must be about nine times smaller than in the surrounding country rock; this difference may be produced by a system of fractures in the strained zone.

The rigidity of granite fluctuates about 6×10^{11} dynes/cm^2. In this thesis we shall assume $G = 10^{11}$ dynes/cm^2 for the strained zone, which will be about the right order of magnitude.

5. Two rough checks. The rate of strain release in the crust (as evidenced by great shallow earthquakes) was found to be approximately constant (Benioff, 1951b). If all non-Pacific earthquakes are excluded, the graph is still linear (fig. 25). The data comprise all earthquakes of magnitude 7-3/4 and over since 1904, computed with the new magnitude-energy equation, Eq. (47). From this graph it appears that the annual release of shallow energy in the Circum-Pacific belt is of the order of 25×10^{22} ergs/year. From Gutenberg and Richter (Seismicity, p. 22, 2nd Ed.) one finds that the California-Nevada region accounts for about 2.8% of this activity, say:

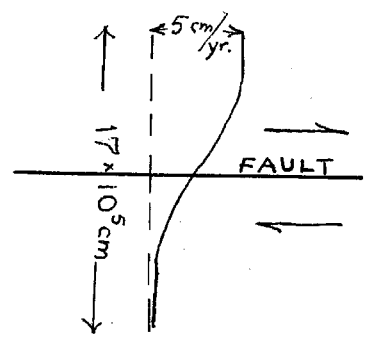

FIG. 26

$$E = 7 \times 10^{21} \text{ ergs/year} .$$

Assume for a moment that the entire strain energy of the region is concentrated in the 10-mile wide strip along the San Andreas fault, which is about 800 km long. If the depth of the strain zone extends to the Mohorovicic discontinuity the volume of the zone is:

$$V = 800 \times 17 \times 35 \times 10^{15} \text{ cm}^3 = 4.7 \times 10^{20} \text{ cm}^3$$

and from Eq. (46):

$$s = \sqrt{\frac{7 \times 10^{21} \times 2}{10^{11} \times 4.7 \times 10^{20}}} = 1.7 \times 10^{-5} \text{ radians per year}$$

FIG 25

CIRCUM-PACIFIC EARTHQUAKES

magnitude 7¾ and over

CUMULATIVE SQUARE ROOTS OF THE ENERGY

computed from Gutenberg & Richter, Seismicity, 2nd Ed.

with the magnitude-energy equation (1955):

$$\log E = 9.1 + 1.75M + \log(9-M)$$

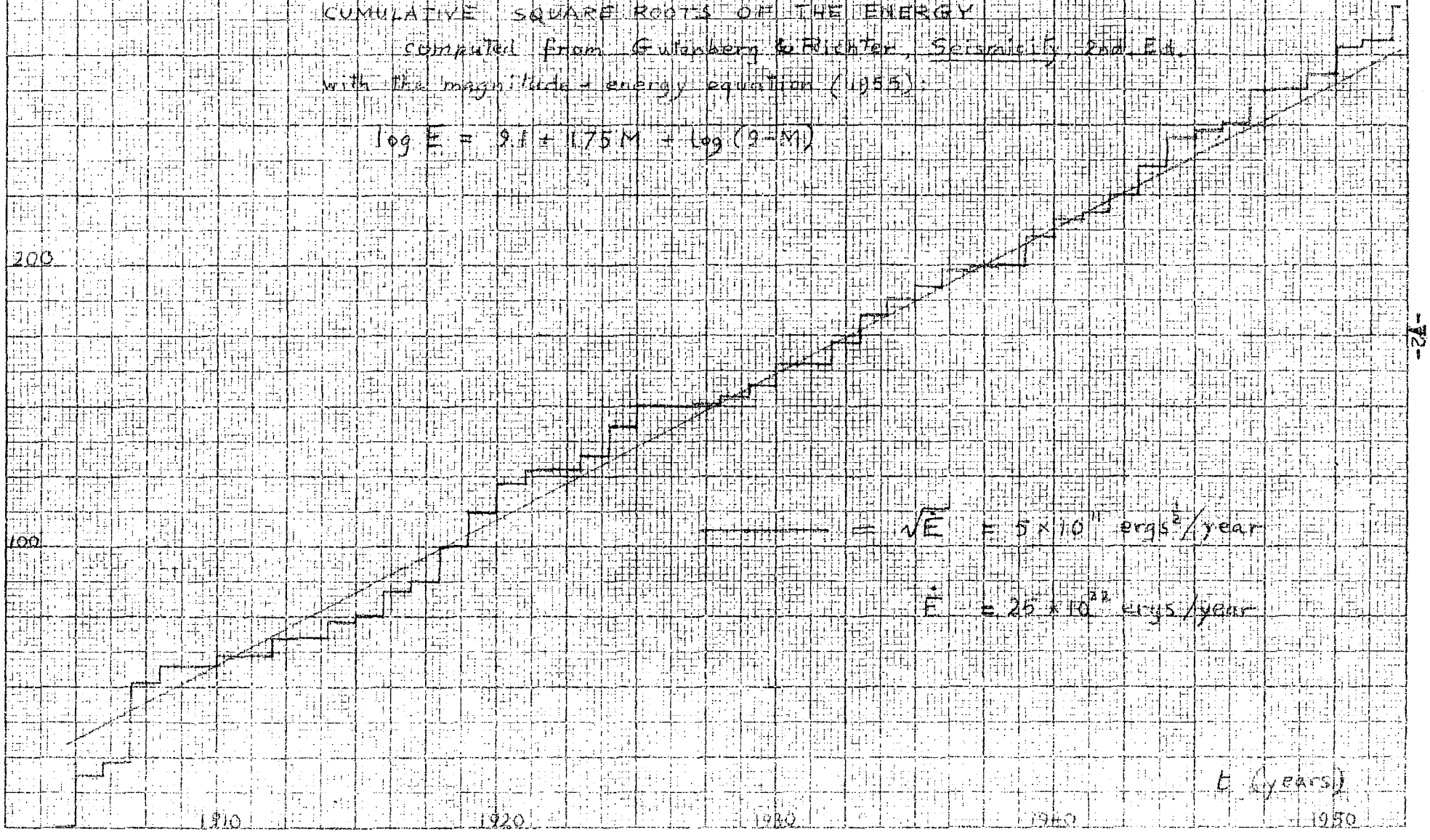

The measured strain across the fault corresponds to a displacement of 2 inches per year, or (fig. 26):

$$s = 0.3 \times 10^{-5} \text{ radians per year .}$$

Comparing both values of the strain it is found that they are only half an order of magnitude apart. Moreover, the discrepancy is in the direction to be expected from our assumption that the entire seismicity of the California-Nevada region is concentrated along the San Andreas fault. A second check can be made as follows: From Eq. (47) the energy released by an earthquake of magnitude 7 is:

$$E = 6 \times 10^{21} \text{ ergs .}$$

In the Southern California region it takes about 11 years to produce an earthquake of this size (Gutenberg and Richter, Seismicity, p. 18, 2nd Ed.).

From the previous check we take the average strain accumulation to be roughly 10^{-5} radians per year, or 11×10^{-5} radians for an earthquake of magnitude 7. Introducing these values into Eq. (46) and solving for the volume we find:

$$V = \frac{6 \times 10^{21} \times 2}{121 \times 10^{-10} \times 10^{11}} = 10^{19} \text{ cm}^3 .$$

The value agrees rather well with Benioff's estimate of 7.6×10^{19} cm^3 for the Kern County active zone, if one considers that the Kern County earthquake was of magnitude 7.6.

CHAPTER VII

DERIVATION OF THE RELAXATION FUNCTION

In the preceding Chapter we have evaluated and summarily checked the order of magnitude of the constants involved in the aftershock problem. The present Chapter is concerned with establishing a mathematical formulation of this problem.

It has been shown (Part I) that Boltzmann's Principle is applicable to igneous rocks under certain laboratory conditions. The following discussion assumes that this behavior may, in first approximation, be extended to the earth's crust and particularly, to the material of the strained zone in which the aftershocks occur.

The most general case of such a material can be represented by a rheological model (Fig. 27), having an arbitrarily large number of spring and dashpot elements connected in parallel. Our treatment of this model is based upon work by Zener (1946), Alfrey (1945), Simha (1942), Gross (1947) and particularly by Sips (1950), whose method will be followed closely.

Let each element of our model (Fig. 27) be composed by a spring of elastic constant α and a dashpot of viscosity constant η.

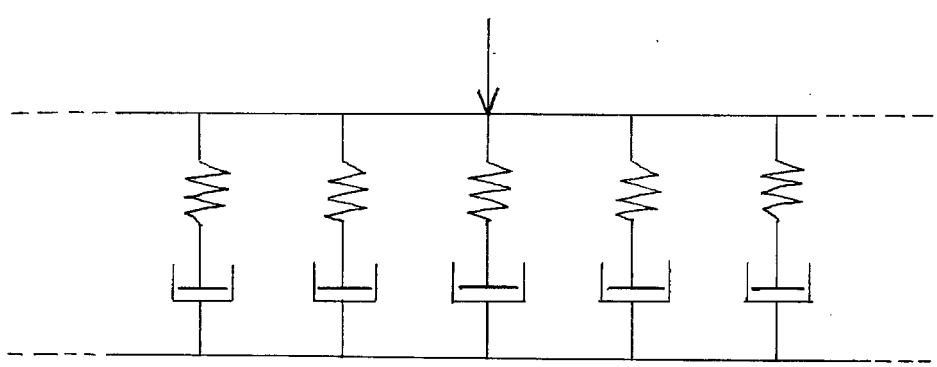

Fig. 27

The stress-strain relation for this element will be (cf. Eq. (10), p. 9):

$$\frac{ds}{dt} = \frac{1}{a}\frac{dp}{dt} + \frac{1}{\eta}\,p \qquad . \qquad (50)$$

Integrating and putting $p(0) = 0$ we obtain:

$$p = a\int_0^t e^{-k(t-\tau)}\,\dot{s}(\tau)d\tau \qquad (51)$$

where $k = \frac{a}{\eta}$.

In order to describe the model we may introduce a density distribution function $N_1(a,k)$ such that $N_1(a,k)$ such that $N_1(a,k)da dk$ is the density of elements whose constants have values between a and $(a + da)$, and k and $(k + dk)$. In this context the word "density" is taken relatively to the total number of elements, so that we have:

$$\int_0^A \int_0^K N_1(a,k)da\,dk = 1 \qquad (52)$$

where A and K are the upper limiting values of a and k. The total stress on the model may now be written:

$$p(t) = \int_0^A \int_0^K \left[N_1(a,k)\,a \int_0^t e^{-k(t-\tau)}\,\dot{s}(\tau)\,d\tau \right] da dk \qquad , \qquad (53)$$

it being understood that $N_1(ak) \equiv 0$ for all $a > A$ and $k > K$. Let us now define a function

$$N(k) = \int_0^A a\,N_1(ak)da \qquad . \qquad (54)$$

We may write Eq. (53) in the following form:

$$p(t) = \int_0^t \dot{s}(\tau) \left[\int_0^K N(k)\,e^{-k(t-\tau)}\,dk \right] d\tau \qquad . \qquad (55)$$

Let now a strain Δs be imposed upon the material in a very short time Δt beginning at $t = 0$. Then:

$$\dot{s} = \frac{\Delta s}{\Delta t} \quad . \tag{56}$$

If the sample is constrained to remain under the same deformation Δs we may write the stress relaxation from Eq. (55):

$$p(t) = \frac{\Delta s}{\Delta t} \int_0^{\Delta t} d\tau \int_0^K N(k)\, e^{-k(t-\tau)}\, dk + \int_{\Delta k}^t 0 \left[\int_0^K N(k) e^{-k(t-\tau)} dk \right] d\tau \quad . \tag{57}$$

Beyond Δt the strain rate is zero and therefore the integral vanishes in that region. Carrying out the integration:

$$p(t) = \frac{\Delta s}{\Delta t} \int_0^K \frac{N(k) e^{-kt}}{k} \left(e^{k\Delta t} - 1\right) dk \quad . \tag{58}$$

The term in parentheses is equal to $k\Delta t$ plus higher-order terms which can be neglected. Thus:

$$p(t) = \Delta s \int_0^K N(k)\, e^{-kt}\, dk \quad . \tag{59}$$

At time Δt this expression tends to

$$p(\Delta t) \approx \Delta s \int_0^K N(k)\, dk \quad . \tag{60}$$

Since the deformation is approximately instantaneous it may be expressed by means of Hooke's Law:

$$p(\Delta t) = G\, \Delta s \quad . \tag{61}$$

Instead of the rigidity G any other elastic constant may equally well be used. Substituting back into (60):

$$G = \int_0^K N(k)\, dk \quad . \tag{62}$$

Dividing Eq. (59) by Eq. (62):

$$p(t) = G\Delta s \frac{\int_0^K N(k) e^{-kt} dk}{\int_0^K N(k)\, dk} \quad . \tag{63}$$

It is convenient to define a "relaxation function" $\psi(t)$ such that

$$\psi(t) = 1 - \frac{\int_0^K N(k) e^{-kt} dk}{\int_0^K N(k) dk} \quad . \tag{64}$$

Then Eq. (63) can be written in the familiar form:

$$p(t) = G\Delta s \left[1 - \psi(t) \right] \tag{65}$$

which defines the stress relaxation under a constant strain Δs.

Let there be additional displacements Δs_1, Δs_2, ... at times t_1, t_2, ..., Eq. (65) then becomes:

$$p(t) = G \sum_{i=0}^{n} \Delta s_i \left[1 - \psi(t - t_i) \right] \quad . \tag{66}$$

Passing to the limit of continuous deformation:

$$p(t) = G \int_0^t \dot{s}(\tau) \left[1 - \psi(t-\tau) \right] d\tau \quad . \tag{67}$$

In the case of earthquake strain accumulation at constant rate U this equation becomes:

$$p(t) = GU \left[t - \int_0^t \psi(t-\tau)\ d\tau \right] \quad . \tag{68}$$

In order to represent the sequence of events during one cycle of aftershock generation we assume the origin of stress and strain at t = 0. If the main earthquake occurs at time T and any subsequent accumulation of stress is neglected, we may write:

$$0 < t < T-\varepsilon \qquad s(t) = Ut$$

$$t = T \qquad -\Delta s = UT - s(T+\varepsilon)$$

$$t > T \qquad s(t) \text{ given; } p(t) = 0$$

This sequence is represented graphically on Fig. 28 (upper part). For $t > T$ the integral (67) may be written in three steps:

$$0 = U\left[T - \int_0^T \psi(t-\tau)d\tau\right] - \left[UT-s(T)\right]\left[1-\psi(t-T)\right] + \int_T^t s(\tau)\left[1-\psi(t-\tau)\right]d\tau \quad . \qquad (70)$$

As the aftershock function s(t) is a datum and the strain p is eliminated, it is possible by Eq. (70) to find the relaxation function $\psi(t)$ which represents the creep characteristics of the material.

I am indebted to Professor A. Erdelyi for suggesting the solution to Eq. (70). Let us put:

$$\int_0^t \psi(\tau)\, d\tau = \Psi(t) \quad . \qquad (71)$$

If we substitute:

$$t - \tau = u \quad , \qquad (72)$$

the first integral in (70) can be written:

$$\int_0^T \psi(t-\tau)\, d\tau = -\int_t^{t-T} \psi(u)\, du = -\Psi(t-T) + \Psi(t) \quad . \qquad (73)$$

Substituting into Eq. (70) and rearranging we obtain finally:

$$\Psi(t) = \frac{s(t)}{U} + \Psi(t-T) + \dot{\Psi}(t-T)\left[T - \frac{s(T)}{U}\right] - \frac{1}{U}\int_{T}^{t} \dot{s}(\tau)\,\dot{\Psi}(t-\tau)\,d\tau \quad . \quad (74)$$

Eq. (74) may be solved by an iteration method already used by A. Cauchy (1840) in the solution of differential equations. The method consists in assuming values for $\Psi(t-T)$ and $\dot{\Psi}(t-T)$ and constructing the curve $\Psi(t)$ by points.

The procedure involves some degree of trial and error and is generally laborious. About the relaxation function $\dot{\Psi}$ nothing is known except that

$$\dot{\Psi}(0) = 0 \quad , \qquad \text{and}$$

$$\dot{\Psi}(\infty) = 1 \quad .$$

Actually $\dot{\Psi}$ may be nearly unity already when the aftershock sequence dies out. Moreover, $\dot{\Psi}$ is a uniformly increasing function.

Once the relaxation function is determined we may immediately find the mean viscosity η_m:

$$\eta_m = G\int_{0}^{\infty}\left[1 - \psi(t)\right]\,dt \quad . \quad (75)$$

Formula (75) can be easily verified by referring to Eq. (64) which may be written:

$$1 - \psi(t) = \frac{1}{G}\int_{0}^{K} N(k)\,e^{-kt}\,dk \quad . \quad (76)$$

Therefore

$$G\int_{0}^{\infty}\left[(1 - \psi(t)\right]\,dt = \int_{0}^{K} N(k)\,dk \int_{0}^{\infty} e^{-kt}dt. \quad (77)$$

Integrating and writing out the function N(k) as defined in Eq. (54):

$$G \int_0^\infty \left[1 - \psi(t) \right] dt = \int_0^A \int_0^K \frac{a}{k} N_1(ak)\, da\, dk \quad . \tag{78}$$

The right-hand integral represents the average value of $\frac{a}{k}$ which is precisely η by definition.

It is also possible to calculate the amount of energy expended in overcoming the viscous resistance:

$$E_v = V\dot{s}\,\eta_m \quad . \tag{79}$$

This energy represents the heat generated in the earthquake sequence.

The computation of the relaxation function has been carried out for the Manix earthquake sequence (fig. 22).

It should be noted that the curve shown as Ψ is only one of a number of possible curves, depending upon the assumptions made in the course of computation. Thus it has been arbitrarily assumed that the strain reaches zero at the end of the aftershock sequence. This assumption gives the minimum values for the viscosity, as can be seen by the dashed line (fig. 28) which represents another possible solution.

2. Minimum viscosities from aftershock sequences. If we assume that the strain reaches zero at the end of the sequence, we may write approximately:

$$\int_0^\infty \left[1 - \psi(t) \right] dt \approx \int_0^T \left[1 - \psi(t) \right] dt \tag{80}$$

since T is always larger than the duration of the sequence. Now, it is seen that:

$$\int_0^T \left[1 - \psi(t) \right] dt = T - \int_0^T \psi(t)\, dt$$

$$= T - \Psi(T) \quad . \tag{81}$$

From the iteration formula (Eq. 74) we obtain, putting t = T:

$$\Psi(T) = \frac{s(T)}{U} \quad . \tag{82}$$

Thus we may write the approximate expression for the viscosity:

$$\eta = G\,(T - \frac{s(T)}{U}) \quad . \tag{83}$$

s(T) represents the total creep strain which is obtained from the aftershock graphs. The aftershock graphs reproduced here (figs. 22 and 23) have been scaled according to an older magnitude-energy relation. In order to obtain direct strains we correct the value of S (left-hand scale) using the new formula, Eq. (47); then we multiply through by $(\frac{1}{2}GV)^{-\frac{1}{2}} = (\frac{1}{2} \times 10^{11} \times 10^{19})^{-\frac{1}{2}}$. Putting the aftershock sequence in the form shown in fig. 28 and changing time and strain origins accordingly, we obtain:

$$s(t) = 1.85 - 0.7 \log (t-T) \quad \times 10^{-5}$$

and for Hypothesis B:

$$s'(t) = 1.02 - 0.34 \log (t-T) \quad \times 10^{-5} \quad .$$

We have (from the graph) $s(T) = 4.0 \times 10^{-5}$

The main earthquake strain (Mag. 6.2) is 2.23×10^{-5}

Total accumulated strain 6.23×10^{-5}

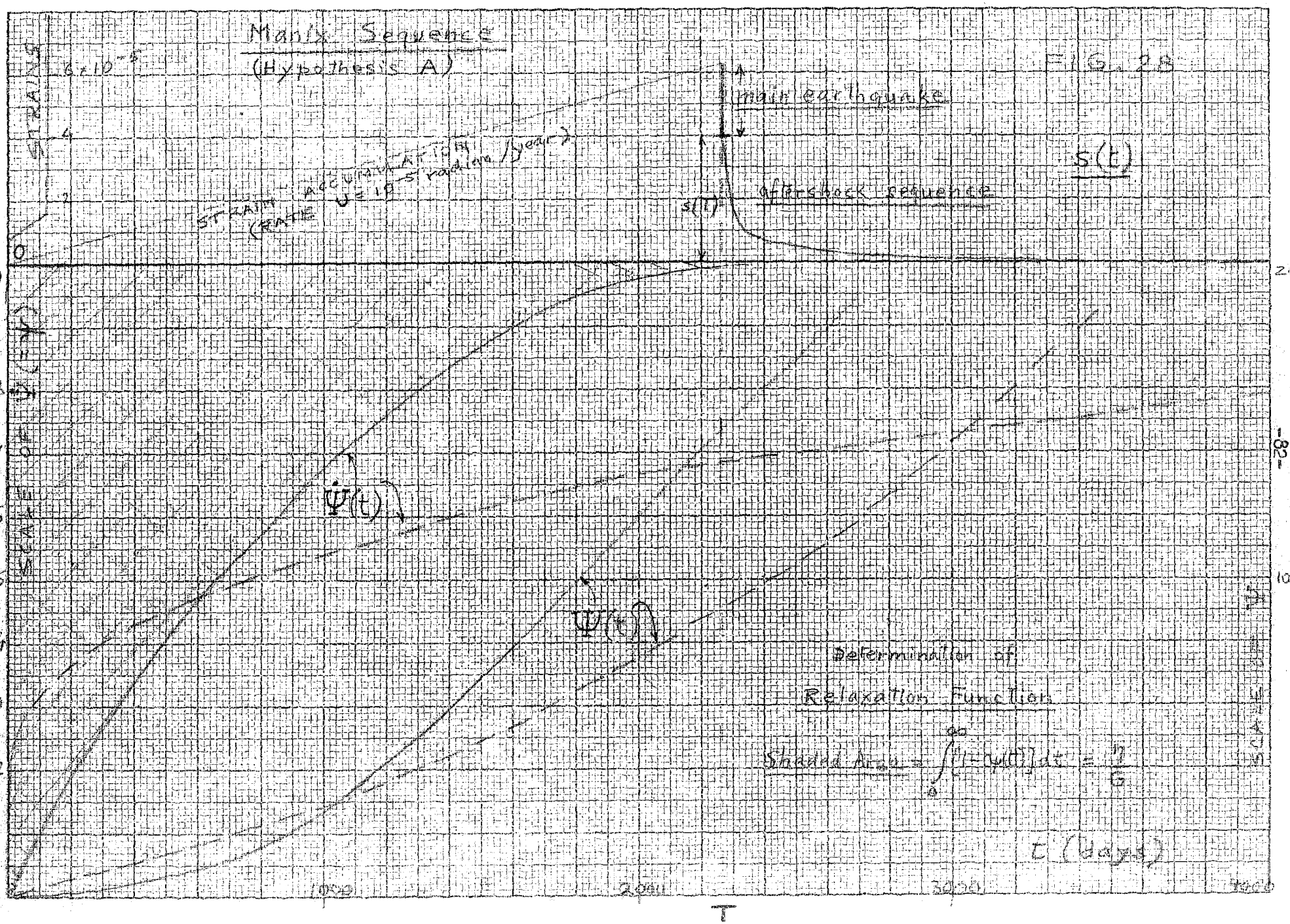
Manix Sequence
(Hypothesis A)
FIG. 28
main earthquake
aftershock sequence
s(t)
STRAIN (RATE ACCUMULATION) $\dot{\Psi}(t)$
$\dot{\Psi}(t)$
$\Psi(t)$
Determination of
Relaxation Function
Shaded Area = $\int_0^\infty [\dot{\Psi}_\infty - \dot{\psi}(t)]\,dt = \frac{1}{G}$
t (days)
T
6×10^{-5}
$\dot{\Psi}_\infty$
$\dot{\psi}(t)$
10^{-5} radians/year
2000
1000
3000
-82-

corresponding to a time of accumulation

$$T = \frac{6.23 \times 10^{-5}}{U} \quad .$$

The strain rate is $U = 10^{-5}$ radian/year $= 2.74 \times 10^{-8}$ rad./day

$$T = 2275 \text{ days} \quad .$$

For Hypothesis A we have (Eq. (83))

$$\eta_A = 10^{11} \left(2275 - \frac{4.0 \times 10^3}{2.74}\right) 86400 = 7.05 \times 10^{18} \text{ poises.}$$

The factor 86400 is a conversion factor of days into seconds.

For Hypothesis B we obtain

$$s'(T) = 0.34 \log 1000 = 1.02 \times 10^{-5}$$

$$\eta_B = 10^{11} \left(2275 - \frac{1.02 \times 10^3}{2.74}\right. 86400 = 1.32 \times 10^{19} \text{ poises.}$$

Hypothesis B gives slightly higher values. Let us repeat the same calculation for the Nevada sequence (fig. 23). We obtain:

$T =$	11,750 days	
$s(T) =$	18.8×10^{-5}	(Hypothesis A)
$s'(T) =$	2.8×10^{-5}	(Hypothesis B)

$$\eta_A = 4.23 \times 10^{19} \text{ poises}$$

$$\eta_B = 9.25 \times 10^{19} \text{ poises}$$

The differences between the two hypotheses are not important or consistent enough to afford any conclusion.

It has been pointed out already that the values of the viscosity obtained by this method are minimum values. However, the error introduced by assuming zero strains at the end of the sequence will hardly be more than one or two orders of magnitude.

This estimate is made on the basis of actual trial-and-error computations, such as gave the dashed curve in fig. 23.

The determination of the viscosity of the earth's crust is a major problem in geophysics. Current estimates, including Haskell's calculation for the post-glacial uplift of Fenno-scandia, are reviewed by Gutenberg (1951). The average estimate for the viscosity is:

$$\eta = 10^{20} - 10^{22} \text{ poises.}$$

These values are in excellent agreement with our general results, obtained exclusively through the use of the Benioff aftershock theory.

3. Conclusions. It has been shown how a method of quantitative analysis based upon the viscoelastic theory can be applied to aftershock sequences. Due to the lack of strain measurements in earthquake zones the problem is still indeterminate, and only rough results can be obtained. It is probable, however, that a procedure essentially similar to the one outlined here may eventually provide a tool for computing crustal strain patterns from aftershock data.

Some of the geophysical problems amenable to this approach would be:

1. Study of the viscosity of the crust and its geographical and depth variations.

2. The question of local heat generation due to earthquakes, and its possible relation to volcanism.

3. The problem of stress-strain behavior of the subcrustal material and its influence on the mechanism of deep-focus earthquakes.

4. An analysis of isostasy based upon actual stress patterns produced by the mountainous overburden.

5. Regional seismicity studies on the basis of strain accumulation, and prediction of earthquakes.

At present many of the fundamental data available for such calculations are still very imperfect; however, we hope to have shown that the Benioff Theory can provide numerically consistent results even at this stage. In addition, the theory could furnish a basis for devising model experiments of great value in connection with some of the problems outlined above.

It would be interesting to find out how the assumption of linearity contained in the viscoelastic approach affects the results. Some clues might be obtained from suitable high-pressure experiments in metals, since "the observed behavior of rocks...is in all respects consistent with that of metals and some other solids" (Griggs in "Colloquium on Plastic Flow", 1951). This remark, which applied chiefly to sedimentary and metamorphic rocks, may now be extended to include some igneous rocks in the range of testing conditions described.

APPENDIX I

In a uniform bar of circular cross section let $p(r, t)$ be the stress at points of distance r to the center of the section subjected to a constant torque M.

The moment necessary to balance p over an annular section of radius r and width dr is:

$$dM = 2\pi\, r dr \cdot p(r,t)\, r \quad . \tag{84}$$

Integrating over the section:

$$M = 2\pi \int_0^R p(r,t)\, r^2\, dr \quad . \tag{85}$$

Since M is a constant we may write

$$\frac{dM}{dt} = 2\pi \int_0^R \frac{\partial p(r,t)}{\partial t}\, r^2\, dr = 0 \quad . \tag{86}$$

In order for the integral to vanish, the derivative of p must change signs at least once within the limits of integration. This implies the existence of non-uniform properties in the section, such as may be caused by differential strain hardening, heat generation or other strain-dependent effects.

In the present experiments we are limited to very small strains so that these differential effects may be considered negligible. Thus we have approximately:

$$\frac{\partial p(r,t)}{\partial t} = 0 \quad . \tag{87}$$

Strictly speaking, this equation is true only for non-dissipative systems (e.g. for the ideal elastic case).

APPENDIX II

1. Maxwell solid. Let r be the radial distance of any point in the section and let $\dot{\theta}$ be the rate of angular strain of the sample per unit length. Then:

$$s = r \int_0^t \dot{\theta}\, dt \tag{88}$$

gives the strain at the point of distance r at the instant t.

The Maxwell equation (Eq. 10):

$$\dot{s} = \frac{1}{E}\dot{p} + \frac{1}{\eta}p$$

degenerates under constant load into Newton's equation, because $\dot{p} = 0$ (see Appendix I):

$$\dot{s} = \frac{1}{\eta}\, p \,. \tag{89}$$

Differentiating Eq. (88) above with respect to time, and equating with (89) we have:

$$p = \eta\, r\, \dot{\theta} \,. \tag{90}$$

On an annular surface of radius r and width dr we have:

$$dM = \eta\, r\, \dot{\theta} \times 2\pi r dr \times r \,. \tag{91}$$

Integrating over the section:

$$M = 2\pi\eta\dot{\theta} \int_0^R r^3\, dr = \frac{\pi}{2}\eta\, \dot{\theta}\, R^4 \,. \tag{92}$$

Since M is constant $\dot{\theta}$ must be constant also. Thus:

$$s = \dot{s}t + \frac{p}{E}$$

and:

$$\phi(t) = \frac{E}{\eta}t \,. \tag{93}$$

2. Voigt solid. The Voigt equation (Eq. 11):

$$p = Es + \eta \dot{s}$$

may be easily integrated as follows:

$$s = \frac{p}{E}\left(1 - e^{-E/\eta t}\right) . \tag{94}$$

For any given instant t, Eq. (94) is identical with Hooke's law. We may therefore write directly the moment-twist equation in the form of Eq. (19):

$$M = \frac{\pi}{2} ER^4 \frac{\theta(t)}{1-e^{-E/\eta t}} \tag{95}$$

and:

$$\phi(t) = -e^{-\frac{E}{\eta}t} . \tag{96}$$

3. Standard linear solid. The stress-strain equation of the standard linear solid is:

$$Es + \eta \dot{s} = p + \frac{1}{\tau} \int p dt \tag{97}$$

which may be integrated as follows:

$$s = p\left[\left(\frac{1}{E} - \frac{\eta}{\lambda}\right)\left(1 - e^{-\frac{E}{\eta}t}\right) + \frac{t}{\lambda}\right] \tag{98}$$

where $\lambda = \tau E^2$.

Again, one can write the moment-twist equation directly:

$$M = \frac{\pi}{2} R^4 \frac{\theta(t)}{\left(\frac{1}{E} - \frac{\eta}{\lambda}\right)\left(1-e^{-E/\eta t}\right) + \frac{t}{\lambda}} \tag{99}$$

$$\phi(t) = \left(1 - \frac{\eta}{E\tau}\right)\left(1 - e^{-E/\eta t}\right) + \frac{1}{E\tau}\, t - 1 \quad . \tag{100}$$

APPENDIX III

The Bingham equation for a plastic-viscous body is (Eq. 22):

$$p = k + \eta \dot{s} \quad .$$

In any section of a twisted bar of such a material there will be an elastic core of radius ρ and a plastic-viscous periphery. If $\dot{\theta}$ is the angular strain rate per unit length of sample, the strain rate at the surface is equal to $R\dot{\theta}$, whereas at the elastic boundary the strain rate is zero. At any radius $r > \rho$ we have then:

$$\dot{s} = \frac{R\,\dot{\theta}\,(r-\rho)}{R-\rho} \tag{101}$$

since in any linear solid the strain rate must be a linear function of the radius.

Substituting (101) into the Bingham equation:

$$p = k + \frac{\eta R\dot{\theta}(r-\rho)}{R-\rho} \quad . \tag{102}$$

At this point it is convenient to introduce a stress function F (Prager and Hodge, 1951) such that

$$-\frac{\partial F}{\partial r} = p \quad . \tag{103}$$

The function F is defined over the entire cross-section and it is conventionally zero along the contour of the section. For all $r > \rho$ the stress function will be:

$$-F_p = \frac{\eta R\dot{\theta}(r-\rho)^2}{2(R-\rho)} + kr + C \quad . \tag{104}$$

The value of the integration constant is found from the condition that F_p vanish at the contour:

$$C = -\frac{\eta R\dot{\theta}(R-\rho)}{2} - kR \quad . \tag{105}$$

For all $r < \rho$ the stress function has the well-known form for the elastic case (Prager and Hodge, ibid.):

$$F_e = -\tfrac{1}{2} E \theta_o r^2 + C' \quad . \tag{106}$$

In order to make the problem solvable we assume:

a) continuity of the stress function at $r = \rho$:

$$F_p(\rho) = F_e(\rho)$$

which gives the value of the constant of integration C':

$$C' = \tfrac{1}{2}E\theta_o\rho^2 + \frac{\eta R\dot{\theta}}{2}(R-\rho) + k(R-\rho) \quad . \tag{107}$$

b) continuity of stresses at $r = \rho$:

$$\frac{\partial F_e(\rho)}{\partial r} = \frac{\partial F_p(\rho)}{\partial r}$$

which gives:

$$\rho = \frac{k}{E\theta_o} \quad . \tag{108}$$

Now that the position of the boundary is determined we can integrate the stress function over the cross-section to find the torque M:

$$M = 2\int_A F dA = 4\pi \int_0^R F r dr \tag{109}$$

or:

$$\frac{M}{4\pi} = \int_0^\rho F_e\, r dr + \int_\rho^R F_p\, r dr \quad . \tag{110}$$

Carrying out the integration one finally obtains:

$$M = \frac{2}{3}\pi R^3 k\left[1 - \frac{1}{4R^3}\left(\frac{k}{E\theta_o}\right)^3\right]$$

$$+ \frac{\pi}{6}\eta R\dot{\theta}\left(3R^3 - \frac{R^2 k}{E\theta_o} - \frac{Rk^2}{E^2\theta_o^2} - \frac{k^3}{E^3\theta_o^3}\right) \qquad (111)$$

which is identical with Eq. (23).

REFERENCES

Adams, F. D. and J. A. Bancroft, Internal Friction in Rocks during Deformation; Journ. Geol. 25, p. 597 (1917).

Alfrey, T., Jr., Molecular Theory of Viscoelastic Behavior of an Amorphous Linear Polymer; Journ. Chem. Phys. 12, p. 374 (1944).

Becker, R., Ueber die Plastizität amorpher und kristalliner fester Körper; Phys. Z. 26, p. 919 (1925).

Benioff, H., Earthquakes and Rock Creep, I. Bull. Seis. Soc. Amer., 41, p. 31 (1951).

Benioff, H., (6) Global Strain Accumulation and Release as Revealed by great Earthquakes; Bull. Geol. Soc. Am., 62, p. 331 (1951).

Benioff, H., The Mechanism of Earthquake Generation (unpublished).

Benioff, H., Mechanism and Strain Characteristics of the Fault as Indicated by the Aftershock Sequence, Symposium on the Crust of the Earth (Columbia University Centennial Ed.) Geol. Soc. of Am. Memoir, 1955 (in publication).

Bingham, E. C., Fluidity and Plasticity, New York (1922).

Biot, M. A., Theory of Stress-Strain Relations in Anisotropic Viscoelasticity and Relaxation Phenomena, Journ. Appl. Phys., 25, p. 1385 (1954).

Birch, F. and D. Bancroft, Elasticity and Internal Friction in a Long Column of Granite, Bull. Seism. Soc. Am. 28, p. 243 (1938).

Bridgman, P. W., Studies in Large Plastic Flow, McGraw-Hill, New York (1952).

Bullen, K. E., On the Size of the Strained Region Prior to an Extreme Earthquake; Bull. Seis. Soc. Am. 25, p. 43 (1955).

Burgers, J. M., First Report on Viscosity and Plasticity; Acad. Sci. Amsterdam (1935).

Colloquium on Plastic Flow, Trans. Am. Geoph. U. 32, p. 526 (1951).

Goranson, R., Physics of Stressed Solids, Journ. Chem. Phys. 8, p. 323 (1940).

Griggs, D. T., Deformation of Rocks under High Confining Pressures; Jour. Geol. 44, p. 541 (1936).

Griggs, D. T., Creep of Rocks; Jour. Geol. 47, p. 225 (1939).

Gross, B., On Creep and Relaxation, Journ. Appl. Phys. 18, p. 212 (1947).

Gutenberg, B., Internal Constitution of the Earth, 2nd Ed., Dover, New York (1951).

Gutenberg, B. and C. F. Richter, Seismicity of the Earth and Associated Phenomena, 2nd Ed., Princeton Univ. Press, N. J. (1954).

Gutenberg, B., and C. F. Richter, Earthquake Magnitude, Energy, Intensity and Acceleration, 2nd paper (in course of publication, 1955).

Jeffreys, H., Viscosity of the Earth, 3rd paper, Mon. Not. Roy. Astron. Soc. 77, p. 449 (1917).

Kauzmann, W., Flow of Solid Metals, Trans. Am. Inst. Min. Met. Eng. 143, p. 57 (1941).

Love, A. E. H., Treatise on the Mathematical Theory of Elasticity, 4th Ed. Cambridge Univ. Press (1934).

Ludwik, P. and R. Scheu, Vergleichende Zug-, Druck-, Dreh- und Walzversuche. Stahl u. Eisen 45, p. 373 (1925).

Michelson, A. A., Preliminary Results of Measurements of the Rigidity of the Earth; Journ. of Geol. 22, p. 97 (1914).

Michelson, A. A., The Laws of Elastic-Viscous Flow, I. Journ. Geol., 25, p. 405 (1917).

Michelson, A. A., Id., II, Journ. Geol. 28, p. 18 (1920).

Michelson, A. A. and H. G. Gale, Rigidity of the Earth, Journ. Geol. 27, p. 585 (1919).

Nadai, A., Plasticity. McGraw-Hill, New York (1931).

Nadai, A., and P. G. McVetty, Hyperbolic Sine Chart for Estimating Working Stresses of Alloys at Elevated Temperatures, Proc. Am. Soc. Test. Mat., 43, p. 735 (1943).

Nowick, A. S. and E. S. Machlin, Quantitative Treatment of the Creep of Metals, Nat. Adv. Comm. Aeron. TN 1039 (1946).

Orowan, E., The Creep of Metals, Jour. West of Scotland, Iron and Steel Inst. 54, p. 45 (1946).

Prager, W. and P. G. Hodge, Theory of Perfectly Plastic Solids. John Wiley, New York (1951).

Reiner, M., Deformation and Flow, H. K. Lewis, London (1949).

Richter, C. F., An Instrumental Earthquake Magnitude Scale. Bull. Seis. Soc. Am., 25, p. 1 (1935).

Robinson, E. L., Effect of Temperature Variation on the Creep Strength of Steels, Trans. Am. Soc. Mech. Eng. 60, p. 253 (1938).

Schwope, A. D. and L. R. Jackson, Survey of Creep in Metals, Nat. Adv. Comm. Aeron. TN 2516 (1951).

Shepherd, W. M., Plastic Stress-Strain Relations, Proc. Inst. Mech. Eng. 159, p. 95 (1948).

Simha, R., On Relaxation Effects in Amorphous Media, Journ. Appl. Phys. 13, 201 (1942).

Sips, R., Behavior of Viscoelastic Substances, Jour. Polymer Sc. 5, p. 69 (1950).

Zener, C., Anelasticity of Metals, Tech. Pub. 1992, Am. Inst. Min. Met. Eng. (1946).

Note: References to the work of Cauchy, Hooke, Maxwell, Newton and Saint-Venant may be found in Burgers (1935), Reiner (1949), Nadai (1931), or in historical books.

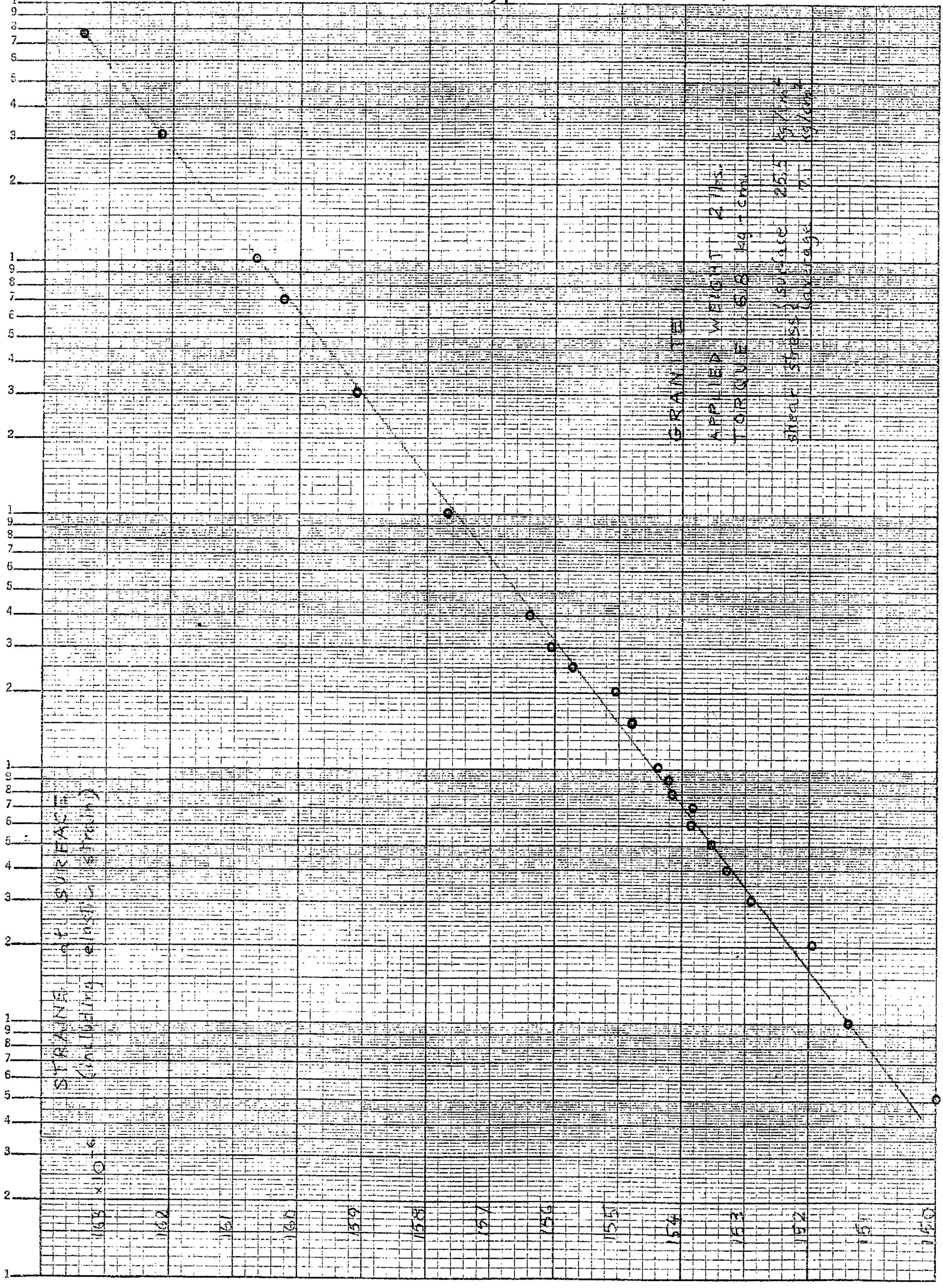
GRANITE
APPLIED WEIGHT 2 lbs.
TORQUE 6.8 kg-cm
shear stress (surface 25.5 lb/in²
(average 17. lb/in²
STRAIN at SURFACE
(including elastic strain)
x10⁻⁶
163
162
161
160
159
158
157
156
155
154
153
152
151
150

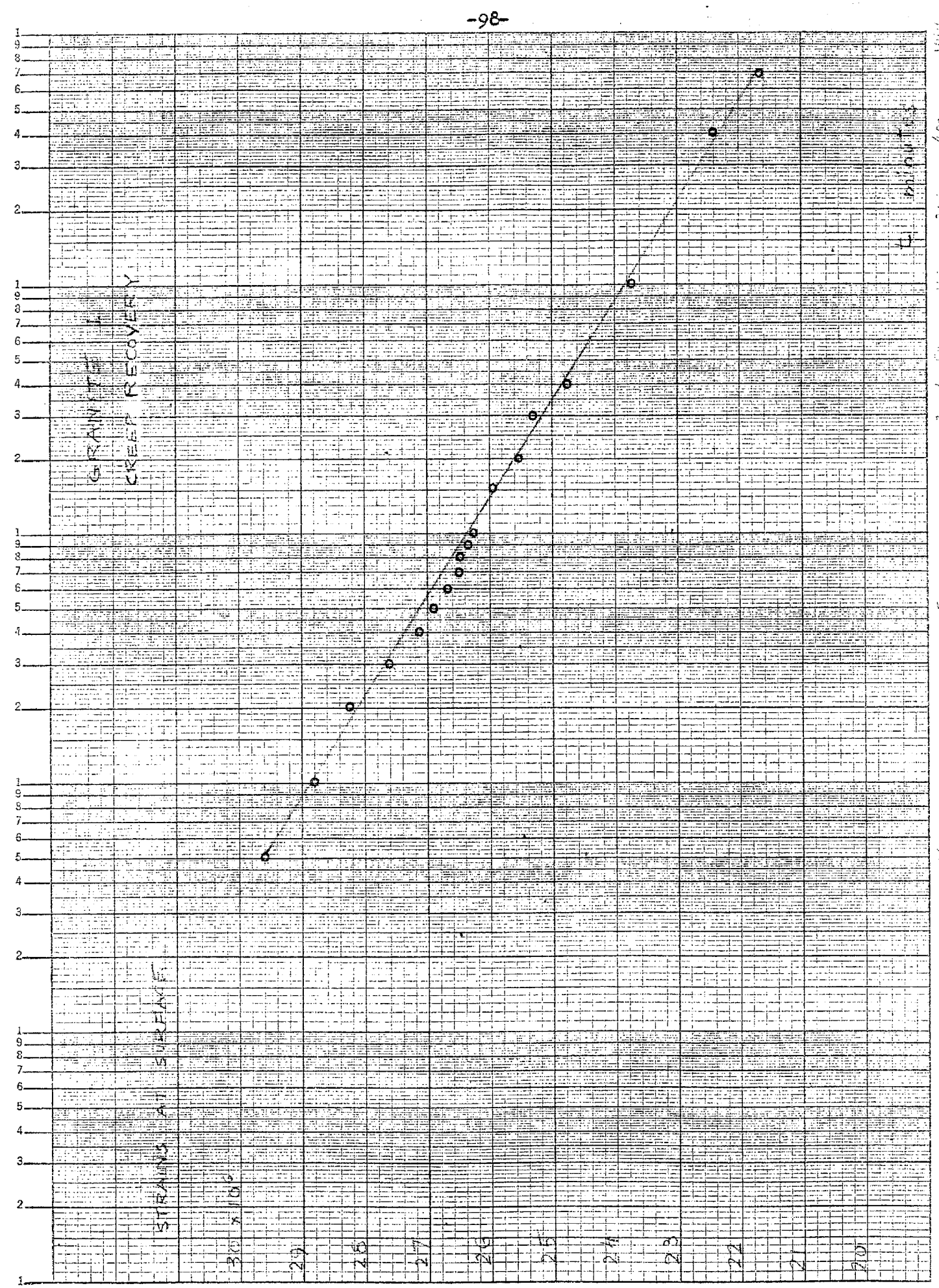
GRAIN SIZE
CREEP RECOVERY
STRAIN, SURFACE
3.0 x 10⁻⁶
29
28
27
26
25
24
23
22
21
20

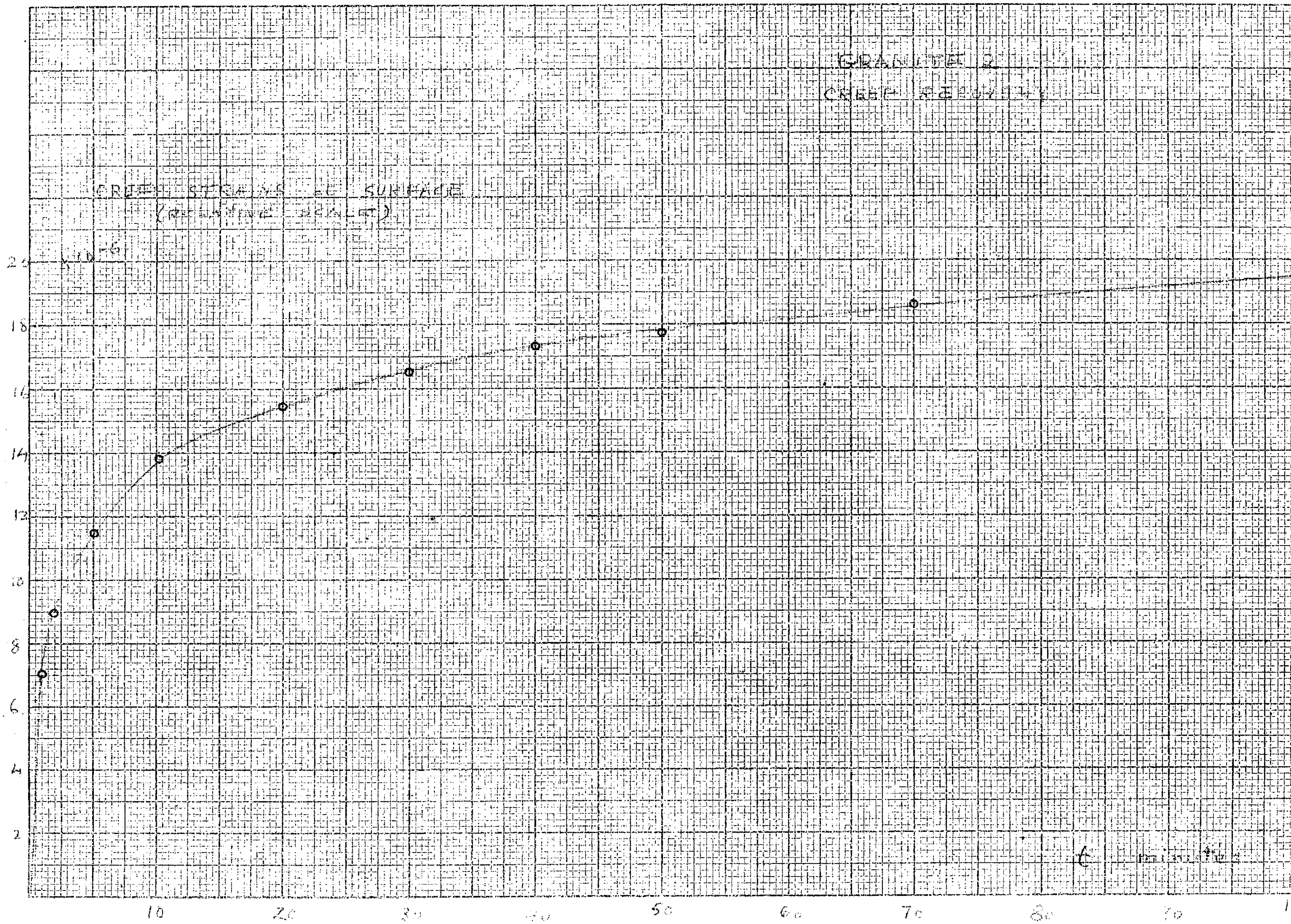
GRANITE 2
SURFACE
x10^-6
20
18
16
14
12
10
8
6
4
2
10
20
30
40
50
60
70
80
90
100
t

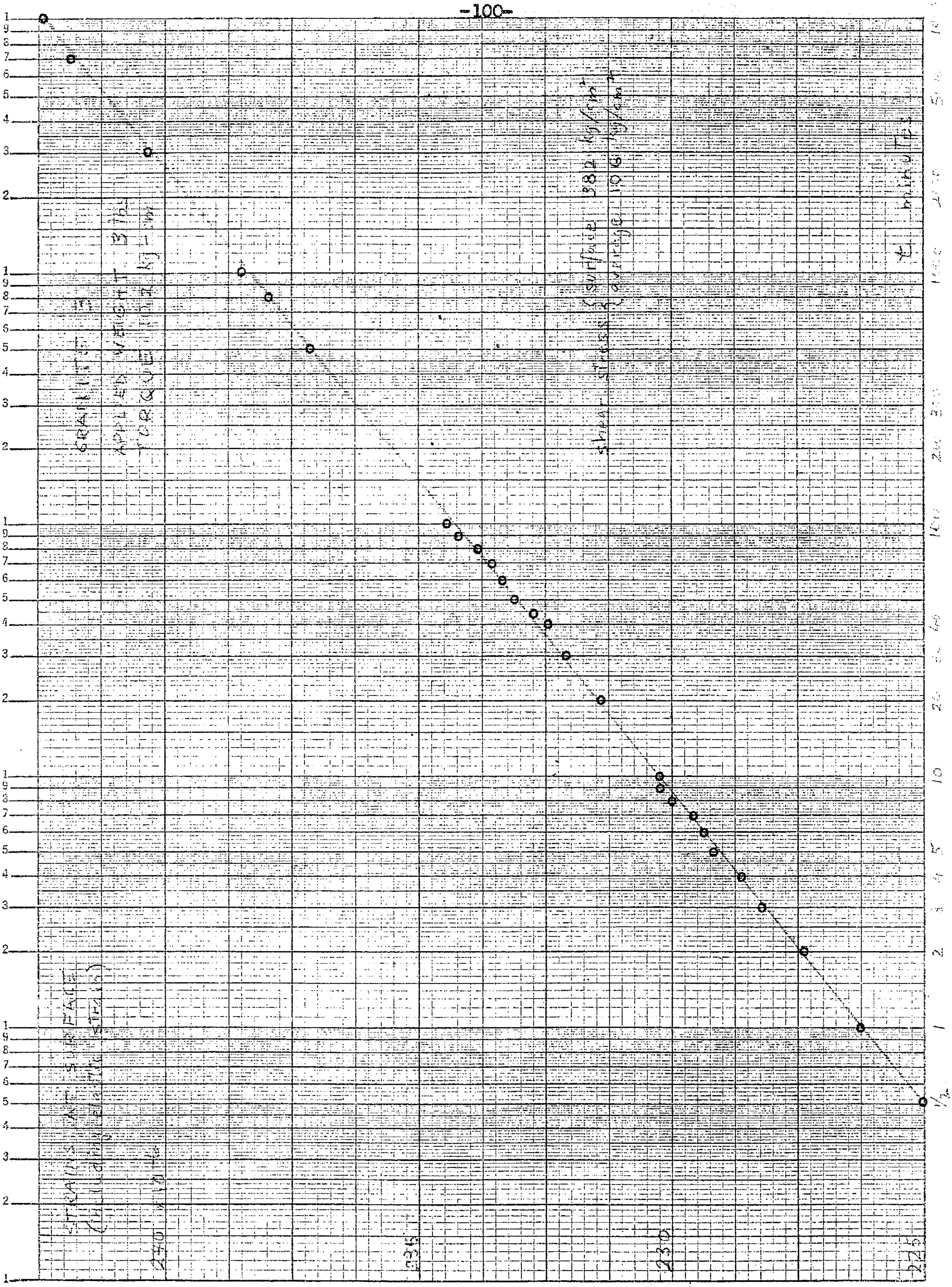
GRANITE
t minutes
240
235
230
225

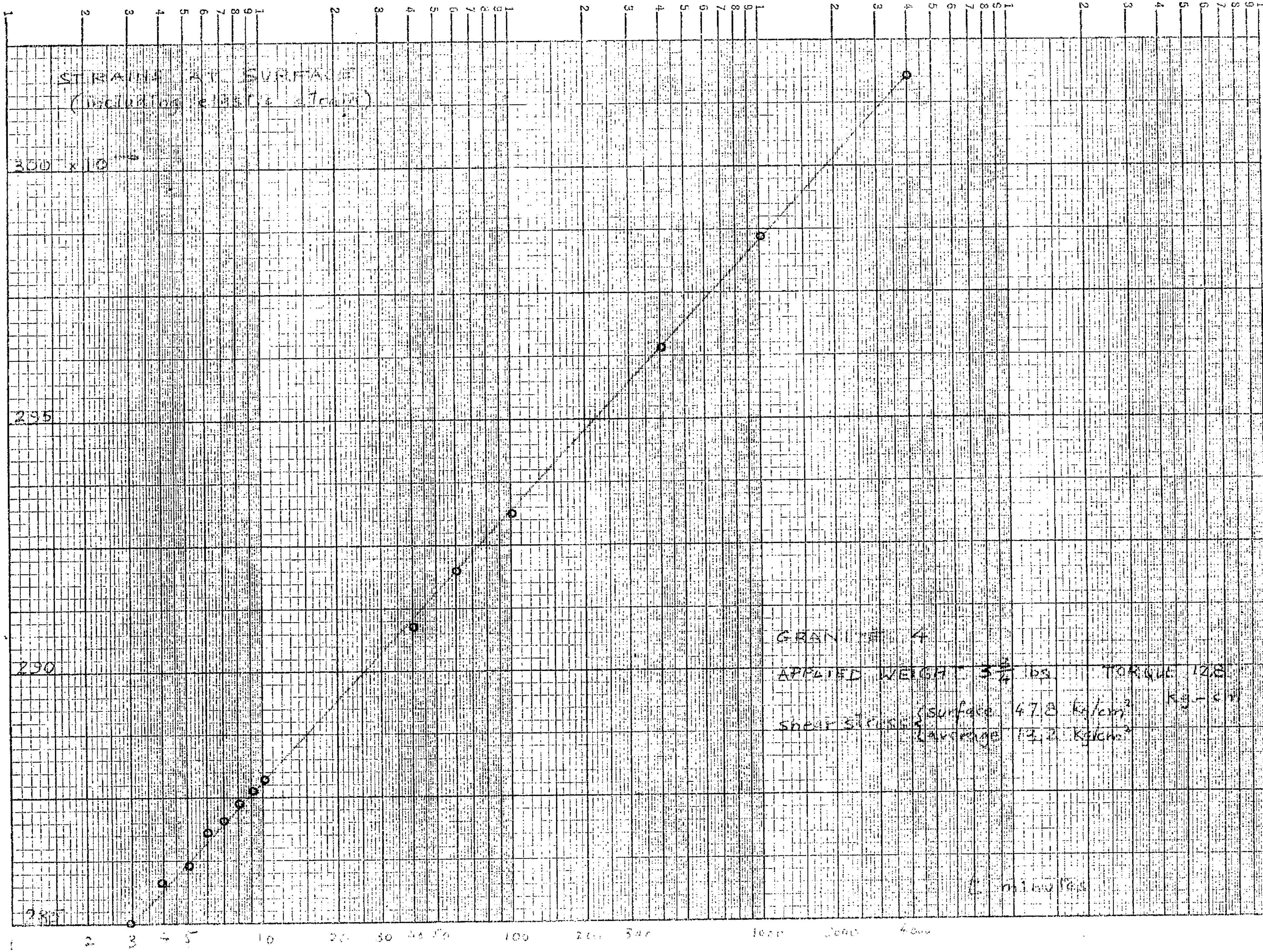
STRAINS AT SURFACE
(including elastic strain)
300 x 10
295
290
285
GRANITE # 4
APPLIED WEIGHT 3¾ lbs TORQUE 128 Kg-cm
Shear Stress {surface 47.8 Kg/cm²
average 14.2 Kg/cm²
t minutes
1 2 3 4 5 10 20 30 40 50 100 200 500 1000 2000 4000

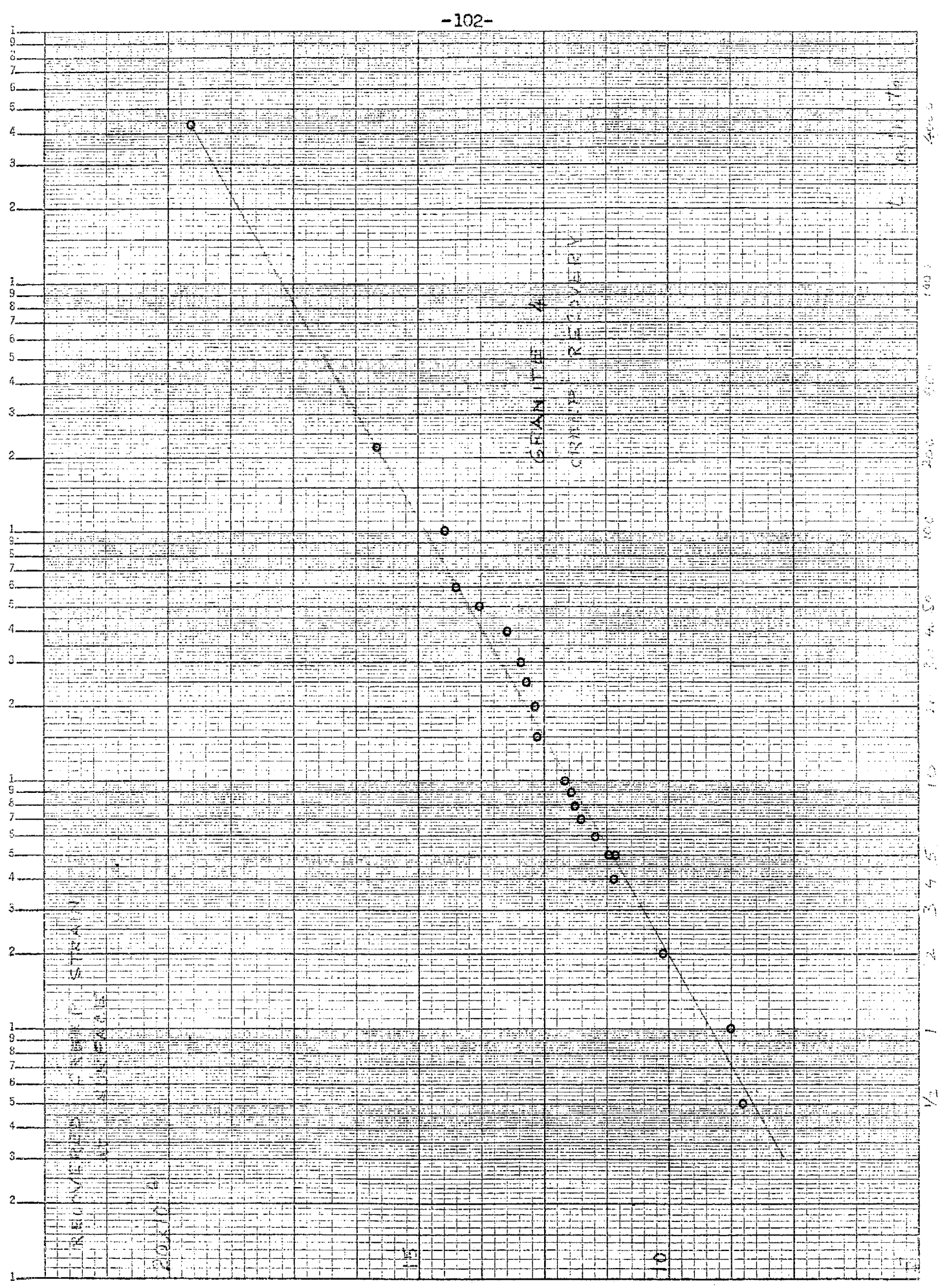
GRANITE
GRANITE

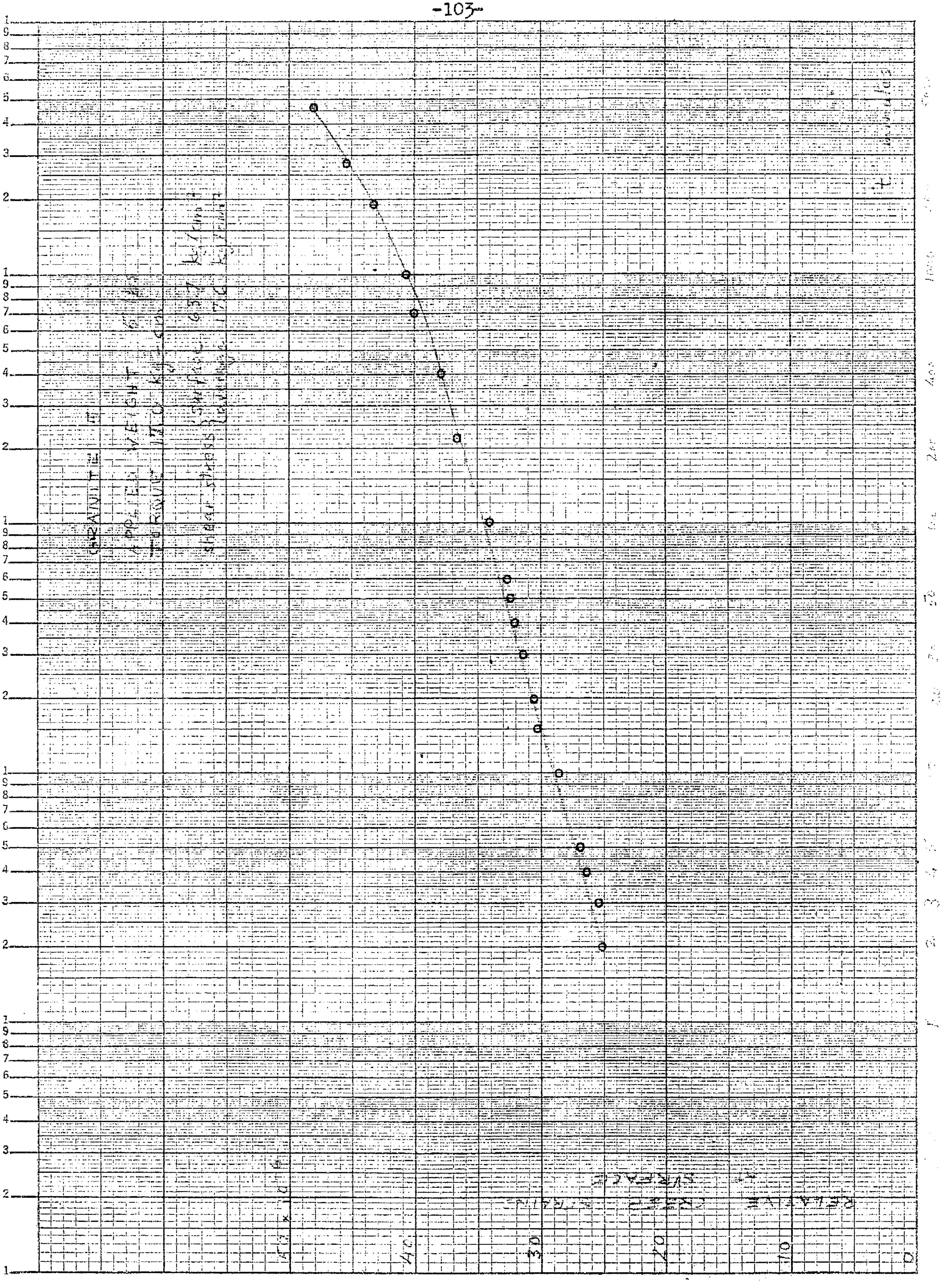

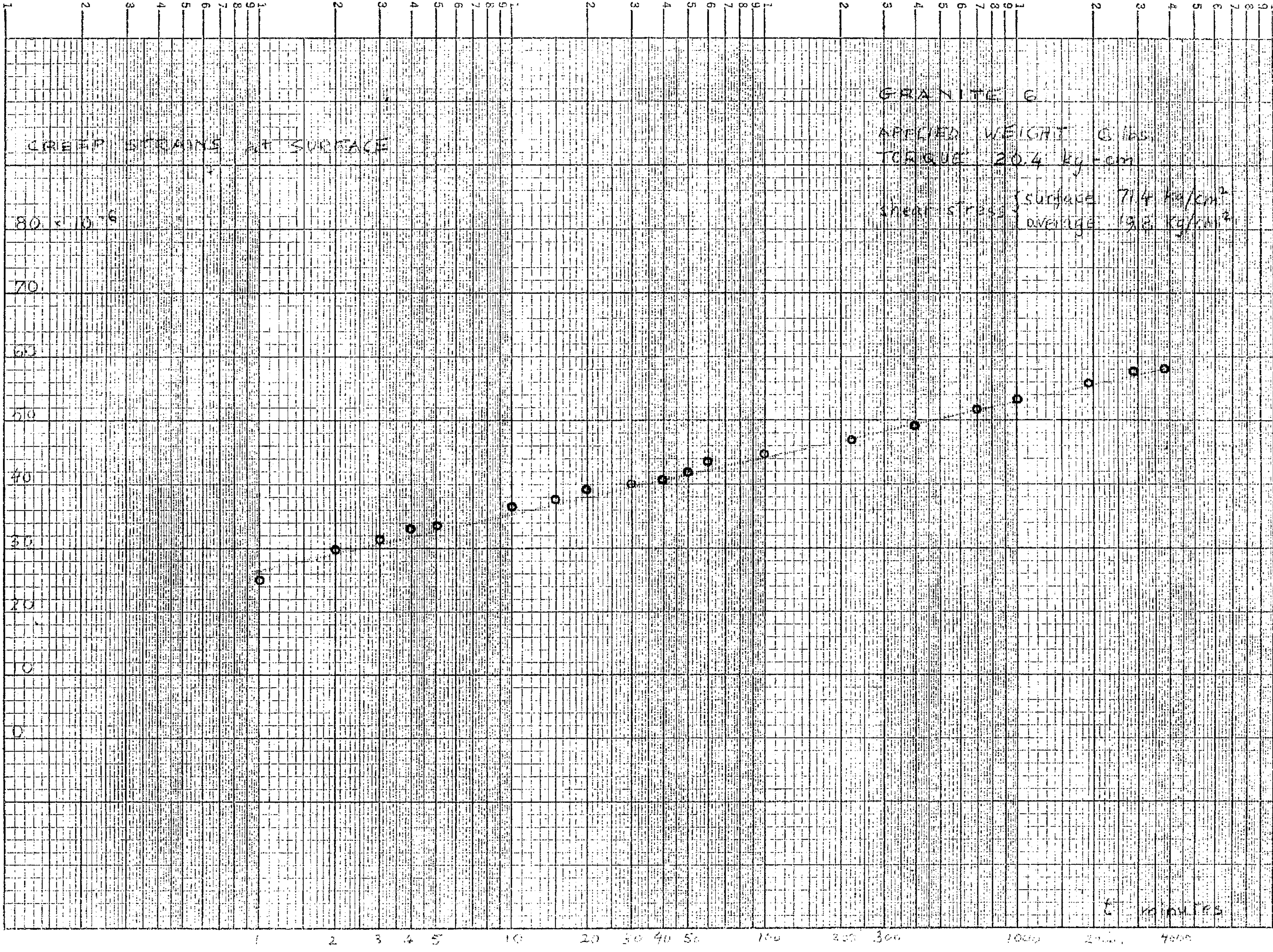
GRANITE 6
APPLIED WEIGHT 6 lbs.
TORQUE 20.4 kg-cm
shear stress {surface 71.4 kg/cm²; average 19.8 kg/cm²
CREEP STRAINS at SURFACE
80 × 10⁻⁶
70
60
50
40
30
20
10
0
1
2
3
4
5
10
20
30
40
50
100
200
300
1000
2000
4000
t minutes

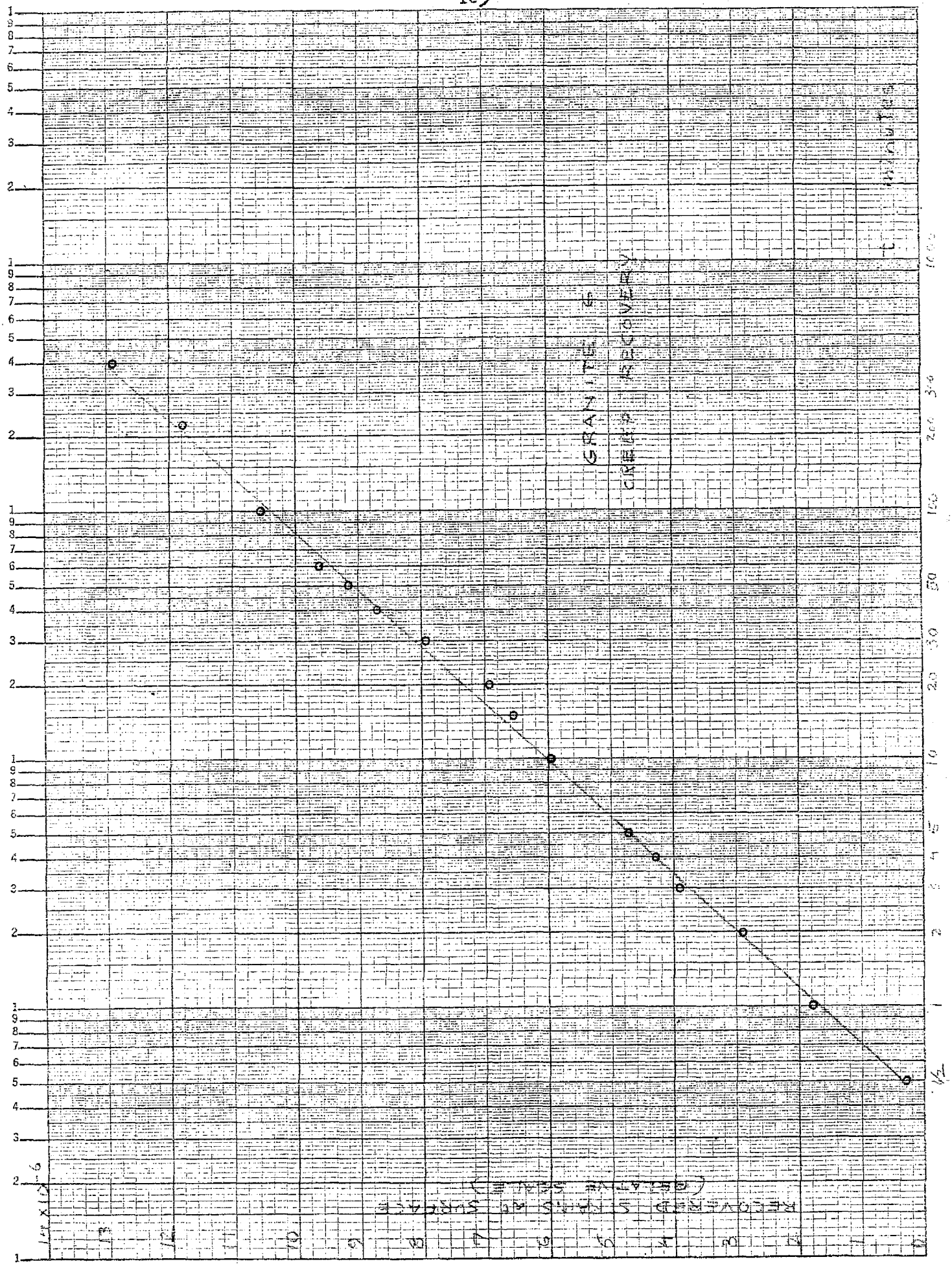
GRANITE
CREEK
RECOVERED STRESS AT SURFACE
(RELATIVE SCALE)

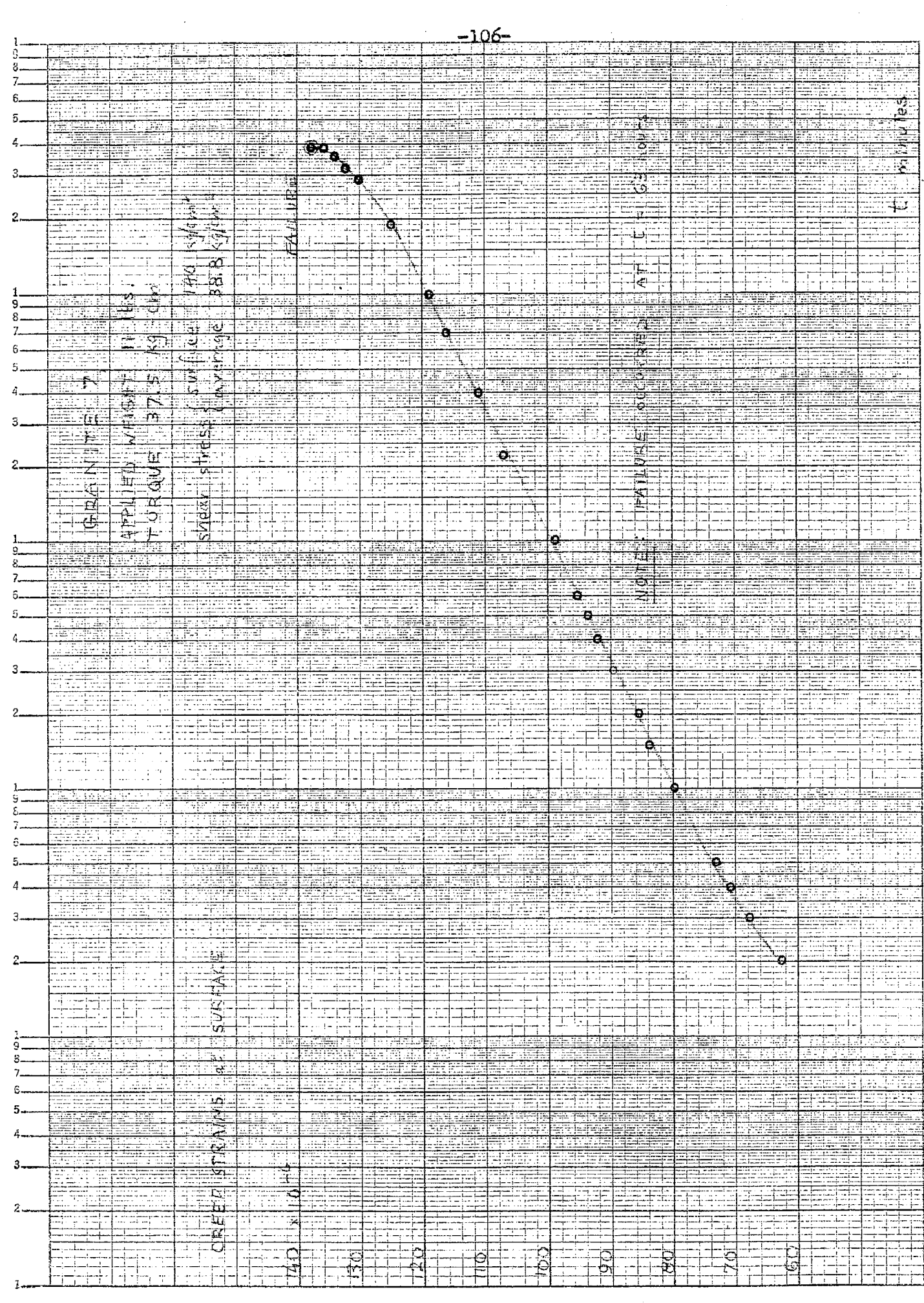
GRANITE
APPLIED WEIGHT 11 lbs.
TORQUE 37.5 kg cm
Shear stress at surface 140 kg/cm²
Shear stress at centre 38.8 kg/cm²
FAILURE
NOTE: FAILURE occurred AT
CREEP STRAINS at SURFACE
t minutes

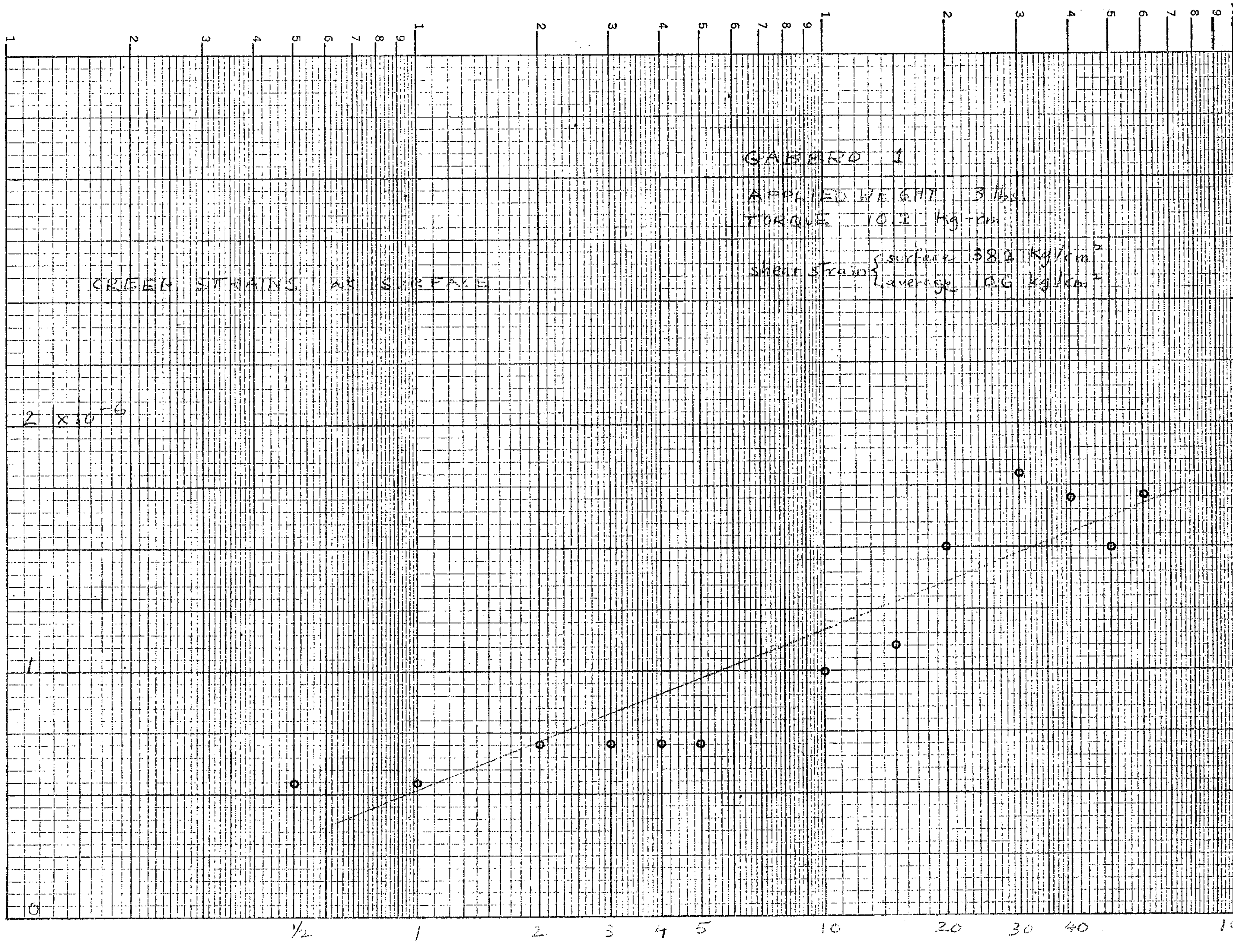
GABBRO 1
APPLIED WEIGHT 3 lbs.
TORQUE 10.2 Kg-cm
Shear Strain {surface 38.0 Kg/cm²
average 10.6 Kg/cm²
CREEP STRAINS AT SURFACE
2 x10⁻⁶
1
0
½ 1 2 3 4 5 10 20 30 40 100

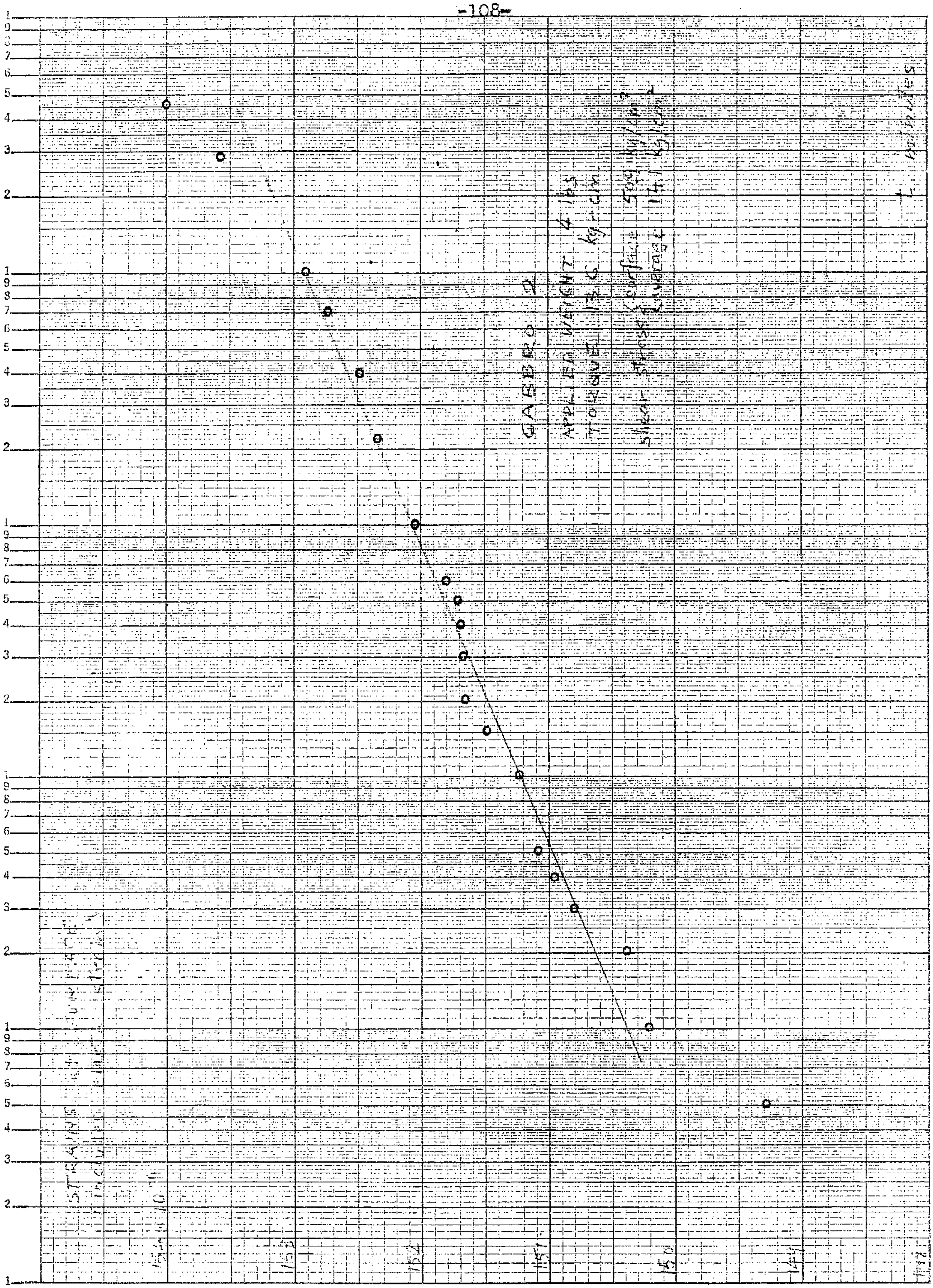
GABBRO 2
APPLIED WEIGHT 4 lbs
TORQUE 136 kg-cm
Shear stress (surface 500 kg/cm²
(average 141 kg/cm²
t minutes
STRAINS ...

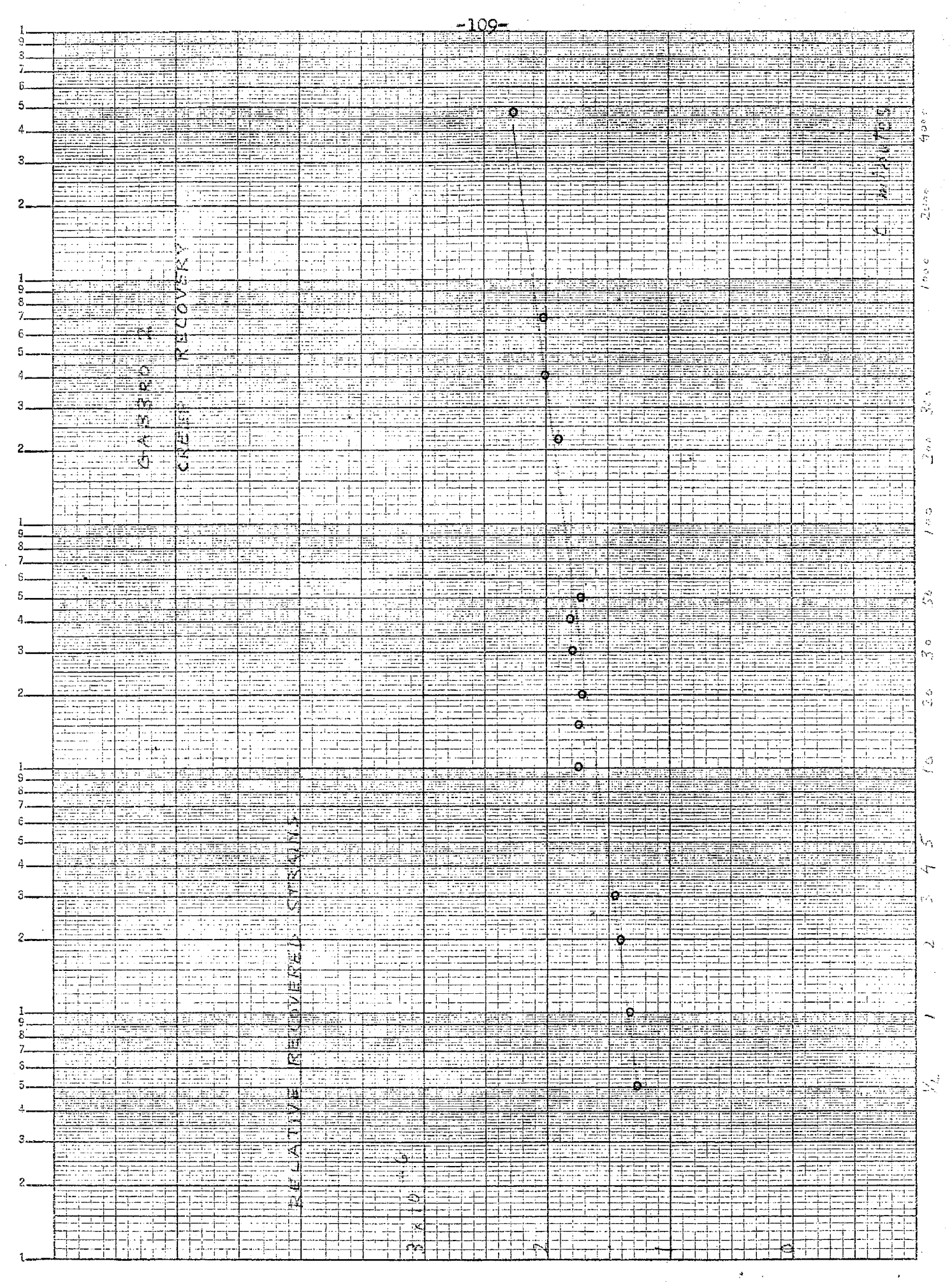
CREEP RECOVERY
RELATIVE RECOVERED STRAIN

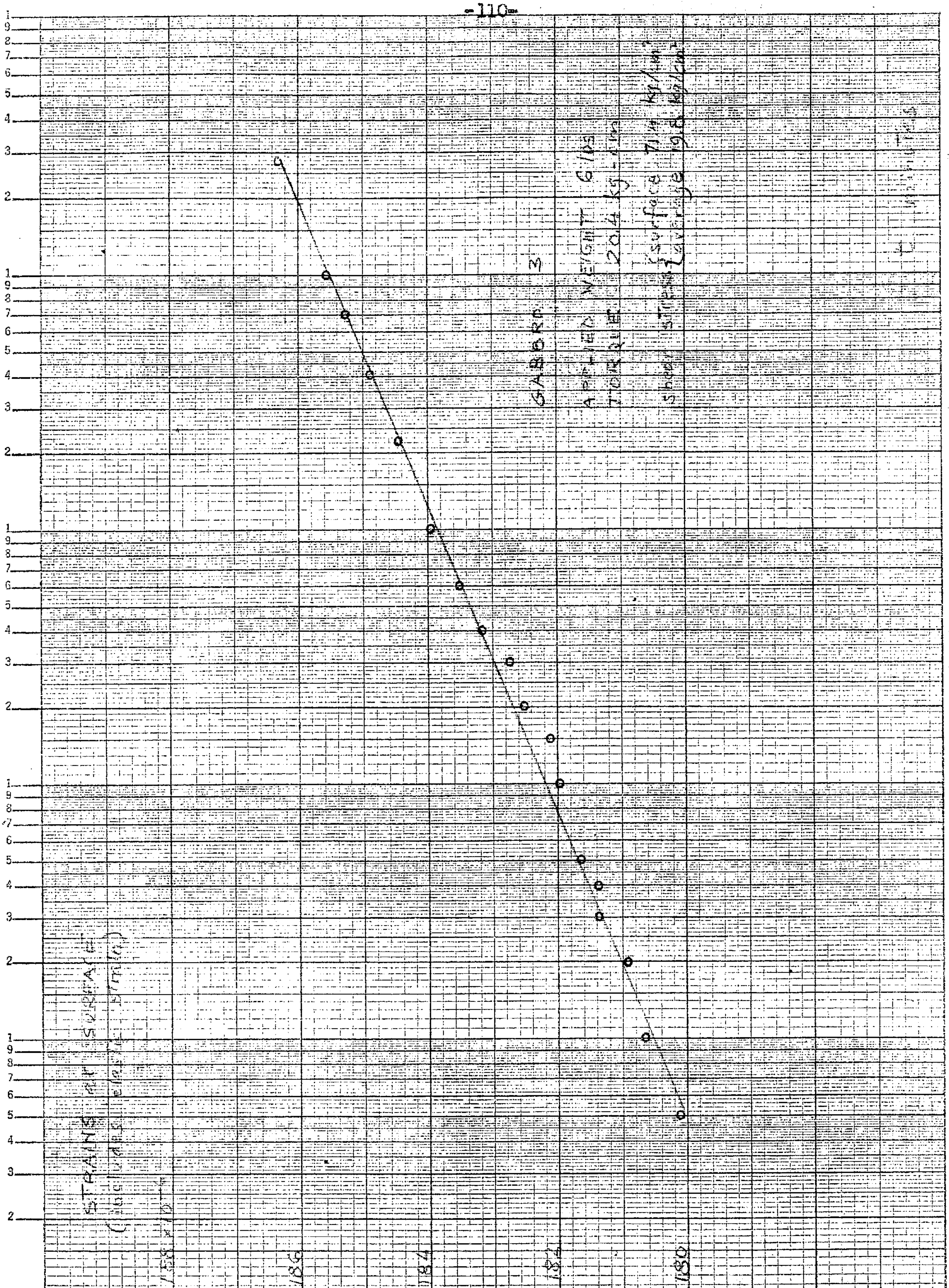
GABBRO 3
TORQUE
186
184
182
180

LOADED AT
APPLIED WEIGHT 11 lbs
TORQUE 3.75 kg-cm
shear stress (surface) 140 kg/mm²
(average) 388 kg/cm²
Note: Data not corrected for calibration of recording pattern
RELATIVE CREEP STRAINS AT CONSTANT
12 x 10⁻⁶
t minutes